SUSTAINABLE ENERGY TECHNOLOGY, ADOPTION, REBOUND, AND RESILIENCE

A Dissertation
Presented to
The Academic Faculty

by

Shahaboddin (Sean) Hashemi Toroghi

In Partial Fulfillment
of the Requirements for the Degree
Doctor of Philosophy in the
School of Building Construction

Georgia Institute of Technology
May 2019

SUSTAINABLE ENERGY TECHNOLOGY, ADOPTION, REBOUND, AND RESILIENCE

Approved by:

Dr. Daniel Castro-Lacouture, Co-advisor
School of Building Construction
Georgia Institute of Technology

Dr. Valerie M. Thomas, Co-advisor
School of Industrial and System Engineering
Georgia Institute of Technology

Dr. Xinyi Song
School of Building Construction
Georgia Institute of Technology

Dr. Mathew Oliver, Minor Advisor
School of Economics
Georgia Institute of Technology

Dr. William Drummond,
School of City and Regional Planning
Georgia Institute of Technology

Date Approved: January 11th, 2019

Dedicated to my beloved mother, *Fatemeh-Shamsolmolouk*,

in ever loving memory of my father, Dr. *Hossein H. Toroghi*,

and my lovely sister, *Hale*.

ACKNOWLEDGEMENTS

First and for most, I would like to express my deepest gratitude to my advisors Dr. Valerie M. Thomas and Dr. Daniel Castro, and my minor-advisor Dr. Matthew Oliver for their support, guidance, and supervision throughout all the stages of this dissertation. Without their help and guidance, this dissertation would not have been possible.

I also would like to extend my thanks to my committee members. My sincere thanks to Dr. Xinyi Song from the School of Building Construction and Dr. William Drummond from the School of City and Regional Planning, for their enormous support and guidance.

Last but foremost; I would like to thank my parents. While my father, Dr. Hossein H Toroghi, passed away years ago, he was and always will be my role model through my life. Without their support, guide, and endless patient, I would not be where I am today.

TABLE OF CONTENTS

LIST OF TABLES

LIST OF FIGURES

LIST OF SYMBOLS AND ABBREVIATIONS

ACF	Autocorrelation Function
ACS	American Community Survey
AIC	Akaike Information Criteria
ADF	Augmented Dickey Fuller
AR	Autoregressive
ARIMA	Autoregressive Integrated Moving Average
BIC	Baysian Information Criteria
BTU	British Thermal Unit
CDD	Cooling degree Days
DG	Distributed Generation
DHS	Department of Homeland Security
DOE	Department of Energy
DRE	Direct rebound effect
DSM	Digital Surface Model
EIA	Energy Information Administration
FiT	Feed-in-Tariff
GHG	Greenhouse Gas Emission
GIS	Geographic Information System
GWh	Giga Watt hour
HDD	Heating Degree Days
KBP	Khazzom-Brooks Postulate
kWh	Kilo Watt hour
LiDAR	Light Detection and Ranging

MA	Moving Average
ML	Machine Learning
NREL	National Renewable Energy Laboratory
PACF	Partial Autocorrelation Plot
PV	Photovoltaic
RECS	Residential Energy Consumption Survey
RMSE	Root Mean Suare Error
TWh	Terra Watt hour

SUMMARY

While in the United States centralized generation system and distribution network are the basis of the current electric infrastructure, the recent surge in uptake of solar photovoltaic (PV) systems introduces a new avenue to decentralize this system. Furthermore, PV systems can substitute the grid electricity and increase the share of renewable energy sources. While by 2018, five states in the U.S. (California, Hawaii, Nevada, Massachusetts, and Vermont) could reach a 10% threshold for the share of solar sources in generating electricity, at the country level this share is still less than 3%; whereas in some other countries, such as Germany and Japan, it has already reached more than 6%. This dissertation examines the diffusion of PV systems from three perspectives, addressing three gaps in knowledge: an empirical study of the diffusion of PV systems in Georgia, a method to estimate renewable rebound effect, and a framework to quantify the resilience capacity of an electric infrastructure system with emergency generators.

Three studies present the primary contributions of this research. *Study 1* examines the diffusion of PV systems in Georgia, identifies characteristics of adopters and patterns of adoption, and forecasts the future adoption of PV systems. *Study 2* introduces a new approach to estimate the direct rebound effect, subsequent of a major adoption of PV systems. *Study 3* presents a state-of-the-art framework that quantifies the resilience capacity of an electric infrastructure system with emergency electricity generators.

The main findings of the *first study* are: 1- median income, electricity rate, and percentage of the Green party voters have positive impact on the diffusion of PV systems in the residential sector, while percentage of Republican voters has negative impact, 2-

adoption of PV systems in the utility sector is in the third phase of diffusion (early majorities), while the residential sector is in the second phase (early adopters), 3- electricity rate, buildings with 10-19 units, and white race have the highest positive impact on selecting the size of a PV system, and 4- the future adoption of PV systems in the residential sector in Georgia for the next four years is estimated to increase by 300% in annual electricity generation, which reduces up to an additional 6,700 ton CO_2e per year. The main findings of the *second study* are: 1- through an econometric data-driven approach, a novel computational method is developed that estimates the direct rebound effect triggered by the future adoption of PV systems, 2- the proposed framework estimates a 5.8% rebound under a moderate diffusion of PV systems in Fulton county, which is equivalent to a 4.5 megawatt hour increase in annual electricity consumption, or an average of 3,300 ton CO_2e per year. The main finding of the *third study* is a state of the art resilience assessment framework, in which four dimensions of a resilient system are quantified, the contribution of emergency electricity generators to improve the resilience capacity is counted, and end-users are categorized by their types. The advantages of the proposed framework are presented through numerical examples.

The findings of the *Study 1* provide a benchmark for the future adoption of PV systems and highlight the impact of socio-economic and location-based factors in the diffusion of PV systems in Georgia. These findings can be used to shape a more effective policy, aiming to increase the share of PV systems, or to evaluate the effectiveness of a policy. The finding of the *Study 2* opens a new avenue to compute the rebound effect and can support development of a policy to mitigate the renewable rebound effect in a targeted region. The findings of the *Study 3* can help system designers to customize the design of a

resilient system based on its characteristics. The introduced framework can further be used to investigate improvement of the resilience capacity in an electric infrastructure system by increasing the penetration of PV systems, or other decentralized electricity generators in a region.

CHAPTER 1. INTRODUCTION

The United States generated more than 4,000 Terawatt hours in 2017 [1]. A vast majority of the electricity generated in the U.S. is from the centralized generation and distribution systems spread across the country. The electric infrastructure system in the U.S. consists of more than 6,413 power plants and provides electricity to more than 300 million people through approximately six million miles of high-voltage transition lines [2,3]. Despite the benefits of renewable energy systems, previous studies showed some potential economic, social and environmental consequences of achieving a targeted share of renewable energy [4–6]. However, without an accurate analysis of the diffusion, their positive and negative impacts cannot be thoroughly explored. While it may assume benefits of installed PV systems should be evaluated by computing the generated electricity by the PV system, as an one-to-one substitution of the grid electricity, previous empirical studies showed the adoption of PV systems results in an increase in electricity consumption, which is defined as the rebound effect [7]. Several renewable energy technologies, including rooftop photovoltaic (PV) systems are categorized as decentralized energy generation systems. This inherent characteristic of PV systems can change the existing approach to design a resilience electric infrastructure system.

1.1 Electricity Generation: Trend

During the past 40 years the electricity generation in the world increased from 6,298 TWh to 25,082 TWh, a constant 3.3% annual growth, except for one year between 2008 and 2009 due to the economic crisis [8]. In 2017, out of total 28.6 trillion kWh total consumed energy in the U.S, equivalent to 97.7 quadrillion British Thermal Unit (BTU),

37.2% was used to generate electricity, out of five main energy sources: natural gas, petroleum, coal, nuclear power, and renewable energy (e.g. hydroelectric power, solar, wind, geothermal, biomass) [9,10]. More than 60% of the electricity generated in the U.S. comes from fossil fuel sources, well understood to be the main source of carbon emissions. Figure 1 illustrates the annual net electricity generation by all sources in the U.S. and its annual growth rates from 1949 to 2017 [1]. Although in the US the annual electricity generation growth rate keeps declining in the past decade, the energy generated from solar sources has been increasing [11].

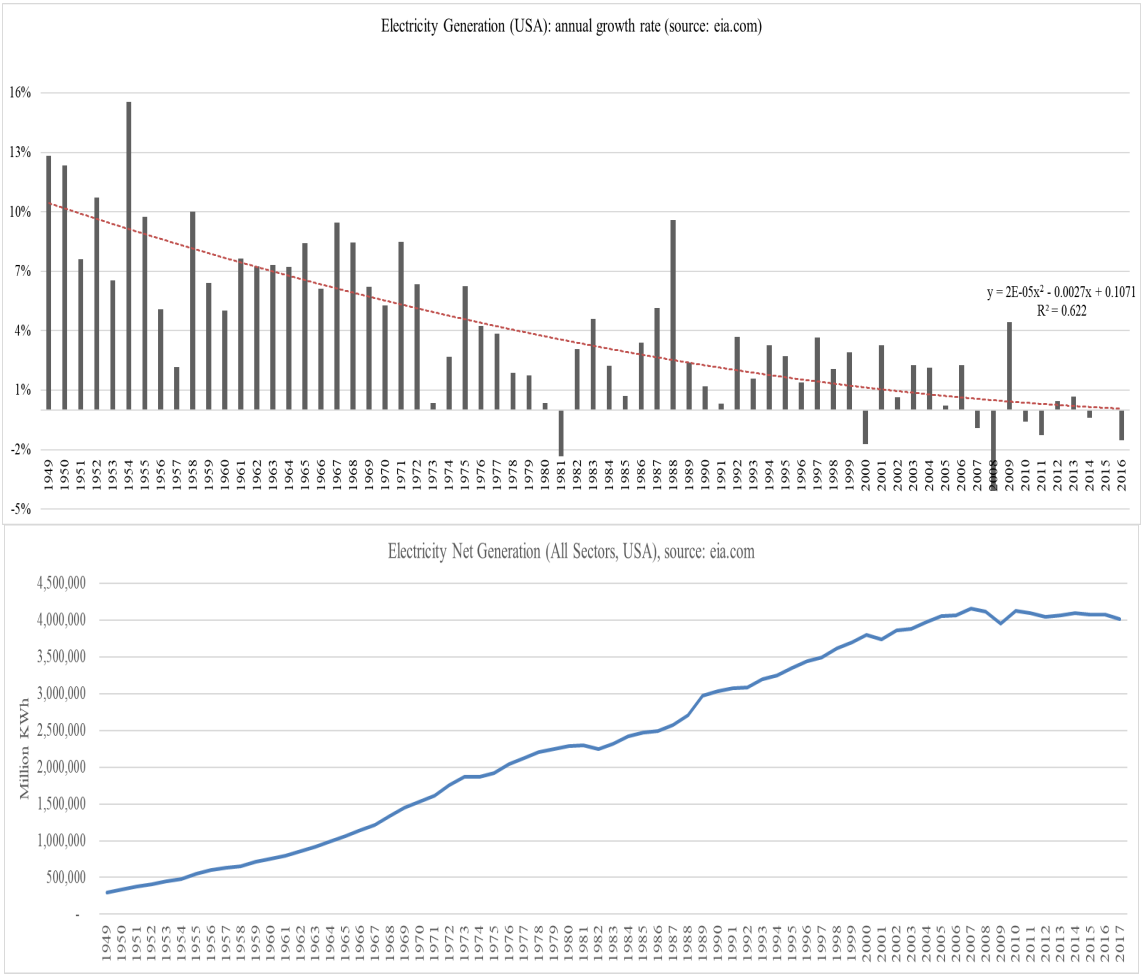

Figure 1 – Electricity generation in the USA: annual growth rate [11]**.**

1.2 Electricity generation: sources

In the U.S. the main source of energy for producing electricity is fossil fuels [1]. In 2017, natural gas and coal had a 60% share of the energy source for generating electricity in the U.S. [12] (Figure 2). In the same year, the share of renewable resources for generating electricity was 10%, and 2% for solar sources. PV system is one of the renewable energy generation systems that converts solar radiation to electricity.

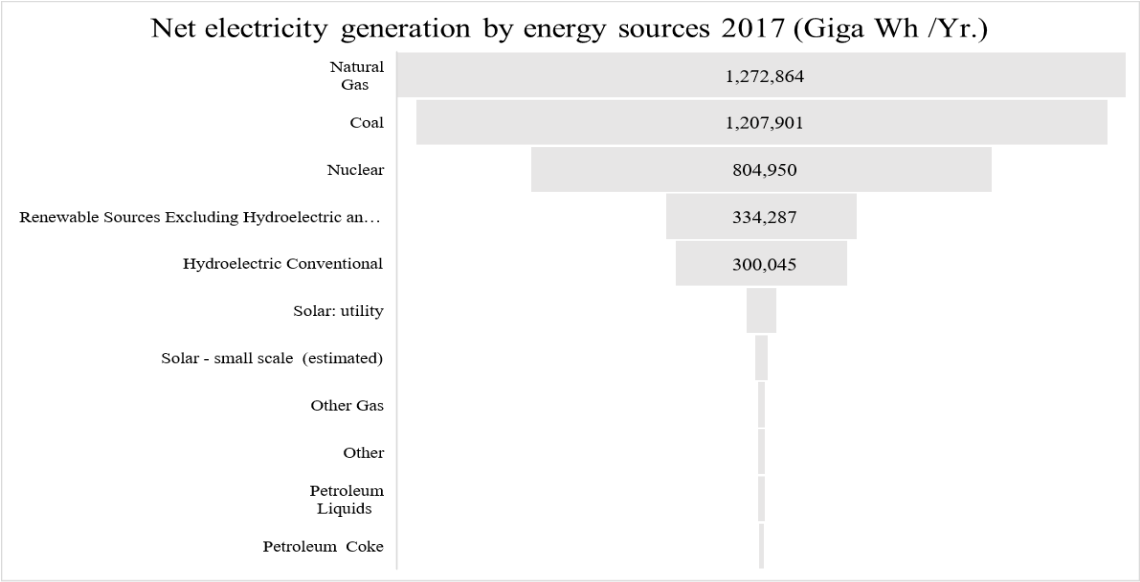

Figure 2 - Electricity generation by energy sources - USA 2017 [11]**.**

Figure 3 shows the annual growth rate of electricity generation from solar sources in the U.S. Among the reasons for this increase the most important ones are: decline in cost along with the improvement in the efficacy of the PV panels, increase of public awareness about global warming, and state and federal incentives. The cost of electricity generated by photovoltaic systems declined from $0.28 per kilowatt hour in 2011 to $0.06 in 2017, or a 79% reduction [13–15].

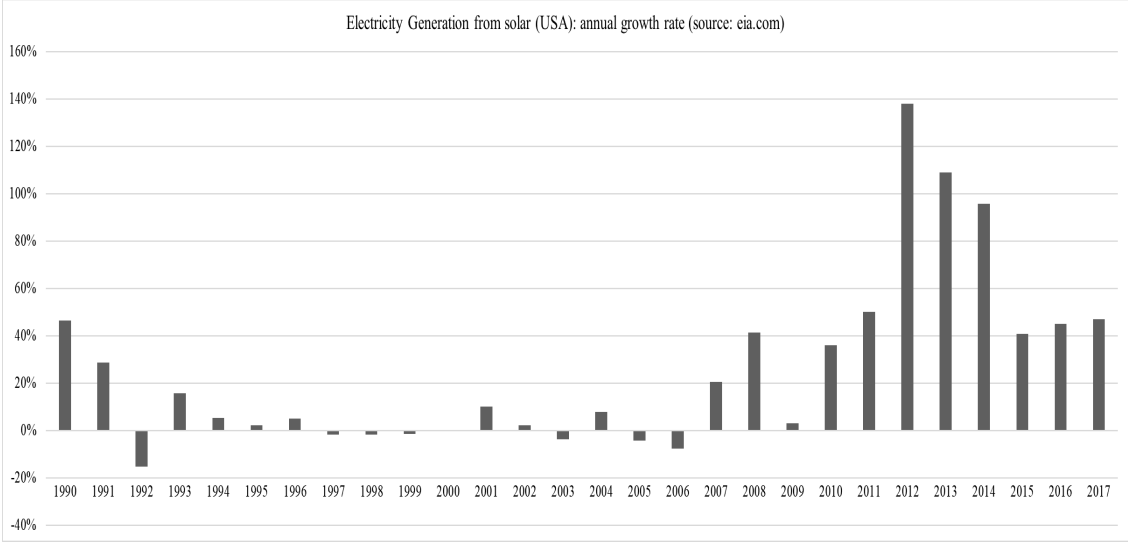

Figure 3 – Electricity generated from solar sources in the USA: annual growth rate [12]**.**

In the U.S., in terms of states with the highest aggregated capacity of the solar systems, California with annual capacity of 22,777 kWh per year has the highest rank and Georgia with 1,556 kWh per year is ranked 10th [16] (Figure 4). In 2018, the share of solar systems and other renewable energy sources in generating electricity was 5.1% in Georgia [17] (Figure 5).

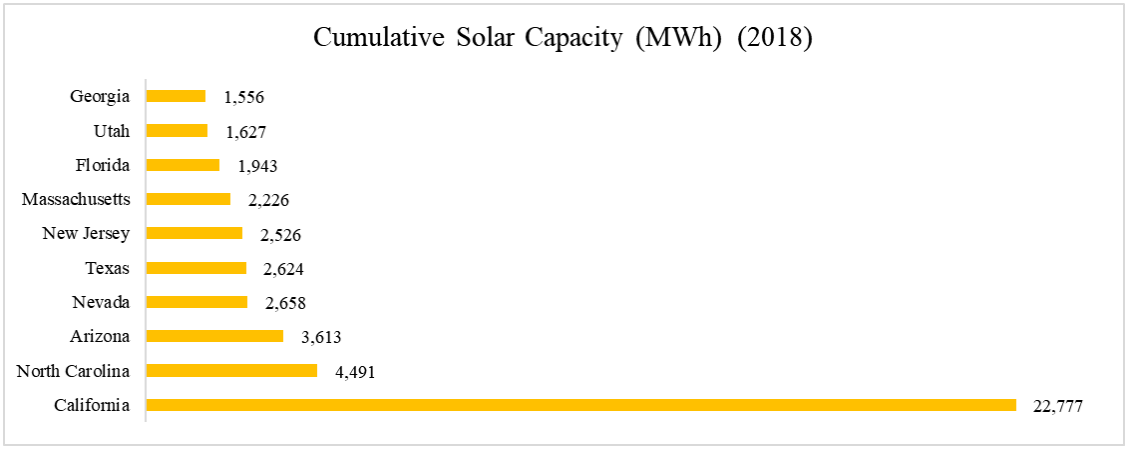

Figure 4 - Top 10 ranked states by cumulative solar capacity (kWh/yr.) [16]**.**

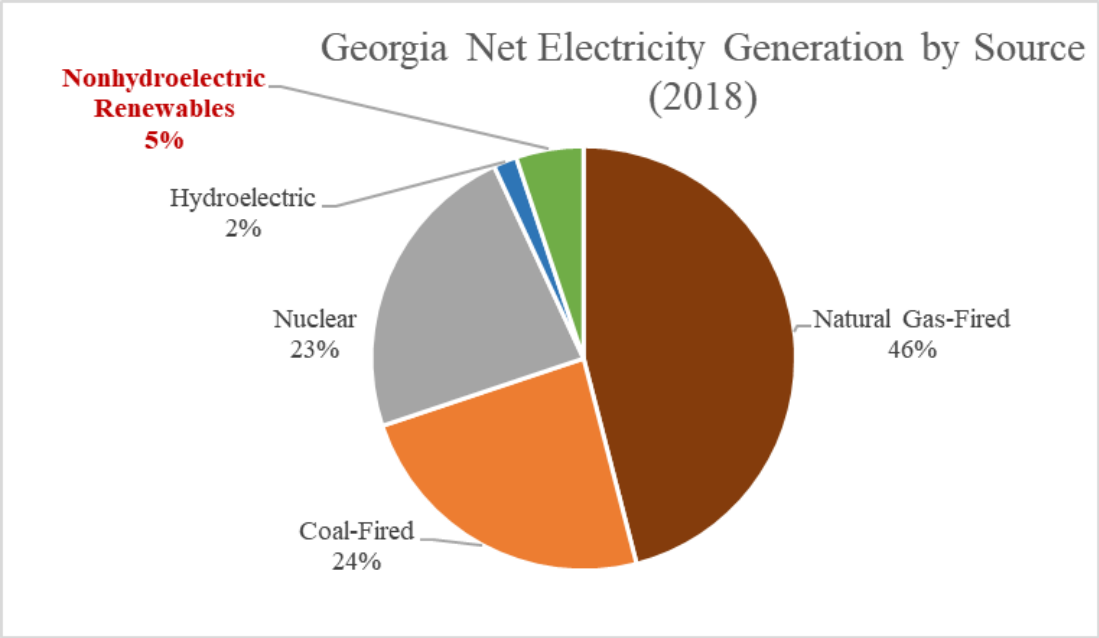

Figure 5 - Electricity generation by energy source: Georgia in 2018 [17].

1.3 Rebound Effect

The phenomenon of rebound effect explains how the perceived energy saving from adopting a more efficient system is not achieved, because of changing consumer behavior. This can occur directly by consuming a portion of saved energy or indirectly by spending money from the saved cost of energy on other products and services. Recent studies showed that the introduction of more energy efficient products such as vehicles, home appliances, and space heating and cooling systems, results in rebound effect, ranging between 1% to 87% [18]. Two major factors determining rebound effect are elasticity of demand expressed as responsiveness of demand to the price of a service or product, and the ability to substitute for other inputs [19–21]. Several intergovernmental organizations raised concerns about the negative effects of rebound effect on global sustainability [22,23]. To address this issue, several policy-driven suggestions are proposed, among which are reducing energy consumption, migrating to renewable energy generation technologies, and

increasing in environmental efficiency [24,25]. Past research suggested that the first step in developing a policy to deal with the issue of rebound effect is to identify its magnitude and targeted areas [26]. Ironically, the migration to renewable energy generation can also trigger rebound effect, as an empirical study on the adoption of PV systems in Australia has caused rebound effect ranges between 5.4% to 8% [7].

1.4 Resilience system

In the U.S., a range of hazardous incidents threat the electric infrastructure system, which can be categorized as natural disasters, physical attacks, or cyberattacks [27]. Two years after establishing a national policy on critical infrastructure security and resilience in 2013, the Department of Homeland Security (DHS) published a report addressing the concern on energy sector security and resilience as a guide to manage risks for the critical infrastructure systems industry [28,29]. In the DHS report of 2015, to enhance the security and resilience of electric infrastructure systems three federal priorities were set: 1- develop tools to enhance awareness of a potential disruption, 2- plan a coordinated response to the disruptive event, and 3- ensure an actionable intelligence communication on threats between government and industry [29]. This report also stated the goal of increasing infrastructure resilience to all-hazards with a list of required actions: enhance system design for resiliency, improve preparedness and mitigation measures, improve system response and recovery, and analyze and manage interdependencies among critical infrastructure systems [29]. In 2017, the Department of Energy (DOE) in a report to Congress evaluated U.S. energy security and summarized the undertaken efforts to improve energy security into five categories: 1-considering the economy impacts, 2-providing diversity and resiliency, 3-establishing both well-functioning and competitive markets, 4-

addressing the national security objectives, and 5- addressing environmental considerations [30]. It is clear that there is a need for a framework to evaluate the resilience capacity of an electric infrastructure system. Such a framework provides a mean for policy makers and system designers to evaluate the resilience capacity of a system prior to the occurrence of a hazardous incident. Furthermore, not only the introduction of renewable energy technology such as a PV system directly address as the environmental concerns, as expressed in the report of the DOE to congress in 2017, but also it can contribute toward improving the system resilience. However, it is crucial to consider the resilience aspect of PV systems, when installing them. Studies about the aftermath of recent hurricanes (e.g. Irma , Harvey, Maria) showed that while several PV systems could survive, they were not able to provide energy to customers because their design required them to connect to the main grid system [31].

CHAPTER 2. PROBLEM STATEMENT AND RESEARCH OBJECTIVES

2.1 Motivation and Gaps in Knowledge

Although the growth rate in electricity generation from solar systems (PV) in Georgia has been positive for the past decade, there is little knowledge about future adoption of PV systems. Furthermore, the adoption of the PV systems, despite its contribution to mitigate the negative effect of global warming, can affect the management of the balance between demand and generation of electricity. From the economic perspective, since the source of the energy for a solar system is the sun radiation, in the long term, it introduces a cheaper source of electricity to consumers compared with the grid electricity as the primary source of electricity. This introduction of a cheap energy source can lead to a rebound effect. In economic theory rebound effect is the reduction in gains from the adoption of a technology with higher efficiency. Translating this to the area of renewable energy technology, in the long term the lower cost per unit of electricity compares with the rate of grid electricity – the conventional electricity provider – creates the potential for renewable rebound effect. Renewable rebound effect is the increase in electricity consumption because the PV systems provide the electricity at a lower rate.

Moreover, decentralized emergency electricity generators, including PV systems can contribute to improving the system resilience capacity by delivering service (electricity) directly to the end-nodes during a shutdown of the primary electricity provider due to a mishap. The widespread U.S. electricity system, with more than 6,000 power plants and

six million miles of high-voltage transmission lines, supports the well-being of more than 300 million customers and economic growth. Hence, it is crucial to maintain a reliable and sustainable flow of electricity at all times. Since it is neither feasible nor practical to design a system to resist against all threats and risks, the federal government emphasized on the resilience concept. While the governmental published guidance and suggestions emphasized on improving the resilience capacity of the electric infrastructure systems, the contribution of PV systems to improve resilience capacity of an electric infrastructure system has not yet been addressed [32–36].

Neither of the mentioned areas have yet been explored thoroughly. These gaps in the current state of knowledge may result in an unclear assessment of future adoption of the PV systems, inaccurate estimate of the demand after the adoption of the PV systems, and undermine the contribution of the PV systems to improve the resilience capacity of an electric infrastructure system.

2.1.1 The diffusion of the PV systems in Georgia.

Currently, solar systems in Georgia have only 2% share of electricity generation by source, PV systems have a potential to increase the share of solar energy in generating electricity. The current state of knowledge in future adoption of the PV systems in Georgia is minimal. An assessment on the current and future state of the diffusion of the PV systems requires a multi-step analysis of the historical data of the installed PV systems. At the state level, a quantitative analysis is required to link the socio-economic and location-based features to the current adoption of the PV systems. In addition, spatial assessment methods are required to analyze the current state of this adoption from the geographical perspective

and identify any existing patterns. Developing a forecasting model is needed to generate a benchmark for the future adoption of the PV systems in Georgia.

2.1.2 Renewable rebound effect

Introducing a new technology that reduces the cost of a service or good either by improving the efficiency or change the needed resources at a lower cost, can increase the demand, known as the rebound effect. While the rebound effect is a well-known phenomenon in the economic field, first introduced by Jevons in 1865, just recently some empirical studies found that the rebound effect triggered by the adoption of PV systems, a renewable electricity generation technology [7,37,38]. In the current state of knowledge, no econometric framework exists to estimate the renewable rebound effect.

2.1.3 Quantitative approach to examine the resilience capacity of an electric infrastructure system enhanced with PV systems.

Among the definitions of the resilience and its required elements, a well-cited definition introduced fours dimensions of resilience [32,39,40]: robustness, redundancy, resourcefulness, and rapidity. However, existing resilience metrics emphasize on overall system performance to quantify the resilience capacity of a system, without quantifying the resilience dimensions. This gap in knowledge leads to an unclear evaluation of system resilience in each of the mentioned areas. Furthermore, the existing methods do not differentiate among end-users type, which results in an inaccurate evaluation of resilience capacity for a system such as an electric infrastructure system, which supports a range of customers from other critical infrastructure systems to ones in the residential sector. Finally, existing resilience metrics only identify permanent service providers as their inputs

for evaluating the resilience capacity. This results in ignoring the contribution of emergency electricity generators, including PV systems, to improve resilience capacity. The mentioned gaps in knowledge lead to inaccurately estimate the resilience capacity of an electric system.

2.2 Research Objectives

Referring to the declared gaps in the current state of knowledge, this dissertation is aimed at analyzing the diffusion of PV systems from two perspectives: existing PV systems, and future adoption of PV systems.

2.2.1 Research objective one: analysis the uptake of PV systems in Georgia, past and future

The first research objective addresses the first gap in knowledge, the adoption of PV systems in Georgia. This study divides this objective into two perspectives; each represents a separate period for the adoption:

Perspective 1- study the installed PV systems: identifying the possible impact of socio-demographic and location-based factors on the adoption of the PV systems in Georgia, exploring the historical data of the installed system.

Perspective 2- study future adoption of PV systems in Georgia: employing time series analysis to identify and characterize the historical data of the installed PV systems in Georgia and developing a forecast model to estimate the future diffusion of the PV systems; and developing a predictive model employing machine-learning techniques to forecast future adoption of PV systems. The result of this study provides a benchmark for

the state agencies and policy makers and helps them to compare the outcome of an incentive or a policy with the business as usual scenario. Furthermore, it assists utility companies to prepare their distribution management system for feed in electricity in case of implementing a Feed-in-Tariff (FiT) policy.

2.2.2 Research objective two: develop an econometric framework to assess the renewable rebound effect.

The second research objective addresses the second gap in knowledge by developing a data-driven econometric framework to estimate the rebound effect of PV systems, as a renewable energy generation technology. The proposed approach employs multi-stage data-driven methods to extract the required information and then through an econometric framework estimates the renewable rebound effect. This econometric data-driven framework assists utility companies and policy makers to estimate the rebound effect results from implementing renewable energy generation systems such as PV systems, prior the adoption occurs. Not only employing the proposed framework help the utility power management system to balance demand-supply, but also it helps policy makers to estimate more accurately the benefits of adopting PV systems.

2.2.3 Research objective three: develop a framework to assess resilience capacity of a system with the temporary service providers.

Due to the third gap in knowledge, identified and explained above, the third research objective of this dissertation aims to develop a framework, which quantifies the four dimensions of resilience of an electric infrastructure system, and is capable of incorporating the contribution of emergency electricity-generator systems, including PV systems.

Furthermore, this framework differentiates between end-user types in its computation of resilience capacity. The outcome of this objective provides policy makers and system designer a new approach to examine the resilience capacity of an electricity infrastructure system. Furthermore, another application of the proposed framework is to identify strengths and weaknesses of a system at its each resilience dimension.

2.3 Research Methodology

The goal of this dissertation is to address the three research objectives presented above. This section presents the research methodology for each objective briefly, and later in the corresponding chapters, they are discussed more in detail.

To address the first research objective, the adoption of the PV system in the state of Georgia, first the required historical datasets are collected and multiple data preparation techniques including merging and filtering are applied to make them ready for the analysis in the next steps. A comprehensive literature review was conducted to identify the explanatory variables. Two models are developed to answer two hypotheses, in which they assess the impact of explanatory variables (e.g. political affiliation, socio-economic, physical buildings, solar radiation, electricity price) on the uptake of PV systems in the residential sector and selection of the PV system size. Two statistical tests are run to assess the two hypotheses. Special analyses, employing two methods, then examine patterns of PV system diffusion in three sectors: utility, non-residential, and residential. The first method, directional distribution, examined the overall pattern of diffusion, and the second method, univariable Moran's I cluster analysis, investigates the existence of clustering evidence. An univariable time-series analysis technique is employed to develop a time

series model in the following three steps. The first step identified the characteristics of the historical data. In the second step, based on the identified time series characteristics, a univariate time-series forecasting models are developed employing the autoregressive integrated moving average (ARIMA) technique. In the third step, residual analysis technique assessed the results. Finally, two machine-learning techniques are employed to develop two predictive models for the uptake of the residential PV systems. An extension of the explanatory variables and historical dataset of the installed PV systems in the first analysis formed the sample for the training and test sets.

To address the second objective of this dissertation, first a comprehensive literature review is conducted, and an econometric model is developed based on existing definition of direct rebound effect. A data-driven approach is employed to compute or extract each input of this model, including electricity consumption, income level, electricity rate, and electricity generated by PV systems. To estimate electricity consumption, a regression-based model is developed that predicts electricity consumption by socio-economic and location-based explanatory variables. A geographic information system (GIS) based simulation model is developed to compute potential solar radiation. The proposed framework then estimates the renewable rebound effect in Fulton County resulting from the adoption of PV systems under two scenarios: moderate and aggressive. The results of this estimation are compared with the existing empirical studies on renewable rebound effect.

To address the third research objective, first through a comprehensive literature review the existing resilience definition and metrics are identified. A resilience framework is then developed based on existing definition of the four dimensions of resilience:

robustness, *redundancy*, *resourcefulness*, and *rapidity*. The literature review was also employed to categorize end-users by their type. The proposed formulation for the quantification of the four dimensions of resilience incorporates the end-user type and emergency electricity generators including PV systems. Through two numerical examples, the resilience capacity of an electric system under a range of scenarios is assessed and advantages of the proposed framework are compared with the previously proposed metrics.

2.4 Thesis Structure

The adoption of a sustainable technology is the focal point of the three objectives in this paper. The first objective examines the diffusion of PV systems in Georgia via four main assessment means: 1-statistical to evaluate the impact of a range of explanatory variables on the adoption of PV systems, 2-spatial to assess and explore existing patterns in the installed PV systems, 3- time series to identify characteristics of historical dataset of installed PV systems in Georgia and forecast its future adoption, and 4-machine-learning to develop a predictive model for the update of PV systems in the residential sector. Then through a data-driven approach, an econometric framework is presented to estimate renewable rebound effect results from the adoption of PV systems. The last objective of this dissertation, not only present a new quantitative framework to assess the resilience capacity of a system, but also it merges the two knowledge areas of resilience system and sustainable technology by incorporating the contribution of PV systems to improve resilience capacity.

This dissertation is structured as follows. Chapter two presents three problem statements and the research objectives of this thesis. Chapter three addresses the first

research objective, in which, historical dataset on the diffusion of the PV systems is analyzed and characterized to develop the expressed models and predict the future adoption of the PV systems in Georgia. Chapter four covers the second objective of this dissertation. In this chapter, to estimate the renewable rebound effect, a data-driven econometric framework is introduced, and through a case study of Fulton County in Georgia, the proposed framework estimates the renewable rebound effect for a future adoption of the PV systems under two scenarios. Chapter four presents a resilience metric framework, that assesses the resilience capacity of an electric infrastructure system with temporary emergency electricity generators such as PV systems. Chapter five concludes this research and suggest future works and extensions of the proposed frameworks and assessments. Figure 6 illustrates the relationship of the chapters.

2.5 Contribution and Significance

Increasing the share of renewable energy sources in electricity generation not only reduces GHG emission, but also has long-term economic and social benefits. Evaluating the significance of a policy aims to induce consumers to utilize PV systems requires a benchmark for the future adoption of PV systems, representing the business as usual scenario. Moreover, the role of consumers is an important input for assessing the outcome of a policy. From the perspective of the utility companies and the grid management system, knowing the geographical pattern of the currently installed PV systems helps to prepare the required infrastructure to manage the supply-demand balance in the case of implementing a FiT policy. Furthermore, the estimate of the renewable rebound effect for the future adoption of the PV system increases the accuracy of the future demand prediction. This study investigates the profile of the consumers of the PV systems in

Georgia. Multiple approaches are employed to assess the significance of the relationship between installed PV systems and explanatory variables (e.g. socio-economic, built environment, physical structure, solar radiation), to identify existing patterns of the installed PV systems, and to estimate the future adoption of PV systems in Georgia. While recent empirical studies showed the rebound effect resulting from the adoption of PV systems, this study introduces a data-driven econometric framework to estimate the renewable rebound effect.

The other significant innovation of this study is the proposed evolutionary framework to assess the resilience capacity of an electric system. The proposed framework quantifies four dimensions of resilience, incorporates contribution of the decentralized emergency electricity generators, including the PV systems, to improve the resilience capacity of the electric infrastructure system. Furthermore, the proposed framework introduces a new approach to quantify the resilience capacity by separating the end-users by type.

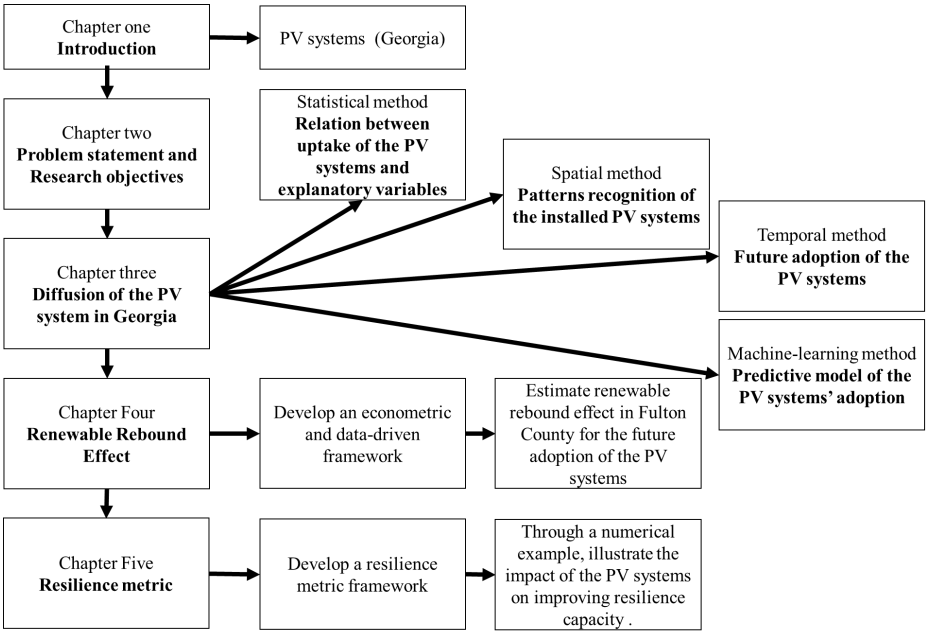

Figure 6 – Thesis structure.

CHAPTER 3. DIFFUSION OF PV SYSTEMS IN GEORGIA: PAST AND FUTURE

3.1 Introduction

Forecasting the future adoption of PV systems in Georgia provides a benchmark to compare the outcome of a policy or an incentive program. Furthermore, it guides utility companies to prepare the electric infrastructure management system in case of implementing a Feed-in-Tariff (FiT) program. FiT is a mechanism that allows investors and individuals to install PV systems at a lower cost by providing a monetary reward for the generated electricity [41]. When the utility company purchases a portion of the electricity generated by the PV system, the fed electricity to the grid system changes the resource-demand balance, known as solar intermittency. From a second perspective, with respect to the historical dataset of installed PV systems, to study the diffusion and recognize its spatial pattern have its merit in policy and the marketing fields. It reveals the effect of socio-economic and location-based factors on the adoption of PV systems and helps to recognize the concentration of systems in geographical basis.

This study departs from the existing body of knowledge by 1- introducing a four-step assessment framework, in which the analysis of the adoption of the PV systems is assessed from four perspectives, each employs an analysis method (e.g. statistical, spatial, temporal, machine-learning); and 2- this assessment is unique in its kind in the state of Georgia. From the time perspective, research objectives of this chapter are divided into two categories, each focusing on a separate timeline of adoption:

1. The installed systems

   Two meta-data analysis methods assess the historical data of installed PV systems in Georgia. This part aims to identify and observe the major factors affecting the diffusion of PV systems in the residential sector, and explore any existing patterns in installed PV systems on three sectors: residential, non-residential, and commercial. Statistical and special techniques are employed.

2. The future adoption of PV systems

   The goal of this section is to forecast the adoption of PV systems in Georgia. At the state level, a forecasting model is developed to estimate the future adoption of PV systems, and at the census tract level, a forecasting model is developed to predict the probability of each census tract to adopt at least one PV system. Two analysis techniques are employed to address these goals: time series analysis and machine-learning methods.

To achieve these objectives, the remaining of this chapter is organized as follows. After a brief literature review, the proposed research approach and steps are expressed in section two. Section three presents the dataset of installed PV systems in Georgia. Section four presents the result of four analyses, followed by a discussion presented in section five, and section six presents the concludes.

3.2 Literature Review

3.2.1 Background on solar policy in Georgia

While there is a federal tax return incentive, that covers up to 30% of the installation cost of the PV systems in the residential and commercial sectors, at the state levels the

policies and incentives vary [42]. California passed a law mandating the installation of the PV systems for newly built houses, while some other states such as Arkansas and Wyoming currently do not have a particular incentive program toward the adoption of the PV systems [43]. In Georgia, there is one statewide policy, the "Solar Power Free-Market Financing Act of 2015", that allows purchase of the electricity generated by the PV systems, that are financed by a third party, from residents and businesses [44]. At the local level, there are some incentive programs for the installed PV systems, including the "Solar Buy Back" program by the Georgia Power utility company, "Green Power" incentive program by the TAV authority, "Right Choice Sun Power" rebate program by the Jackson EMC utility company, and "Solar Photovoltaic" program by the Gray Stone utility company Rebate Program [45–48].

3.2.2 Factors impacting diffusion of PV systems

Following the work of Hagerstrand (1952) and Rogers (1962) on diffusion of a technology, as the first perspective to the adoption of PV systems, this thesis examines the factors influencing the diffusion of PV systems as a sustainable energy technology [49,50]. While past studies divided these factors into two main categories, psychological and social, an extension of their work adds location, built environment and physical based factors [9,51]. The psychological factors include perceived cost, positive and negative feelings about the technology, procedural and disturbance fairness, and trust[51]. The social factors are summarized into three main groups: socio-political, community, and market acceptance [9]. While several studies focus on economical parameters on the diffusion of the renewable energy technologies [52], some recent studies include demography, behavioral, and economic factors in modeling the adoption of the renewable energy technologies [53–

55]. In previous studies, through a statistical methods, a range of demographic and location parameters are picked to estimate the adoption of the PV systems, including ownership, housing unit type, mortgage rate, age, unemployment, density, race, political party, income, education, and population [56–59]. Early studies showed that environmental concern and saving money are the main reasons for adopting the renewable energy generation systems [60]. Later studies showed the role of socio-economic factors on uptaking the PV systems including income, number of bedrooms, number of households, education[56,58,61].

While in the previous studies, the results of employed statistical methods showed a link between environmental location and demographic factors, and the adoption of PV systems in the residential sector, in this area the literature is still growing. Sommerifeld et. al. (2016) identified 15 demographic and location factors and assessed their relationship with the adoption of the PV systems in the residential sector in Australia [58]. A study in Germany by Schaffer and Burn (2015) showed solar radiation, house density, homeownership, per-capita income, and neighborhood-effect have the highest impact on the adoption of the residential PV systems [62]. Another study in Germany showed low household income and rental occupations are the main barriers for the adoption of the residential PV systems [61]. A study in Sri Lanka, employed spatial method to assess the influencing factors on the adoption of PV systems [63]. Gooding et. al. (2013), through spatial method, introduce a prediction method for the adoption the PV systems in seven cities of UK by developing an indicator [56]. The input variables of their proposed indicator are: physical capacity (solar radiation) and socio-economic factors. Richard Snape (2015) employed spatial assessment technique to assess the socio-psychological drivers of the PV systems' adoption in the UK [64]. In the U.S., Rai et. al. (2016) showed in the northern

area of California, financial returns and operation cost, including maintenance cost, are the main determining factors for the adoption of the PV systems, and peer effect and installers are among the other influencing factors [53]. Calvin Kwan (2012) assessed influence of 25 socio-economic, political party and local environment of spatial distribution of the residential PV systems in the U.S., and found the following variables have the highest p-value, indicating the statistically significance positive influence on the count for the installed PV systems: amount of solar insolation received, cost of electricity, amount of financial incentives, median home value, proportion of population with median household income between $25,000-$100,000, proportion of population with at minimum a college education, proportion of population that are white, Hispanic Latino, or registered democrats [65]. Wolske et. al. (2017) showed in California, Arizona, and New Jersey household constraints, such as age, income, gender, income, and education, can influence the uptake of the residential PV systems [66].

3.2.3 Spatial analysis

While the proposed statistical method illustrates the relationship between the uptake of residential PV systems and expressed explanatory variables in five categories, it lacks in showing a potential pattern or a potential clustering of the installed PV systems. Diffusion of PV systems is inherently a dynamic process with a geographical vector assigned to each system. As a result, it exhibits spatial patterns over time. Such a pattern in diffusion is not limited to the PV system technology, and the initial studies on the diffusion of technologies showed that adoption has a centrifugal form and wave-like pattern [67]. Previous studies employed spatial methods to investigate the adoption of the residential PV systems [63,64,68–73]. These studies are categorized into two main groups:

the ones that analyze the spatial pattern of the existing installed systems, and the ones that examine the potential solar radiation and environmental factors for the future adoption of the residential PV systems.

The spatial analysis of the installed PV system links the geographical information to the analysis of the adoption of the PV systems. Vimpari and Junnila (2017) through spatial analysis of 25 European capital cities showed that the rooftop PV systems are more profitable in a denser area [73]. In the U.S., Noll et. al. (2014) investigated the peer effect on the adoption of the residential PV systems and showed, compare with traditional statistical methods, that the spatial analysis method has an advantage in showing the influence of neighborhood and socio-demographic characteristic of the communities in assessing the adoption of the PV systems [74]. Graziano and Gillingham (2015) employed spatial analysis method to investigate the influence of neighborhoods and built environment on the adoption of the PV systems in Connecticut [59]. The results of their study showed the peer effect and how it fades as the distance increases, and housing density and the share of renters decrease the adoption and higher income increases it.

3.2.4 Temporal analysis

Adoption of PV systems in Georgia is auto-correlated time series data, and its major characteristics can be identified and used for its future forecast. The two main categories of forecasting models are causal models and time series models. Causal models forecast a dependent variable using independent (explanatory) variables. While this method has been widely used in a range of applications, to accurately predict the dependent variable depends on the ability to quantify and predict the explanatory variables. Because too many factors

can influence the demographic variables, and these variables have correlation with the adoption as the impact factors, prediction based on them as explanatory variables may not be feasible. The time series method, on the contrary, determines the future values of the feature based on its historical record. A univariate time series forecasting model identifies characteristics of a variable by analyzing its historical record and predict its future values according to those identified characteristics and past observations. This method only requires one variable to develop and calibrate the model. The capabilities of the univariable time series forecasting method makes it suitable to utilize for the prediction of the PV systems' adoption, considering the available historical dataset.

In the past, time series analysis methods were employed to examine the historical dataset on installed PV systems, identify its characteristics, and then develop a forecasting model to estimate the future adoption of the PV systems. While time series analysis is widely used in other fields such as finance and economy [75,76], its application in the field of renewable energy forecasting has only more recently been explored. Time series analysis techniques have been employed to examine and predict the performance of PV systems, and the common technique the authors of those studies employed to build the forecasting model is autoregressive integrated moving average (ARIMA) [77–81]. While there are more complex methods available to form a forecasting model, ARIMA is a good choice when the goal is just to forecast a parameter. In summary the process of developing a forecasting model, employing the time series technique in those papers is as follows. First, the sample data is assessed to identify the main properties of the feature subject to the assessment, including autocorrelation, stationarity, and seasonality. Second, characterizing these properties, the sample data is fitted into three models, each representing its

corresponding sector. Third, for each model, the residual test is run to analyze the underlying conditions. The last step is testing the applicability of the model by the goodness-of-fit test.

3.2.5 Machine-learning techniques

In recent years, machine-learning (ML) techniques, as a subset of artificial intelligence, are becoming useful as an alternative to conventional techniques for modelling, identification, optimization, prediction, forecasting, and control of complex problems. In the field of renewable energy, ML techniques are employed to estimate the size of a PV system [82], forecast the solar radiation [83,84], and predict the generated electricity via a PV system [79,85–88]. Abuella and Chowdhury (2017) employed random-forest ensemble learning method and support-vector machine (SVM) forecasting model to estimate the output of a PV system. Their model is trained by historical dataset of weather condition (i.e. 14 variables, including cloud cover, precipitation, heat index, and wind speed) and PV outputs. Their model could estimate the output of PV systems with the accuracy of random mean square error (RMSE) equal to *7.2%* [87]. Ahmad et. al. (2018) after comparing ML methods, concluded to predict solar thermal energy tree-based methods – decision tree and random forest, have the highest accuracy, with RMSE range between *6.87%* and *7.12%* [88]. A study by Wang et. al. (2018) showed among ML techniques, random forest also predicts the building energy consumption with a higher accuracy rate [89].

3.3 Dataset

The scope of the studies presented in this chapter is Georgia at the macro level, and its micro-boundaries are the U.S. Census tract and block-group, and County are the selected boundaries. County boundary, due to the availability of presidential election results at this level, is the micro-boundary for analyzing the impact of political affiliation on the uptake of PV systems. For both statistical and machine-learning analysis, the Census tract and block-group boundaries are selected to examine the impact of socio-economic, solar radiation, electricity rate, and physical building features on the uptake of PV systems. The datasets for this study are collected from multiple sources. The uptake of PV systems is extracted from a historical dataset, provided by the Southface organization, and contains the information about the installed PV systems in Georgia since 1999 (Figure 7). For each installed PV system, the following information are recorded: installation completion date, annual generated electricity, capacity, location (longitude and latitude), and sector (residential, non-residential, and utility).

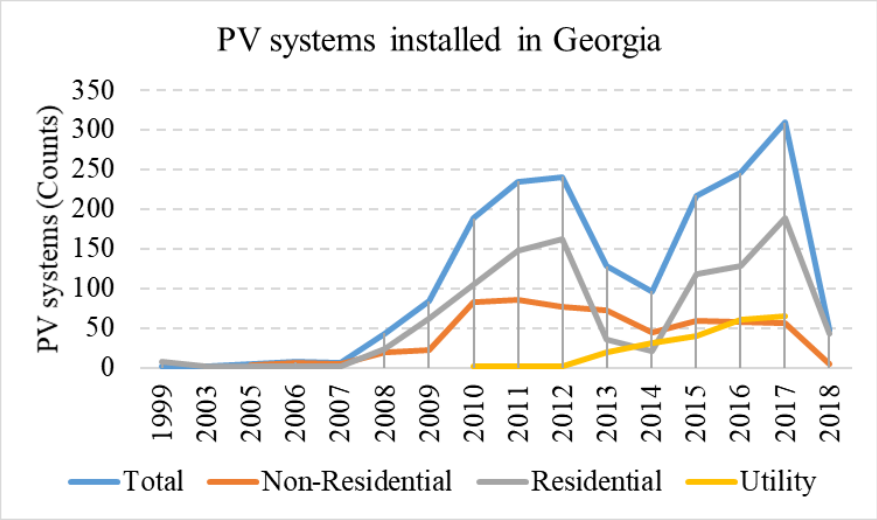

Figure 7 - Installed PV systems in Georgia: residential, non-residential, and utility. [90].

The socio-economic variables, including income, age, race, and education are extracted from the U.S. census. The built-environment and physical-structure information extracted from extracted from the 5-years estimate American Community Survey dataset published by the U.S. Census Bureau. In 2012, the National Renewable Energy Laboratory (NREL) published a state wide, low-resolution solar-radiation map of the U.S., which is used to extract the average solar radiation at the census tract level(Figure 8) [90–92].

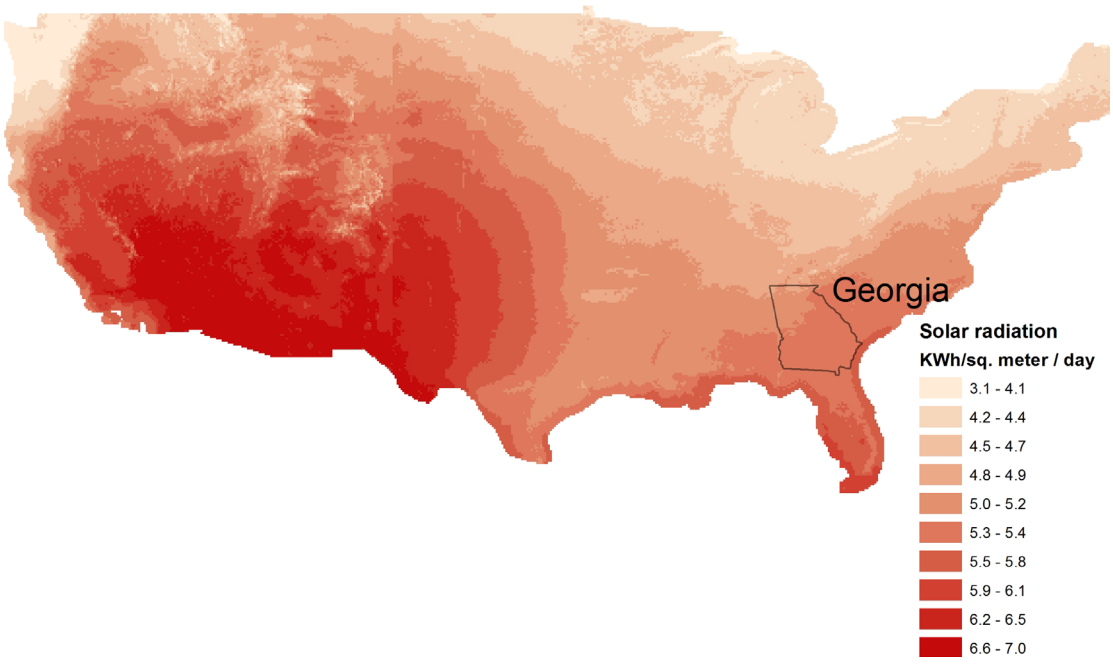

Figure 8 - Solar radiation map, USA [92]**.**

The potential solar radiation in Georgia ranges between 4.7 and 5.5 kWh per square meter per day (Figure 9). Information on the electricity rate is extracted from the published dataset by NREL and EIA.

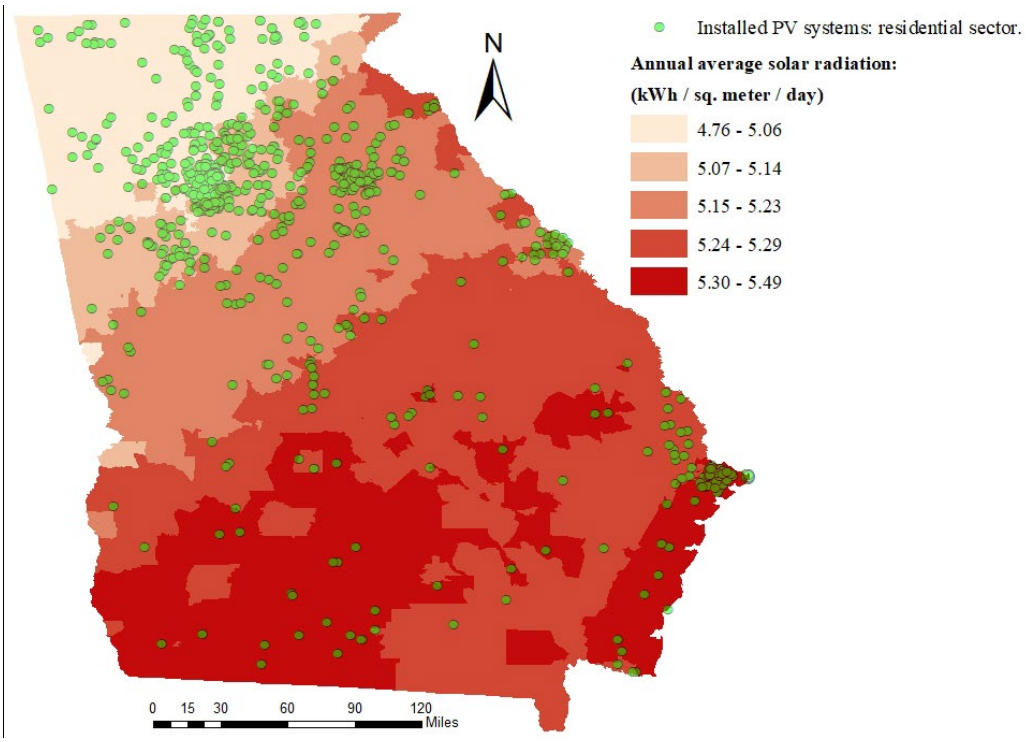

Figure 9 - Potential solar radiation: Georgia [90,92]**.**

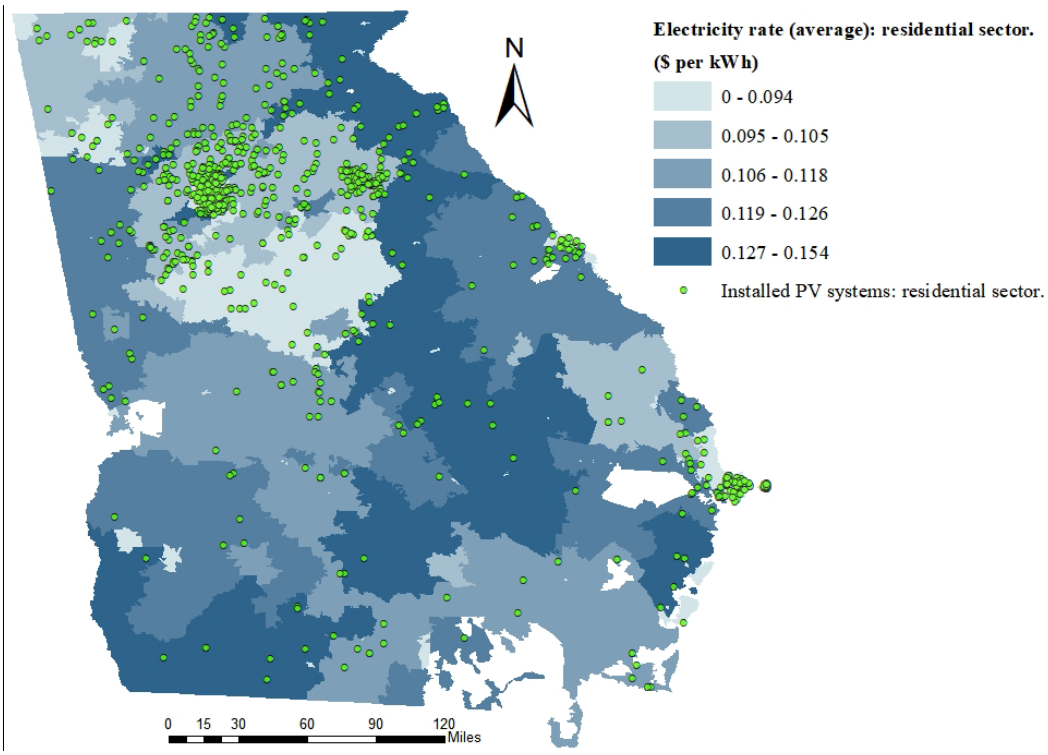

Figure 10 - Electricity rate [90,93]**.**

3.4 Results

3.4.1 Statistical analysis

To examine the relation between the explanatory variables and the adoption of PV systems in the residential sector, two models were developed. Annual generated electricity (kWh per year) by PV systems in the residential sector represents the uptake of PV systems as the dependent variable for both models. The first model examines the impact of political party affiliation on the uptake of PV systems at the County level – micro-boundary. The second model examines the impact of explanatory variables in socio-economic, solar radiation, electricity rate, and physical building categories on the uptake of PV systems in the residential sector. The micro-boundary of the second model is set to the Census block-group level. Georgia is divided into 159 counties, 1969 Census tracts, and 5530 Census block-groups.

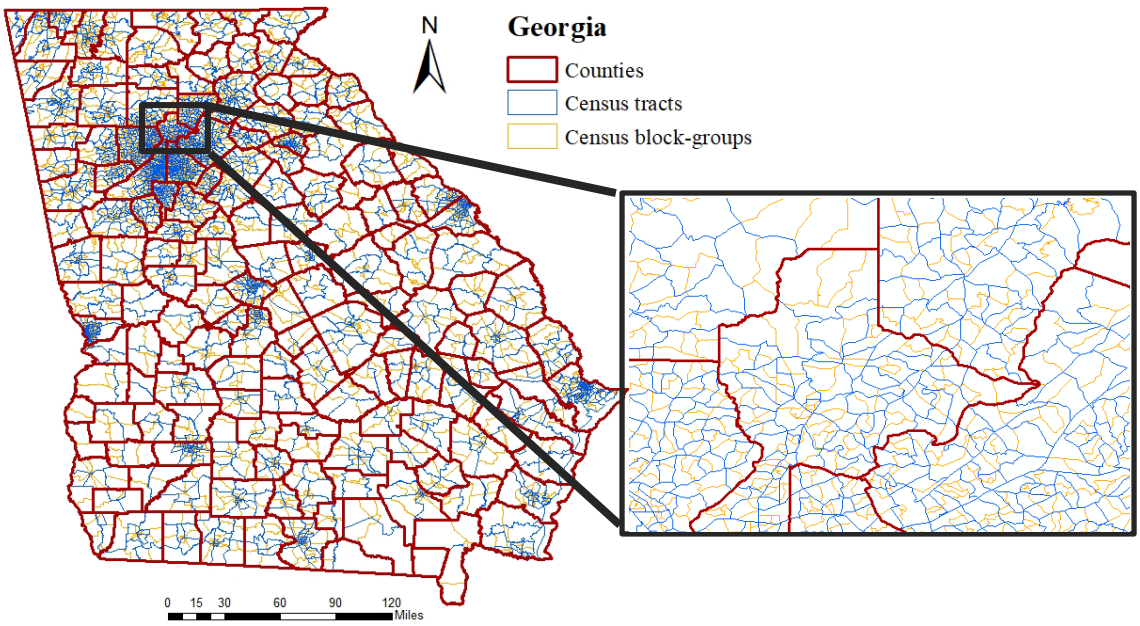

Figure 11 - Boundaries: Counties, Census tracts, and Census block-groups.

3.4.1.1 Model 1

Figure 12 and Figure 13 illustrate a visual representation of the explanatory variables in the first model.

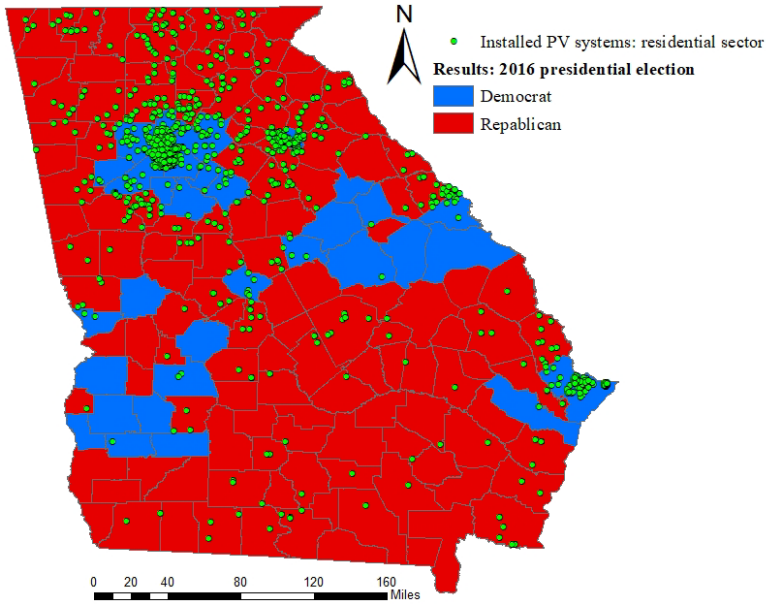

Figure 12 - Results of 2016 presidential election and installed PV systems.

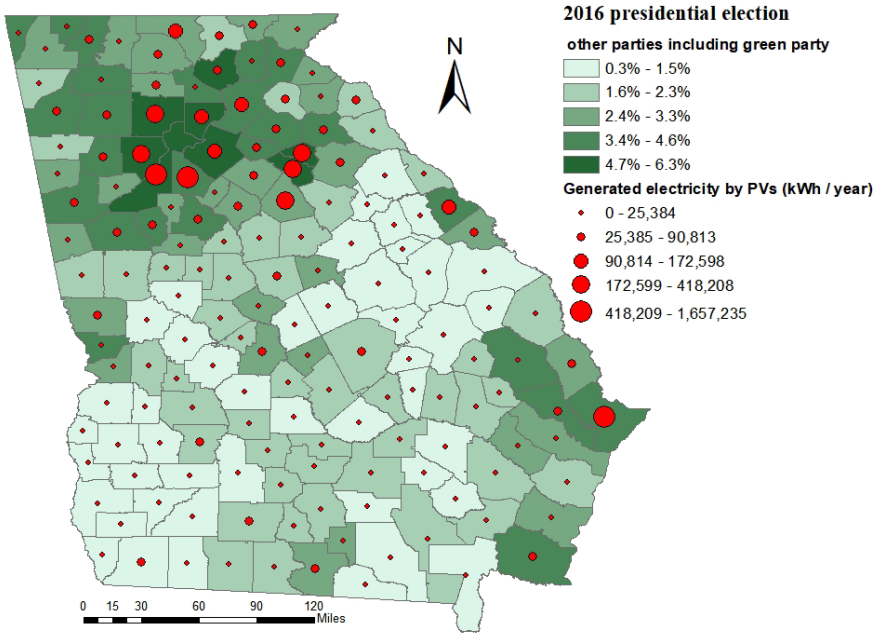

Figure 13 - Results of 2016 presidential election: other parties including green party.

Table 1 presents a summary of the input variables in the first model. Figure 14 is a graphical representation of 2016 presidential election results as the percentage of votes by the parties and the aggregated generated electricity by PV systems at County level suggest there can exist a correlation between these two variables. A logarithmic transformation is applied for a better illustration of variables. Figure 14 suggests there exist a postivie correlation between the counties with a higher percentage of voters affiliate with other parties, including the Green party, and the aggregated annual electricity generated by PV systems in the residential sector. Furthermore, there exists a negative correlation between the counties with higher voters of the Republican party and the aggregated annual electricity generated by PV systems in the residential sector. While the scatter plot shows a positive correlation between a higher percentage of voters in the Democratic party and the uptake of the PV systems, the low p-value suggest such a correlation is not significant.

Table 1 - Statistical analysis 1: variables.

Category	**Variable**	**Min**	**Max**	**Median**	**# of winning counties**
Explanatory variables	Voting results				
	Republican	13.5%	88.8%	67.6%	128
	Democratic	9.8%	30.6%	83.6%	31
	Independent	0.0%	0.1%	0.8%	0
	Others	0.3%	2.0%	6.3%	0
		Min	**Max**	**Median**	**# of counties with minimum 1 PV system**
Dependent variable	Annual generated electricity (kWh / year)	148	1,657,235	12,300	108

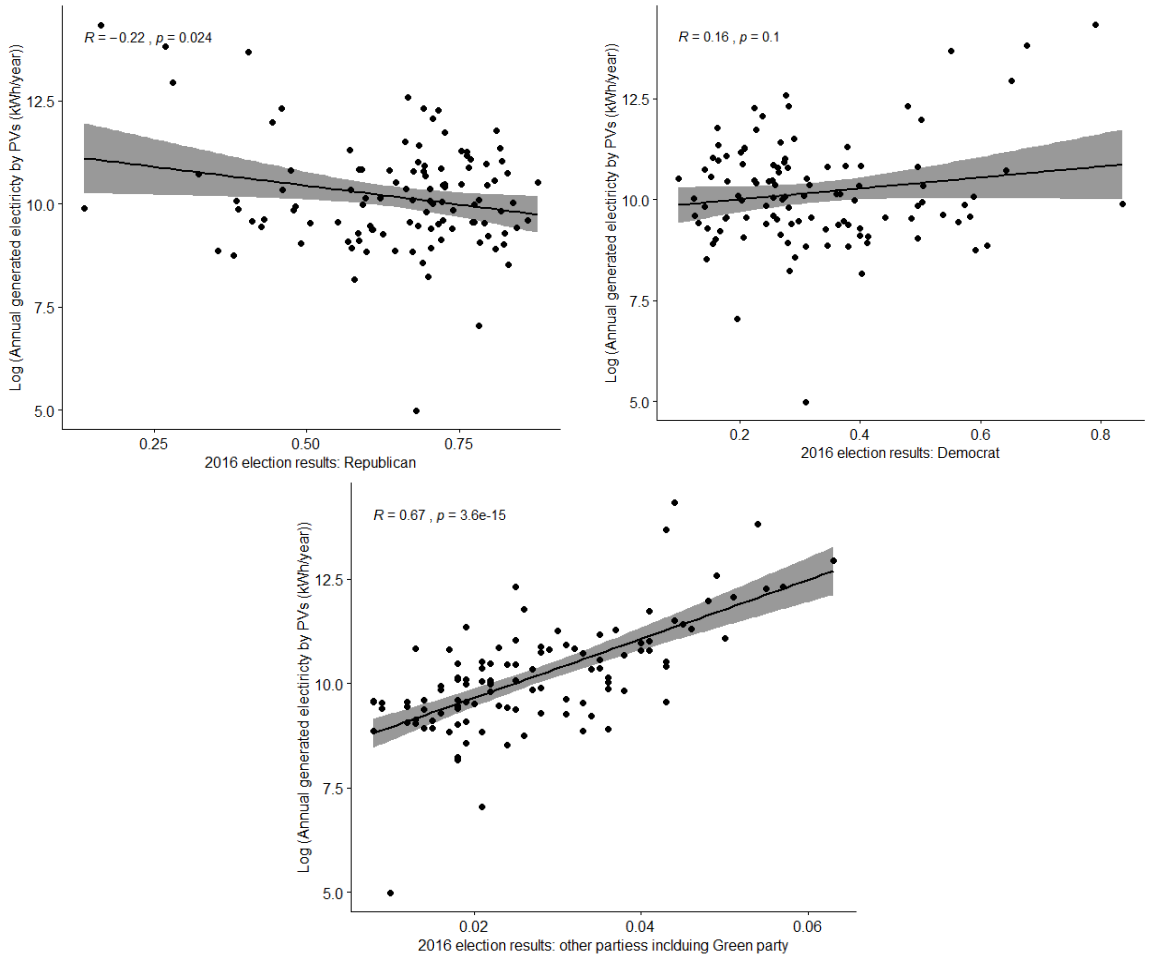

Figure 14 - Scatterplots: 2016 presidential election results vs. aggregated generated electricity by PV systems at the County level.

A linear regression model is then built to investigate the first hypothesis (Equations (1)). In the Equations (1) subscript i represents counties.

Hypothesis 1: A relationship exists between the uptake of PV systems and political affiliation, which can act as a proxy to environmental consciousness.

$$Uptake\ of\ PV\ systems\colon (annual\ electricity\ generated\ by\ PVs\ )_i = c' + \beta'\ (Republican\ votes\ )_i + \gamma'(other\ parties\ votes)_i + \epsilon' \quad \textbf{(1)}$$

In the Equations (1) subscript *i* represents counties. Table 2 presents the results of the test, in which the percentage of votes for *other* parties, shows a significant positive impact on the uptake of PV systems, while the percentage of the Republican voters have a negative impact..

Table 2 –Results: statistical analysis 1.

Test	Estimate	Std. Error	t-value	p-value
Intercept	229,121	85,771	2.67	0.008*
Republican votes (%)	-497,218	108,232	-4.59	1.21e-05*
Other parties including Green party votes (%)	6,150,102	1,355,025	4.53	1.51e-05*
Adjusted R-squared	0.3			
p-value	1.554e-09*			

* indicate statistical confidence at 99% confidence

A diagnosis of residual shows correlation between observed residuals and expected residuals under normality is *0.78.* Table 3 presents a summary of the residual normality tests. Figure 15 illustrates the graphical residual diagnosis.

Table 3 –Results: residual diagnosis (statistical analysis 1).

Test	Statistic	p-value
Shapiro-Wilk	0.634	0
Kolmogorov-Smirnov	0.233	0
Cramer-von Mises	9.037	0
Anderson-Darling	8.315	0

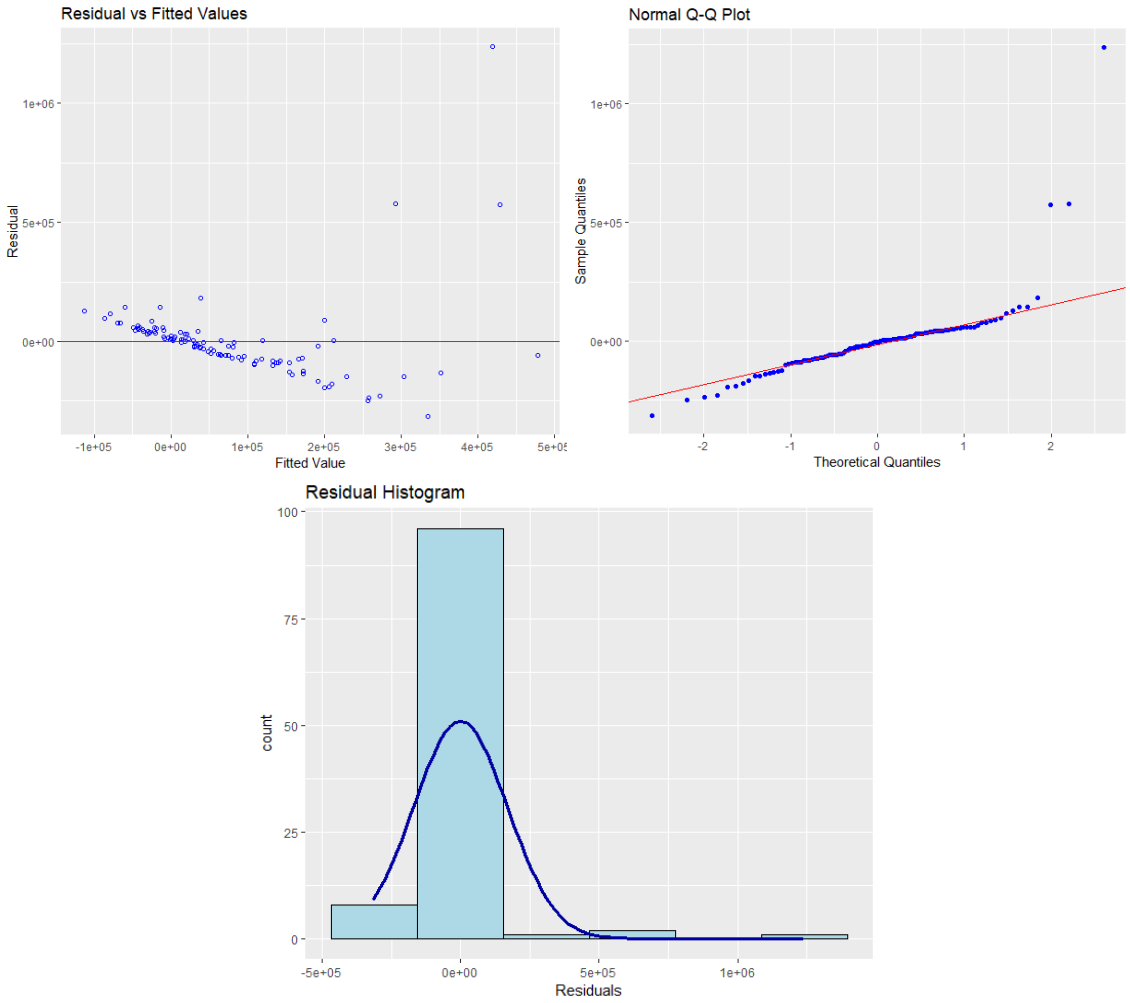

Figure 15 - Residual diagnosis: statistical test 1.

3.4.1.2 Model 2

The second model investigates the impact of explanatory variables in four categories: socio-economic, physical structure, electricity rate, and solar radiation, on the uptake of PV systems in the residential sector. Table 4 presents the candidate input variables. The micro-boundary of this model is the Census block-group and annual generated electricity by PV systems in the residential sector is aggregated at this micro-boundary level. Figure 16 illustrates the aggregated annual generated electricity at the Census block-group level. Figure 17 illustrates the median income (adjusted $ value of 2017) and PV systems.

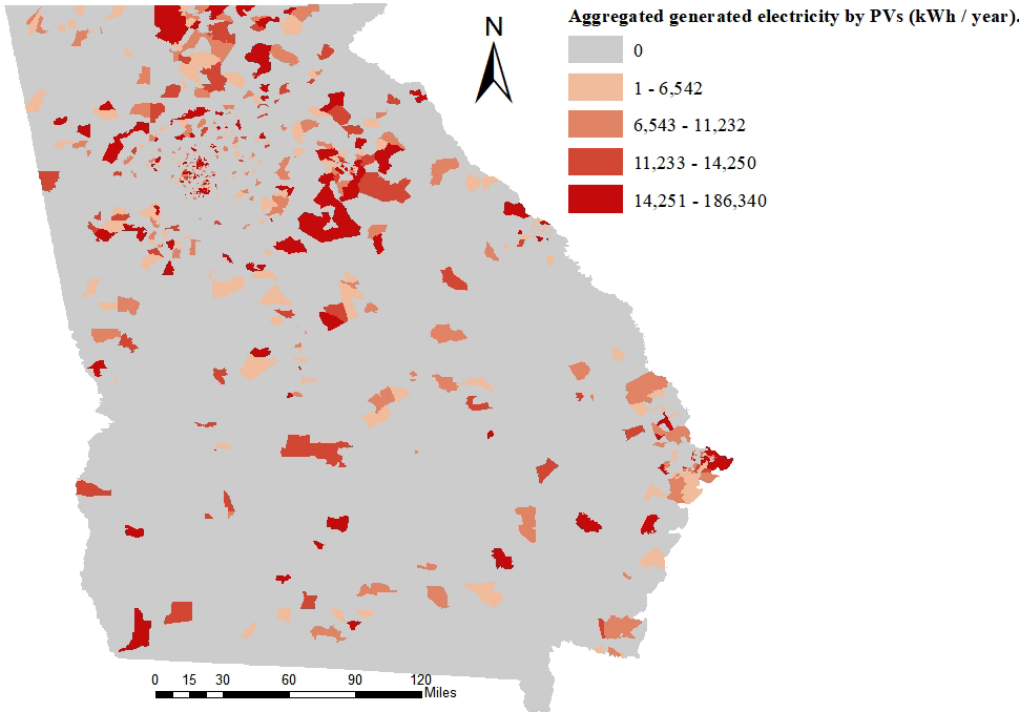

Figure 16 - Aggregated electricity generated by PV systems (residential sector): Census block-group level.

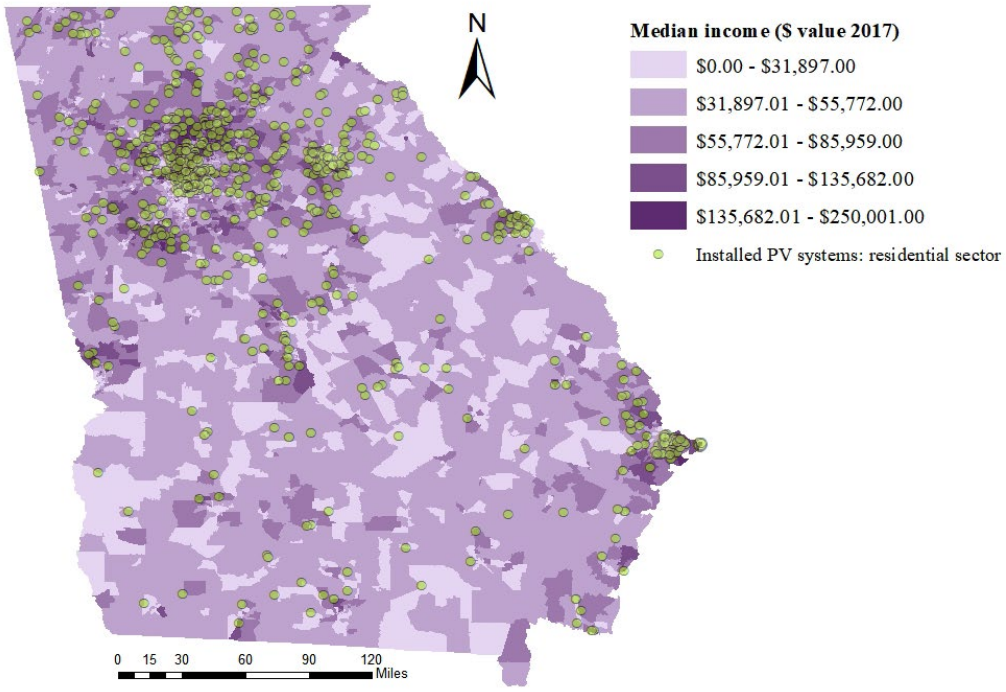

Figure 17 - Median income: Census block-group level.

Table 4 - Statistical test 2: candidate variables.

	Variable	Min	Max	Median	Source
Explanatory variables	Race – White (%)	0	100%	80%	U.S. Census (ACS2003-2017)
	Race – African-American (%)	0	100%	9%	U.S. Census (ACS2003-2017)
	Median income of population over 15 years old. ($)	7,183	250,001	73,323	U.S. Census (ACS2003-2017)
	Education - minimum college degree (%)	18%	100%	66%	U.S. Census (ACS2003-2017)
	Average number of bedrooms	1.12	5.08	3.09	U.S. Census (ACS2003-2017)
	Electricity rate ($/ kWh)	0.048	0.145	0.112	[93]
	Solar radiation (kWh / Sq. meter / day)	4.81	5.47	5.11	[92]
		Min	**Max**	**Median**	
Dependent variable	Annual generated electricity (kWh / year)	25.95	186,340	8,966	[90]

A linear regression model is then built to investigate the second hypothesis. A primary test model is built to test the second hypothesis (Equation (2)).

Hypothesis 2: A relationship exists between the uptake of PV systems and explanatory variables presented in Table 4.

$$Uptake\ of\ PV\ systems\text{: }(annual\ electricity\ generated\ by\ PVs\ )_j = c + \alpha\ (Reace\ )_j + \beta\ (Educatin)_j + \theta\ (Wealth)_j + \gamma\ (Solar\ radiation)_j + \delta\ (Electricity\ rate)_j + \epsilon \quad \textbf{(2)}$$

In the Equations (2) subscript j represents census block-group. To achieve the goal of this section, the extracted variables are merged at the census tract level. The average of the two waves of the Census (ACS) datasets (2008-2012 and 2013-2017) is calculated, and the monetary values are adjusted to the dollar value in 2017. The number of installed PV

systems is each census block-group are mapped, employing the longitude and latitude of the installed PV systems. Based on geographical location, the number of PV systems in each census block-group and their average annual generated electricity are computed. The average value of solar radiation at each census block-group is calculated based on by computing the average solar radiation in each census block-group. The electricity rates are extracted from the "U.S. electric utility companies and rates (2016)" dataset published by NREL [94] and its average is calculated for each census block-group. The boundary of electricity rate is zip code areas. To convert the boundaries, first the electricity rate is assigned to each PV system, and then the average electricity rates of the PV systems in each census block-group is calculated.

Plotting the collinearity pairwise matrix shows some level of multicolliniarity between the explanatory variables (Figure 18).To examine multicoliniarity three-step Farrar-Glauber test is employed. While the correlation graphs show not all the candidates for the explanatory variables have a significant correlation with the uptake of PV systems, a model based on these candidate variables does not satisfy the assumptions of the classical linear regression model, of which there is no collinearity exists between the explanatory variables. In case of approximately linearly relation between pairs of the explanatory variables, the t-value of one or more coefficients will tend to be statistically insignificant. The first step of Farrar-Glauber test is a Chi-square test for the detection of the existence of a multicollinearity, with null hypothesis the regressors are orthogonal. Table 5 presents the results of the first test – Chi-square test –, which shows evidence of multicollinearity. The calculated high value of the Farrar Chi-square shows high significance of existence multicollinearity.

The second step of the Farrar-Glauber test is the Farrar F-test, which locates the multicollinearity. Table 6 shows the results of the Farrar F-test, and illustrates a high value of the F-test for race. The last step of Farrar-Glauber test examines patterns of multicollinearity, by conducting a t-test for the correlation coefficient. The final step of the Farrar-Glauber is the t – test for the pattern of multicollinearity. Table 7 shows the results of the Farrar t-test. Table 8 presents variance infalation factors, which is another indicator of multicolnearity.

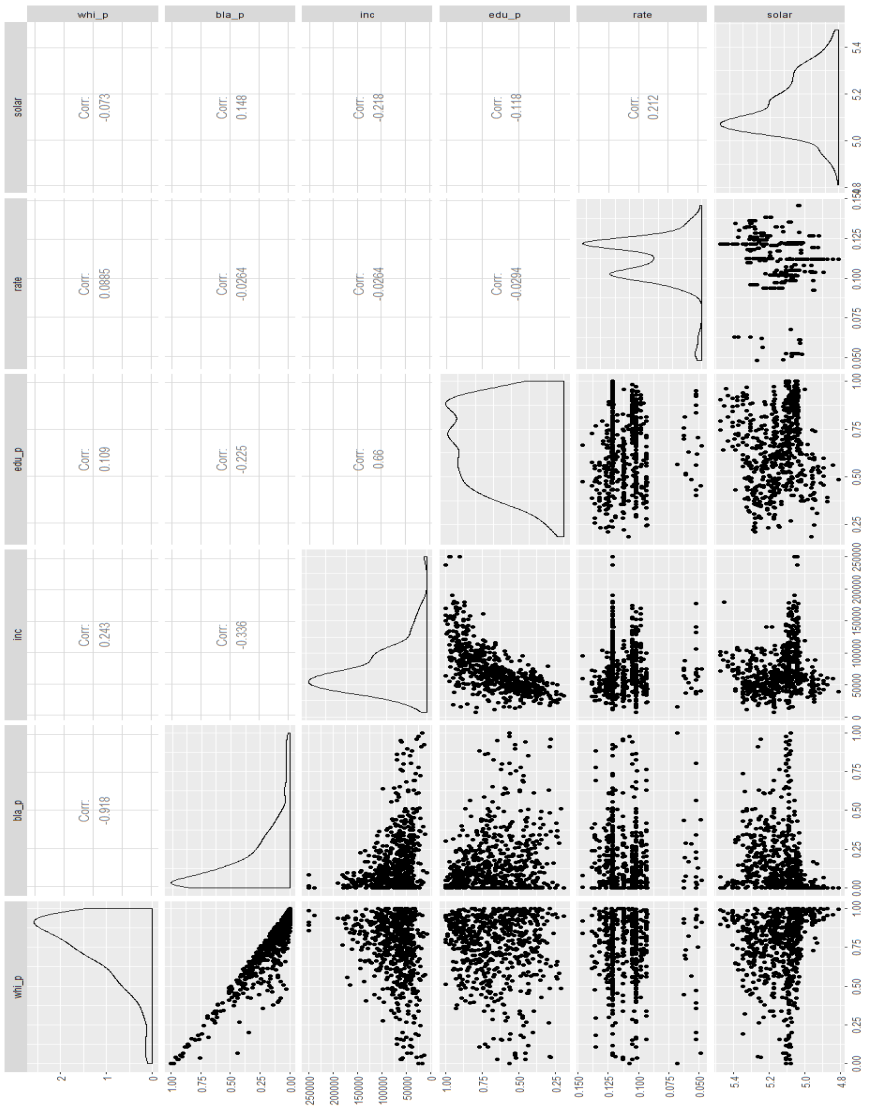

Figure 18 - Collinearity test: pairwise collinearity matrix.

Table 5- Results: Farrar – Glauber test 1: Chi-square.

Overall Multicollinearity Diagnostics	
Farrar Chi-Square	1,737.9
Sum of Lambda Inverse	20.48
Theil's Method	2.71
Condition Number	159.24

Table 6 - Results: Farrar – Glauber test 2: F-test.

Multicollinearity test, Farrar F-test.			
Explanatory variables	**Variance inflation factor**	**Tolerance**	**F-test**
Race – White (%)	7.07	0.14	763
Race – African-American (%)	7.44	0.13	810
Median income of population over 15 years old. ($)	3.57	0.27	324
Education - minimum college degree (%)	2.05	0.48	133
Average number of bedrooms	2.13	0.46	142
Electricity rate ($/ kWh)	1.15	0.88	19
Solar radiation (kWh / Sq. meter / day)	1.13	0.88	16

Table 7 - Results: Farrar – Glauber test 3: t-test.

Pattern of multicollinearity – t-test – partial correllation							
	Race: White	Race: African-American	Median income	Average bedrooms	Education	Electricity rate	Solar radiation
Race: White	0.00	-47.34	-0.28	0.42	-1.58	1.32	1.03
Race: African-American	-42.47	0.00	-0.77	0.20	-1.51	0.94	1.27
Median income	-0.40	-1.11	0.00	13.83	12.84	2.60	-2.33
Average bedrooms	0.77	0.37	20.08	0.00	-6.04	-4.81	1.37
Education	-2.95	-2.89	18.85	-6.15	0.00	-1.49	1.47
Electricity rate	3.29	2.39	4.63	-6.66	-2.00	0.00	5.16
Solar radiation	2.58	3.28	-4.19	1.88	1.98	5.21	0.00
Correlation							
	Race: White	Race: African-American	Median income	Average bedrooms	Education	Electricity rate	Solar radiation
Race: White	1.00	-0.92	0.24	0.20	0.11	0.09	-0.07
Race: African-American	-0.92	1.00	-0.34	-0.24	-0.23	-0.03	0.15
Median income	0.24	-0.34	1.00	0.66	0.66	-0.03	-0.22
Average bedrooms	0.20	-0.24	0.66	1.00	0.26	-0.19	-0.14
Education	0.11	-0.23	0.66	0.26	1.00	-0.03	-0.12
Electricity rate	0.09	-0.03	-0.03	-0.19	-0.03	1.00	0.21
Solar radiation	-0.07	0.15	-0.22	-0.14	-0.12	0.21	1.00

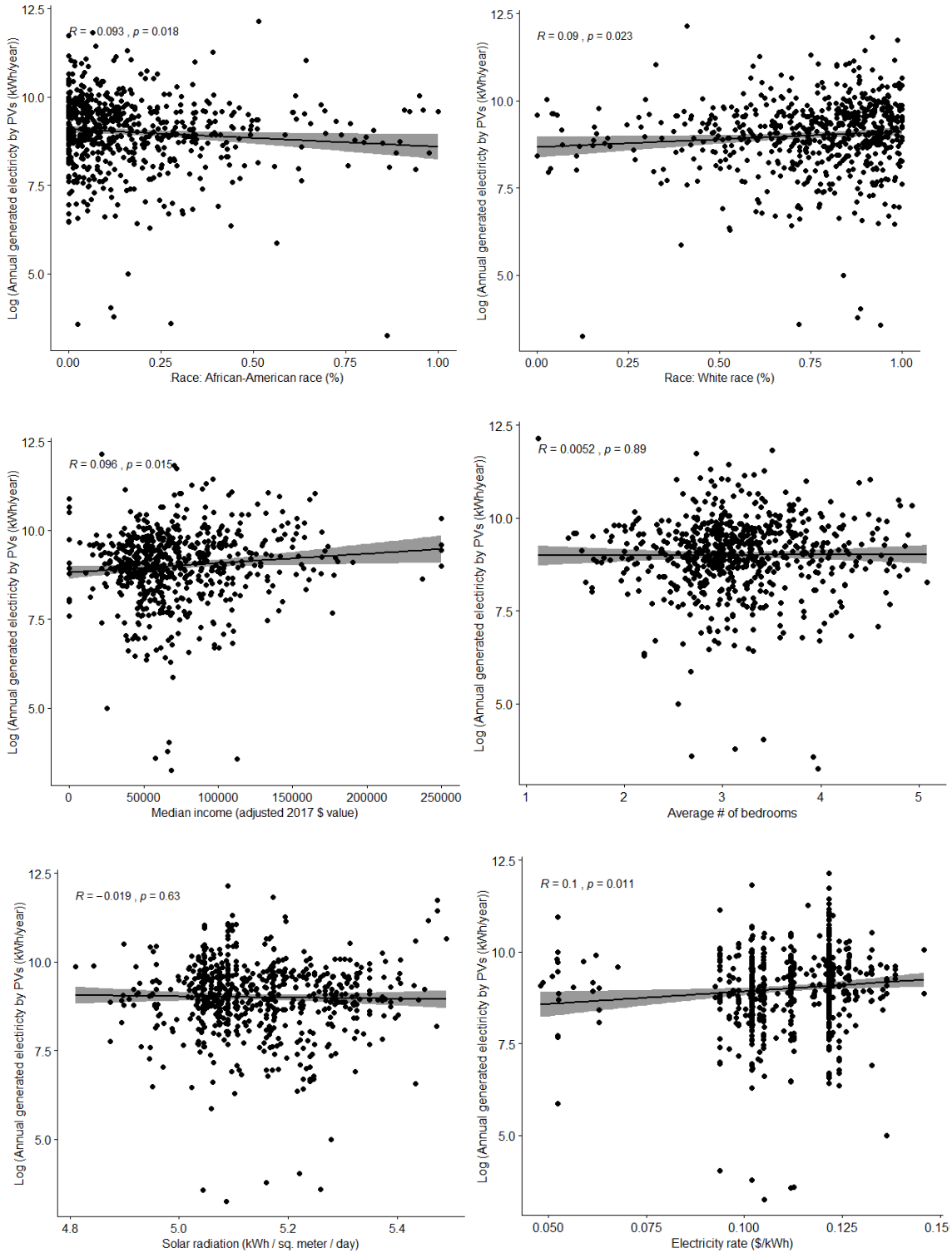

Figure 19 - - Scatter-plots: explanatory variables (candidates) vs. aggregated generated electricity by PV systems at the Census block-group level.

Table 8 - Results: variance inflation factors (VIF) -model 2.

	Candidate explanatory variables						
	Race: White	Race: African American	Education	Median ncome	Average number of Bedrooms	Solar radiation	Electricity rate
VIF	**7.07**	**7.44**	2.05	3.57	2.13	1.13	1.15

According to the results of the Farrar-Glauber test, race (White and African-American), education, and average number of bedrooms are removed from the original model. To investigate the correlation between the candidate explanatory variables and the dependent variable, a scatter-plot for each explanatory variable is generated (Figure 19). According to the scatter-plots, solar radiation does not have a significant correlation with the dependent variable and is omitted from the original model. A logarithmic transformation also applied. Equation (3) presents the modified model.

$$Uptake\ of\ PV\ systems: \log(annual\ electricity\ generated\ by\ PVs)_j = c + \theta\ (Wealth)_j + \delta\ (Electricity\ rate)_j + \epsilon \quad \textbf{(3)}$$

Table 9 presents the results of the second statistical model, in which the percentage of the Republican voters has a negative impact on the uptake of PV systems and the percentage of voters for other parties including the Green party has a positive impact.

Table 9 - Results: statistical analysis 2.

Test	Estimate	Std. Error	t-value	p-value
Intercept	8.001	3.147e-01	2.67	< 2e-16
Median income	3.037e-06	1.100e-06	-4.59	0.0059*
Electricity rate	6.941	2.683e+00	4.53	0.0099*
Adjusted R-squared	0.18			
p-value	0.001*			

* indicate statistical confidence at 99% confidence

To test if the removed explanatory variables are jointly significance, a joint hypothesis testing method is employed. The results indicate the null hypothesis, that the coefiient of the removed explanatory variables are zero can not be rejected, at any significant level. The F-statistic for this joint hypothesis test is about *0.45* and the corresponding p-value is *77%*. A diagnosis of residual shows correlation between observed residuals and expected residuals under normality is *0.95*. Table 10 presents a summary of the residual normality tests. Figure 20 illustrates the residual diagnosis. While a lower p-value suggests a high significance of the results, compare with electricity rate, median income has a lower impact on the uptake of PV systems in the residential sector. The low R^2 value suggests the variables in the model are not concentrated near the fitted line.

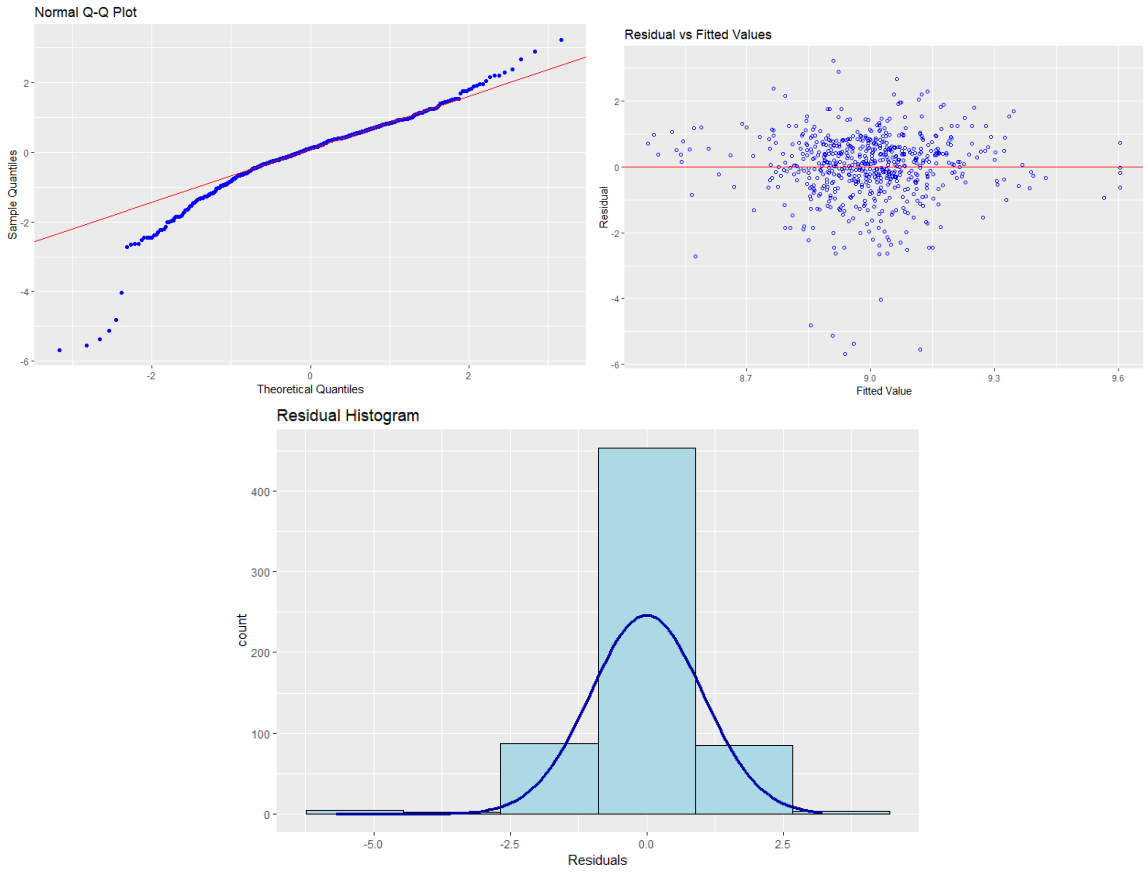

Figure 20 - Residual diagnosis: statistical test 2.

Table 10 –Results: residual diagnosis (statistical analysis 2).

Test	Statistic	p-value
Shapiro-Wilk	0.919	0
Kolmogorov-Smirnov	0.093	0
Cramer-von Mises	37.181	1e-04
Anderson-Darling	9.235	0

Vector values of the first test explain to what extent the percentage of voters of the Republican and Green parties affect the adoption of PV systems in the residential sector. Looking across specifications, results suggest that the null hypothesis cannot be rejected. The results show that the percentage of Republican voters has a negative effect on the uptake of PV systems, while the percentage of other parties including the Green party has positive impact. The results of the second test reveal both wealth and electricity rate have a positive impact on the adoption of PV systems in the residential sector. Other factors, including education, white race, African-American race, and number of bedrooms (as a proxy for the size of a building) have multicoliniarity with wealth and excluded from the model. The correlation analysis indicates there is a minimal relationship between uptake of PV systems in the residential sector and solar radiation.

3.4.2 Spatial analysis

Among existing methods of spatial analysis, two suitable techniques are applied to evaluate the diffusion patterns of PV systems in Georgia: 1- standard deviational ellipse and 2- Moran's I cluster assessment. The s*tandard deviational ellipse* is a common technique to measure the trend for a set of point spatially spread. The result of this technique is an ellipse shape, which its axes (SDE_x and SDE_Y) are the calculated standard distance of points in *x* and *y* directions (Equations (4)).

$$SDE_x = \sqrt{(\frac{\sum(x_i - \bar{X})^2}{n}}\ , and\ SDE_y = \sqrt{(\frac{\sum(y_i - \bar{Y})^2}{n}}\ , \quad \textbf{(4)}$$

where n represents number of features, $x_i and\ y_i$are the coordination of the feature, and $(\overline{X}, \bar{Y})$ is the mean center for of the features.

Moran's I cluster assessment is a measure of spatial autocorrelation, which is characterized by a correlation in a signal among nearby locations in space [95,96]. This technique is widely used for evaluating patterns and identifies whether the feature is clustered, dispersed, or randomly spread. The output is Moran's I index(I), expressed by Equation (5), and z- and p-values to evaluate the significance of the index.

$$I = \frac{n}{S_0}\frac{\left(\sum\sum w_{i,j} z_i z_j\right)}{\sum z_i^2}, \quad \textbf{(5)}$$

where n represents number of features, S_0represents the aggregate of all spatial weights, z_i represents deviation of an attribute for feature i from its mean, and $w_{i,j}$ represents the spatial weight between two features i and j.

Before analyzing patterns of adoption, a visual explanatory analysis was run on the datasets. The historical dataset of the installed PV systems contains data of 1027 installed PV systems in three sectors: 150 units in utility, 368 in non-residential, and 509 units in residential (Figure 21). Figure 22 illustrates the aggregated annual electricity generated by the installed PV systems at the census tract level. The census tract with higher aggregated annual electricity generation via the installed PV systems in the residential sector are located at the north of the state, while the non-residential sector has the highest

concentration at north-west and south of the state. The PV systems in the utility sector are scattered in the Sothern parts of the state.

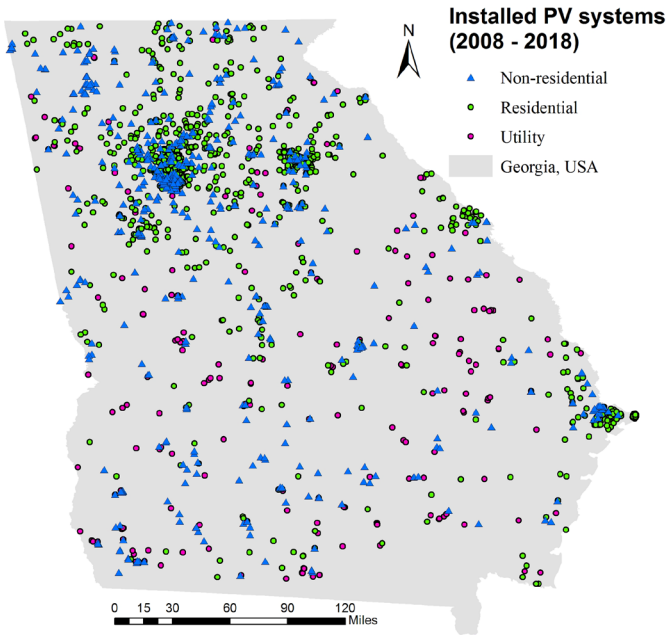

Figure 21 - Installed PV systems in Georgia, between 2008 and 2018.

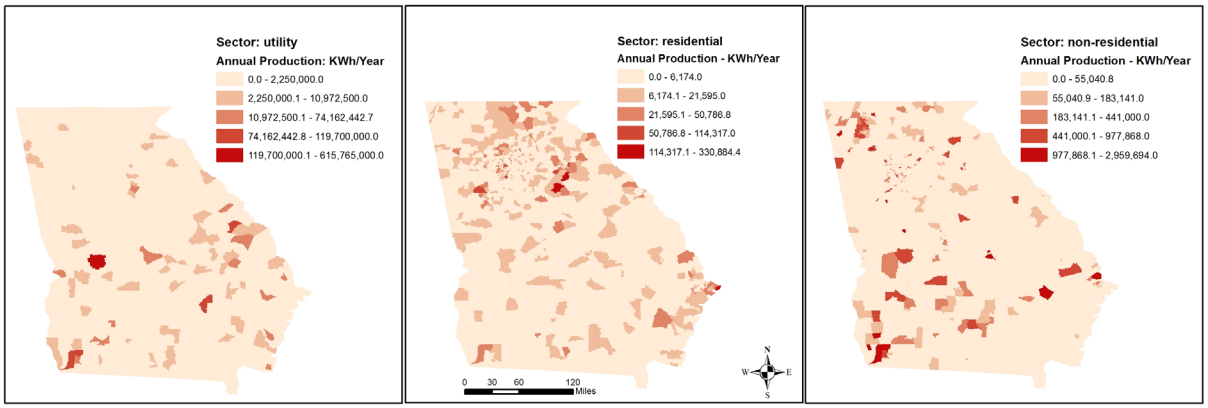

Figure 22 - Annual electricity generated by the PV systems.

Figure 23 illustrates the results of *Standard deviational eclipse*, as the directional distribution of the installed PV systems in each sector. The selected size of the output ellipse is one standard deviation. Both residential and non-residential sectors are

concentrated in the center and north of Georgia, while the concentration is more in the south of the state.

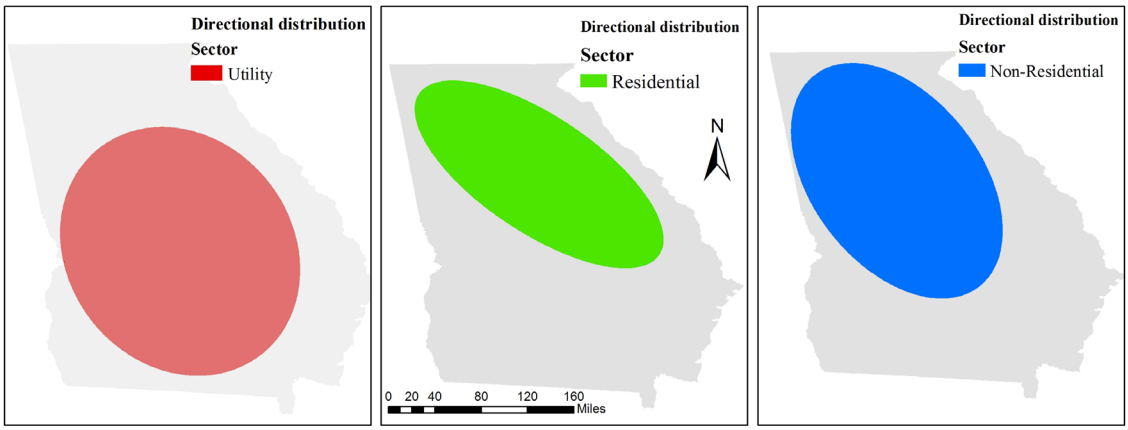

Figure 23 – Results: directional distribution – installed PV systems in three sectors.

In the next step, the installed PV systems in each sector, based on their installation year, are divided into three groups. For each group, the direction distribution method is then applied to form the directional distribution ellipse which reveals more information. The concentration of installed PV systems in the residential sector is at the north part of Georgia. However, a small concentration of PV systems that are installed later at the east side of the state skews the eclipse form and causes it to stretch toward the southeast (Figure 24). In the non-residential sector, the concentration of PV systems was initially in the north part of the state, in Atlanta and Athen and their surrounding areas. Later, the adoption of PV systems in the south areas of the state, inaddition to the north areas, changes the shape of the sllipse and rotate it to aligh with the shape of the state. This indicates the there are enough number of installed PV systems by 2018 spread across the state that the shape of directional distribution ellipse is close to the shape of the state (Figure 25). Installed PV systems in the utility sector are scattered across the southern areas of the state. This scatter

pattern results in the circle shaping of the directional distribution ellipse for the overall installed PV systems (Figure 25). The trend over time shows the PV systems in the utility sector are first adopted in areas closer to the urban areas and then expands across the state.

The univariable Moran's I technique is employed to study the clustering pattern of the installed PV systems in three sectors. The selected feature value is annual generated electricity by PV systems with 999 permutations for the randomization, and spatial weight is created using queen contiguity. The results of this analysis consist of a clustering map, a significance map, and a plot of computed Moran's I index.

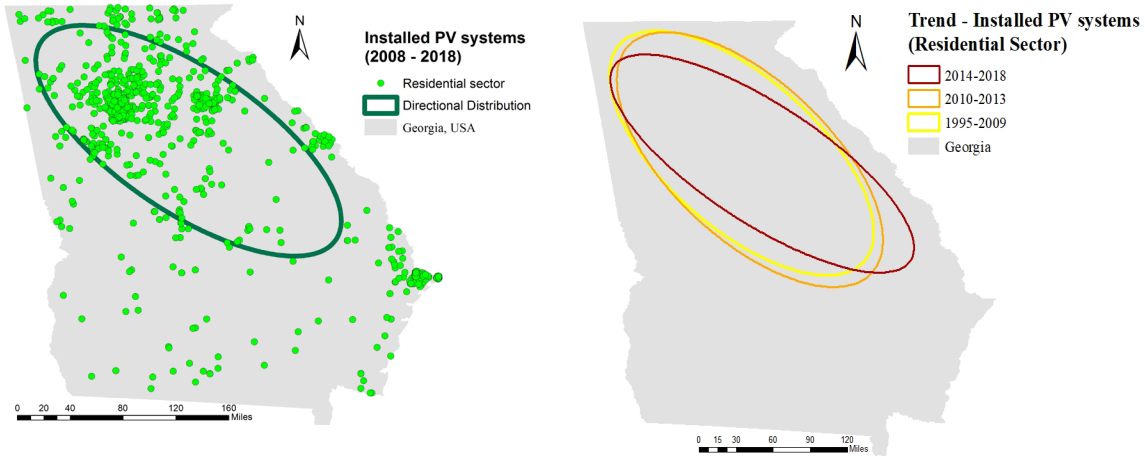

Figure 24 - Results: directional distribution – installed PV systems in the residential sector – Left: overa, Right: over time.

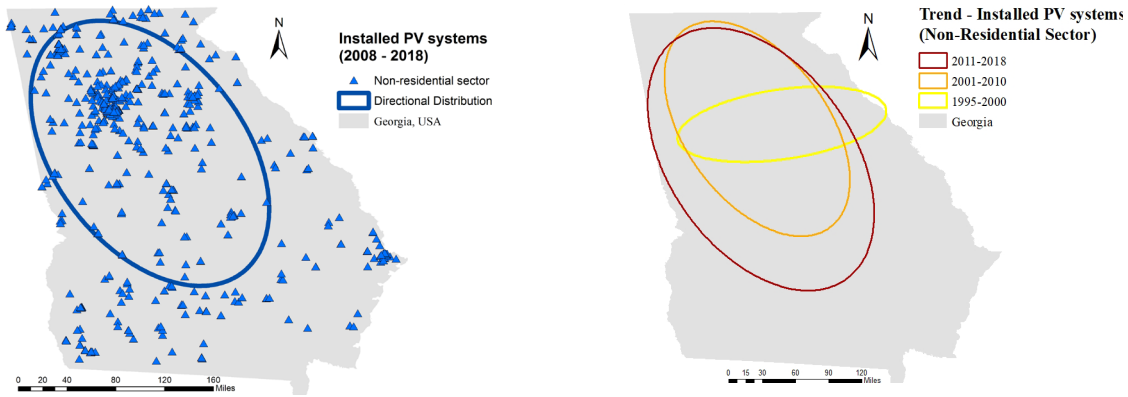

Figure 25 - Results: directional distribution – installed PV systems in the non-residential sector – Left: overa, Right: over time.

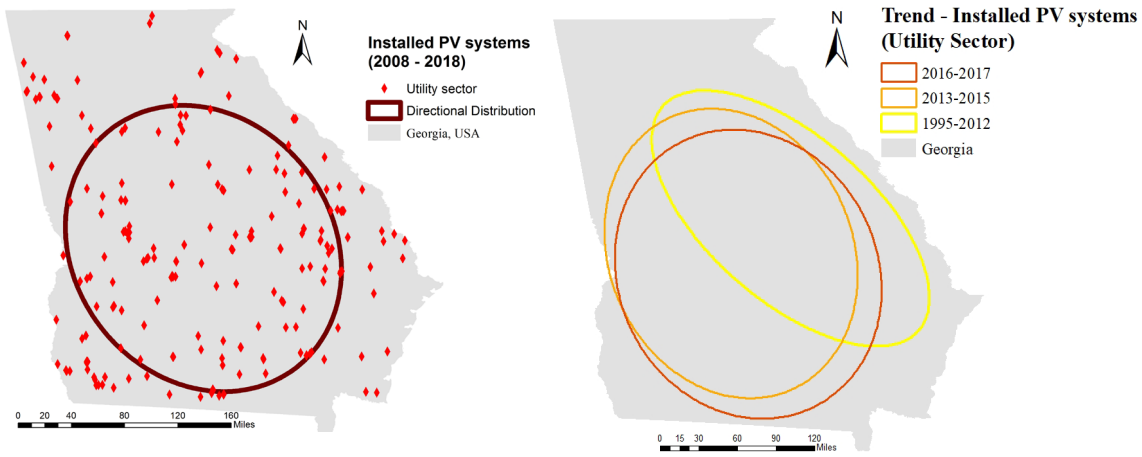

Figure 26 - Results: directional distribution – installed PV systems in the utility sector – Left: overa, Right: over time.

The cluster map is a scatter plot illustrating four classifications: low-low, high-high, low-high, and high-low. The first two classifications represent spatial cluster (cores of a cluster) and the other two classifications represent spatial outliers. These four classifications represent the four corners of the Moran scatter plot, and the location of each census tract, as a point in the four quadrants of the plot.

The results of cluster analyses show some evidence of cluster in the north and center of Georgia for the residential sector, and for the non-residential sector, there exists evidence of clustering scattered across the state (Figure 27 and Figure 28). The result of cluster analysis on the installed PV systems in the utility sector shows evidence of cluster much higher than the other sectors, with high significance level as expressed in Figure 29.

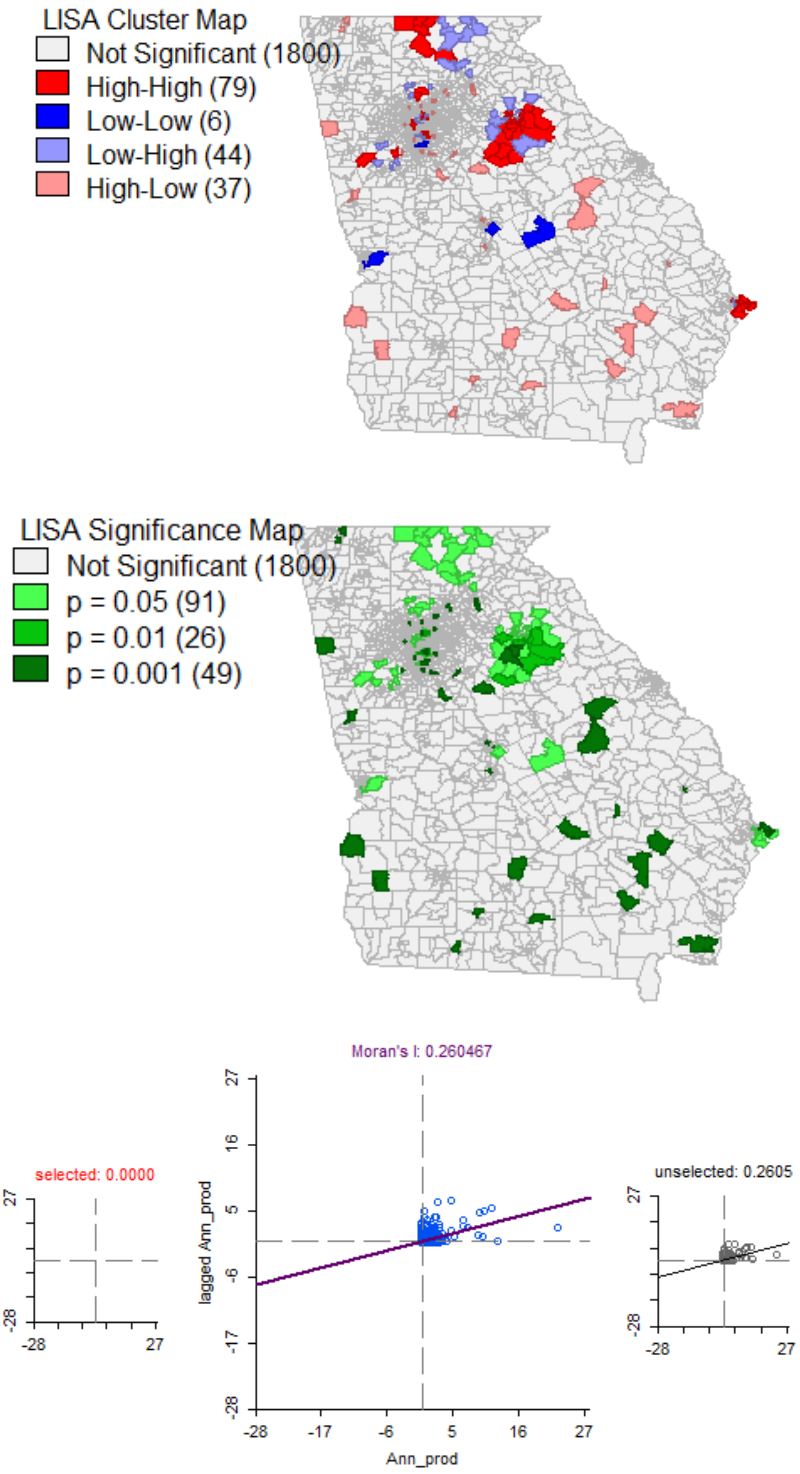

Figure 27 - Results: Moran's I cluster/outlier - installed PV systems in the residential sector.

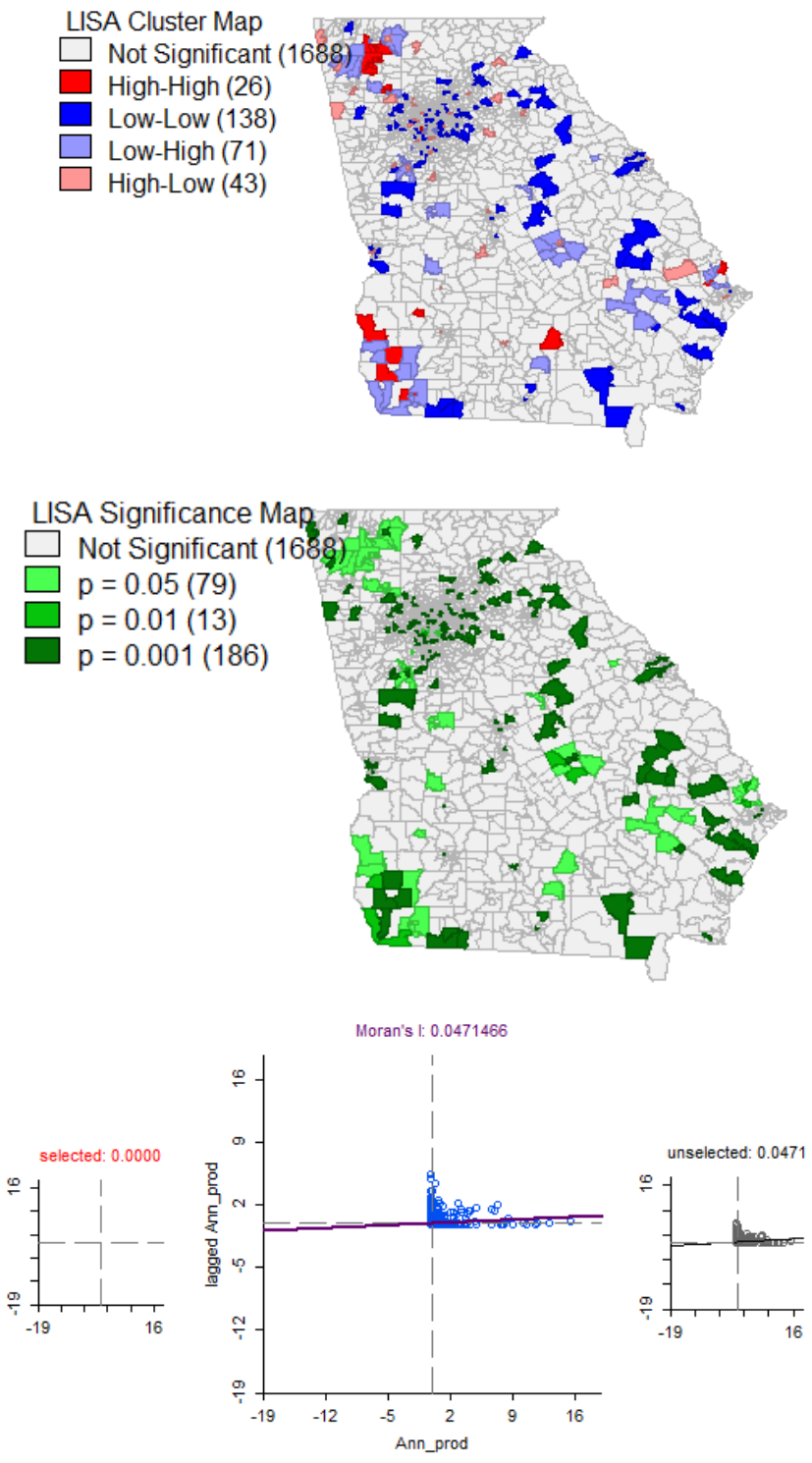

Figure 28 - Results: Moran's I cluster/outlier - installed PV systems in the non-residential sector.

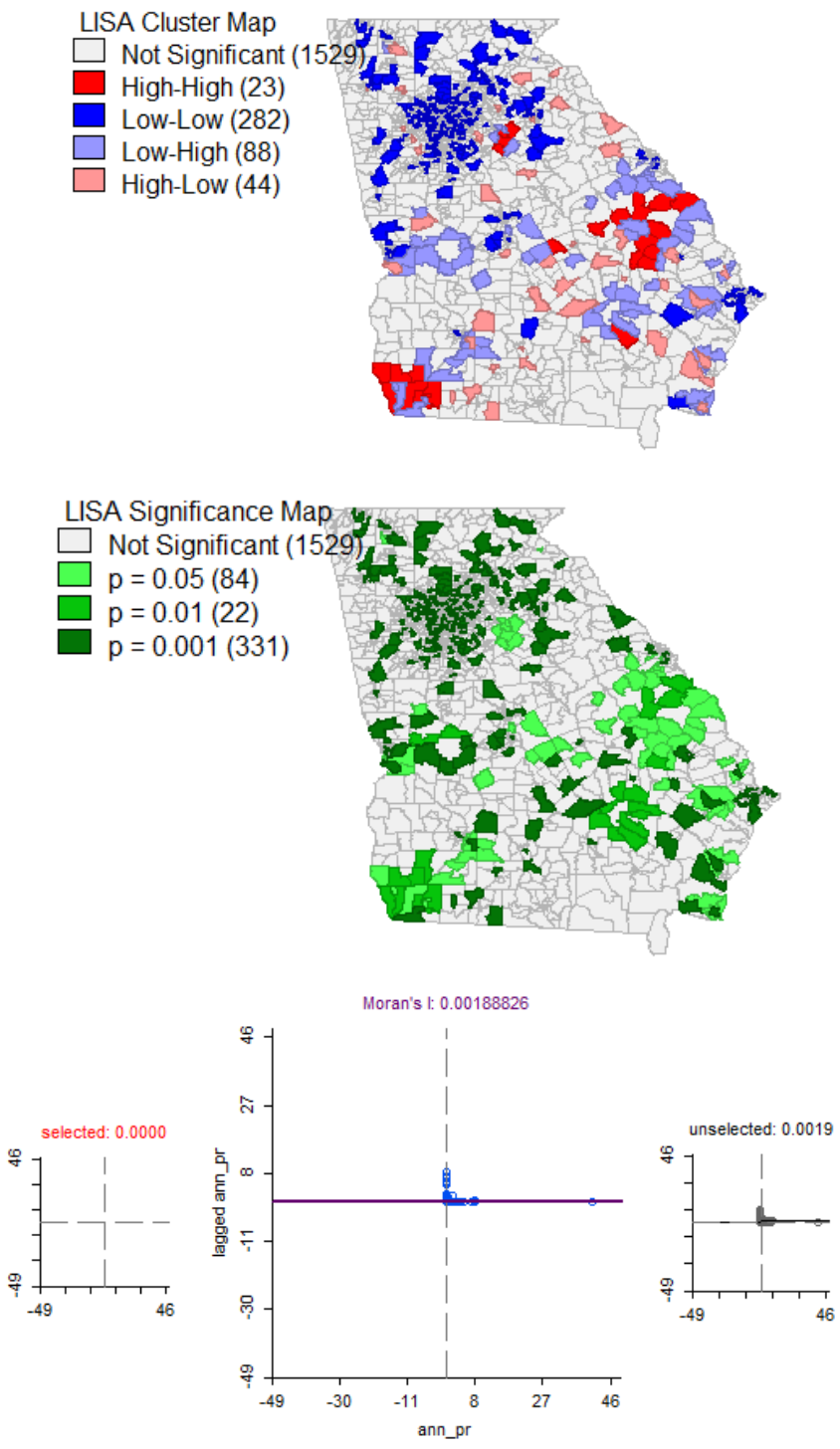

Figure 29 - Results: Moran's I cluster/outlier - installed PV systems in the utility sector.

3.4.3 Spatial regression

A spatial regression with queen continuity of 1 is developed as an extra layer of spatial analysis. The dependant variable in this model is the same as the previous models (aggregated annual electricity generated by the PV system at the Census block-group level). Table 11 presents the explanatory variables of this model.

Table 11 - Input variables: spatial regression.

	Variable	Source
Explanatory variables	Race – White (%)	U.S. Census (ACS2003-2017)
	Race – African-American (%)	U.S. Census (ACS2003-2017)
	Median income of population over 15 years old. ($)	U.S. Census (ACS2003-2017)
	Education - minimum college degree (%)	U.S. Census (ACS2003-2017)
	Average number of bedrooms	U.S. Census (ACS2003-2017)
	Electricity rate ($/ kWh)	[94]
	Solar radiation (kWh / Sq. meter / day)	[92]
	Percentage of the Democratic voter (2016 presidential election	uselectionatlas.org
Dependent variable	Annual generated electricity (kWh / year)	[90]

The results of this spatial regression show the positive impact of the White race on the uptake of PV systems, while the results for the other explanatory variables is not statistically significant.

Table 12 - Results: spatial regression.

Test	Estimate	Std. Error	z-value	p-value
Spatial weighted Annual electricity generated by PV systems	0.24	0.04	6.458	0**
Intercept	-12428.10	25573.10	-0.486	0.627
White race (%)	15838.70	7150.96	2.215	0.027*
African-American race (%)	11769.50	7624.04	1.544	0.123
Median income	0.01	0.03	0.228	0.820
Average # of bedrooms	56.19	1373.18	0.041	0.967
Electricity rate ($/kWh)	-20769.40	15966.50	-1.301	0.193
Solar radiation (kWh/Sq. meter / day)	1408.74	4916.72	0.287	0.774
Democratic voters (%) (2016 presidential election)	5300.19	4057.88	1.306	0.192
Adjusted R-squared	0.12			

* indicate statistical confidence at 90% confidence

*indicate statistical confidence at 99% confidence

3.4.4 Time series analysis

The Ljung-Box Q test on annual electricity generated by PV systems in the residential sector by month (named generated-electricity thereafter) shows whether this historical dataset is autocorrelated [97]; in which the correlation between the values of the series at different lag times (increments by 4 lags) in the generated-electricity dataset are not random and depend on the previous value. Table 13 shows a summary of the Ljung-Box Q test results, in which the p-value is less than 5%. Therefore, employing a time series method, the forecasting model can be created.

Table 13 - Summary results: Ljung-Box Q test.

Lag	Q-statistic	p-value
1	21.75	3.106e-06
5	89.043	< 2.2e-16*
9	128.78	< 2.2e-16*
13	145.38	< 2.2e-16*
17	145.5	< 2.2e-16*
21	149.48	< 2.2e-16*
25	155.22	< 2.2e-16*
29	167.63	< 2.2e-16*
…	…	< 2.2e-16*
89	269.55	< 2.2e-16*
93	280.97	< 2.2e-16*
…	…	< 2.2e-16*
105	298.28	< 2.2e-16*
109	298.74	< 2.2e-16*
113	298.82	< 2.2e-16*

* indicate statistical confidence at 99% confidence

One important characteristic of a time series is seasonality. Seasonal component of a time series is the fluctuation in the dataset related to the calendar cycles. Figure 30 illustrates the result of seasonality test on the generated-electricity dataset, with lag order of 4, with three building blocks: seasonality, trend, and cycle. The trend shows the overall pattern of this dataset and cycle shows increases and decreases that are not seasonal. Trend-cycle component of a time series is estimated by moving average method.

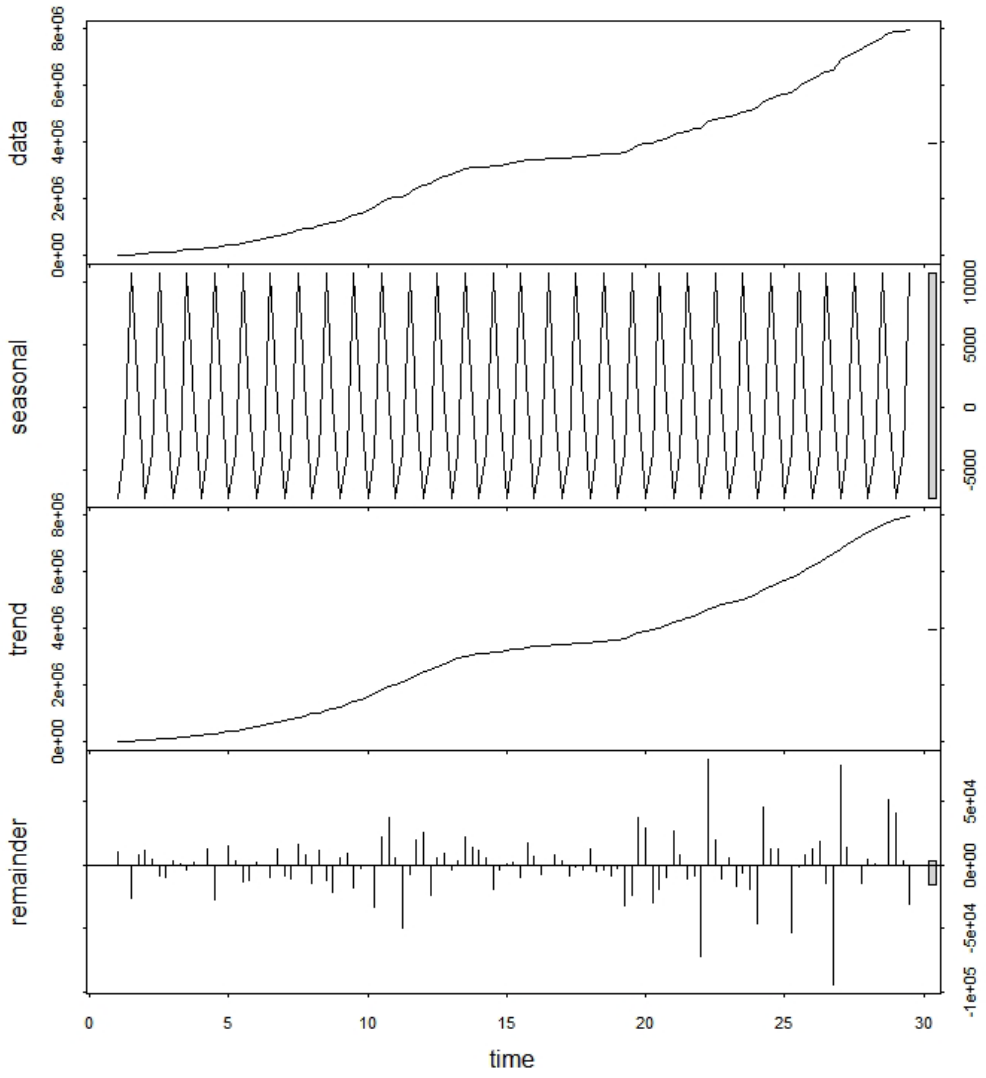

Figure 30 – Results: seasonality test.

The next step is to test *stationary*, one of the most important characteristics of a time series. Augmented Dickey-Fuller (ADF) test is employed to test the null hypothesis that the time series is non-stationary [98]. The result of the ADF test with lag order of 4 is *-2.2312* with p-value of *0.4806*, indicating the null-hypothesis can be rejected and this dataset is stationary. Furthermore, plotting the augmented Dickey-Fuller test on the differenced series illustrated in Figure 31 shows an oscillating pattern around 0 with no

visible strong trend. This suggests that differencing of order 1 term is sufficient and should be included in the model.

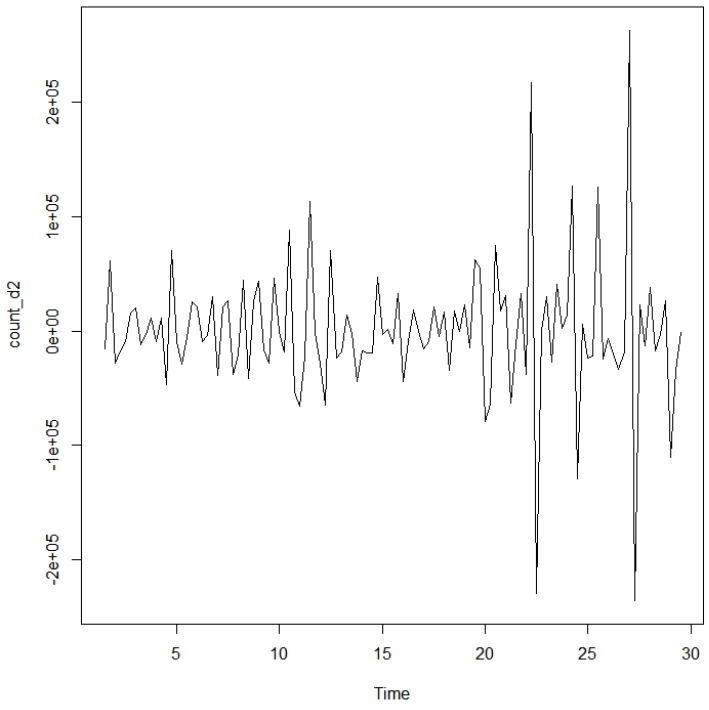

Figure 31 – Results: stationary test - augmented Dickey-Fuller test on differenced series.

Autocorrelation plot (ACF) is a visual test to evaluate if the time series dataset is stationary and useful to select the order of parameters for ARIMA model. Partial-autocorrelation plot (PACF) shows any correlation between a variable and its lags that are not explained by previous lags, which is useful when determining the order of the ARIMA model. Figure 32 illustrates autocorrelation and partial autocorrelation plots, in which blue-dots lines show the 95% significance boundaries. The early spikes on the PACF are due to a carry-over correlation.

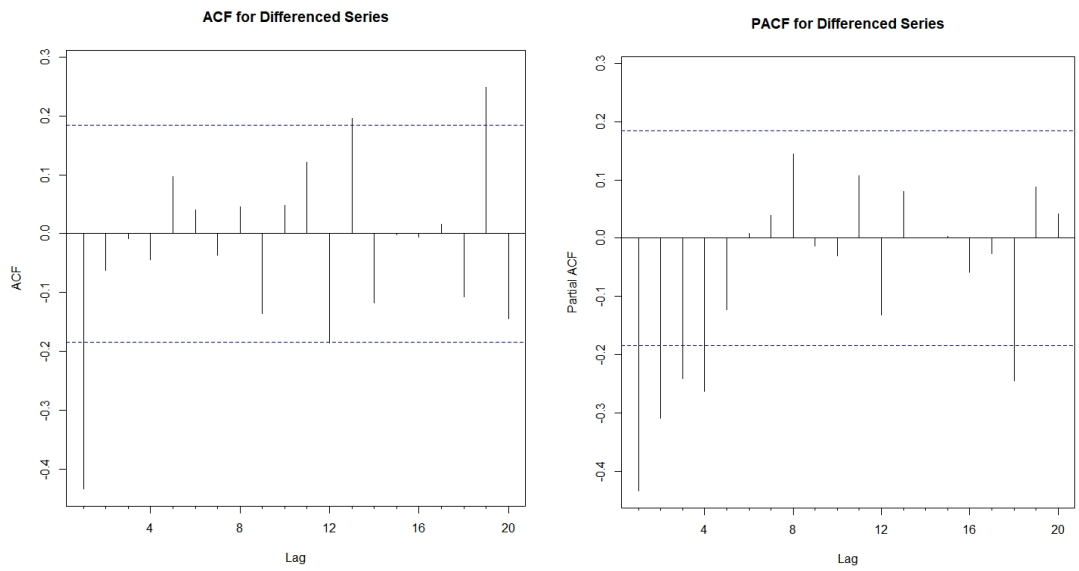

Figure 32 – Results: autocorrelation (left) and partial autocorrelation (right) plots.

3.4.4.1 ARIMA model

The next step is fitting the auto-regressive integrated moving average (ARIMA) model, designed based on a combination of autoregressive (AR) and moving average (MA). ARIMA model consists of three parameters (*p*,*q*,*d*), and searches through a combination of order parameters and picks the set that optimizes fit criteria. Two parameter *p* and *q* describe the orders of AR and MA. Parameter *d* represents the difference order required to transform the original dataset to a stationary time series, and since the dataset is stationary as investigated above, there is no need to apply a transfer method. There are a range of criteria to evaluate quality of fit, among which two most widely used are Akaike information criteria (AIC) and Baysian information criteria (BIC) [99,100]. The lowest BIC and AIC indicate the best choice of variable *p* and *q*. Employ an existing statistic package in R programming platform, suggest parameters (1,1,1) which results in the

highest values of *AIC=2785.16* and *BIC=2790.53*. The results also include ARIMA coefficients that forms the ARIMA model (Equation (8)).

$$\widehat{Y_t} = 0.9854\, Y_{t-1} - 0.7469\, e_{t-1} + E \qquad \textbf{(6)}$$

where

$\widehat{Y_t}$: forecasted value at time t,

Y_{t-1}: AR operator at time $(t-1)$,

e_{t-1}: MA operator at time $(t-1)$, and

E: error.

ACF and PCF plots for model residual test the ARIMA model. If the order parameters are selected correctly, the two ACF and PCf lines should be whithin the thresholds. Figure 33 shows the residual model and ACF and PACF test of the residual. The residual plot shows a white noise and no spike is detected in ACF and PACF plots. The final step in forecasting using the fitted model. Figure 34 shows the forecast plot generated by the fitted ARIMA model. The time increment is four months and this forecast projects next 48 months (12 quarters) from May of 2018, the last time stamp in the historical dataset. The dark shaded area shows the projected aggregated annual electricity generated by PV systems with 80% confidence limits and light shaded area shows the projected values with 95% confidence limits. With 80% confidence, the forecast model predicts that the quarterly electricity generated by the PV systems in the residential sector will increase from 3.3 GWh per year to 10 GWh per year at the fourth year.

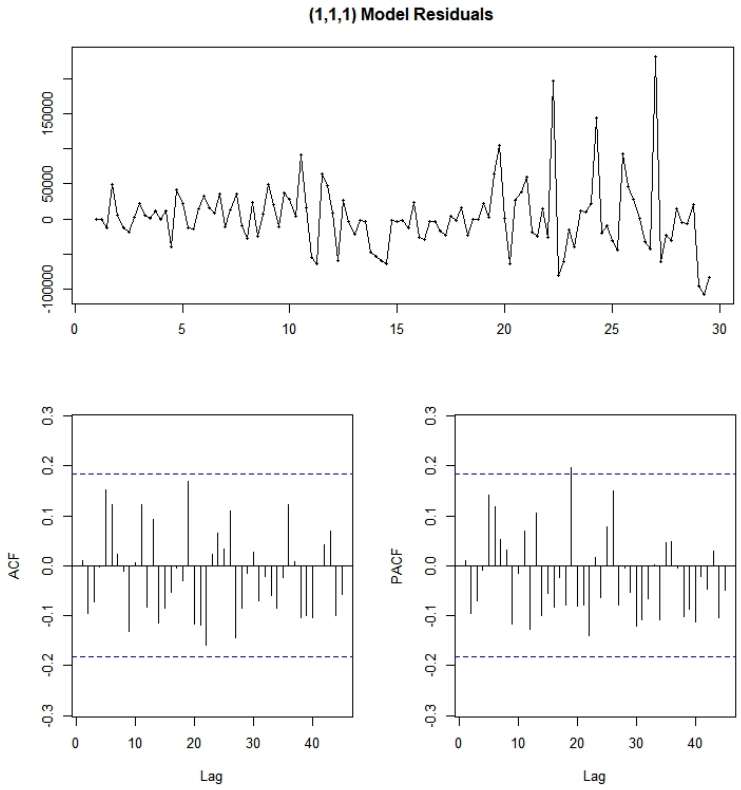

Figure 33 - Results: test ARIMA model.

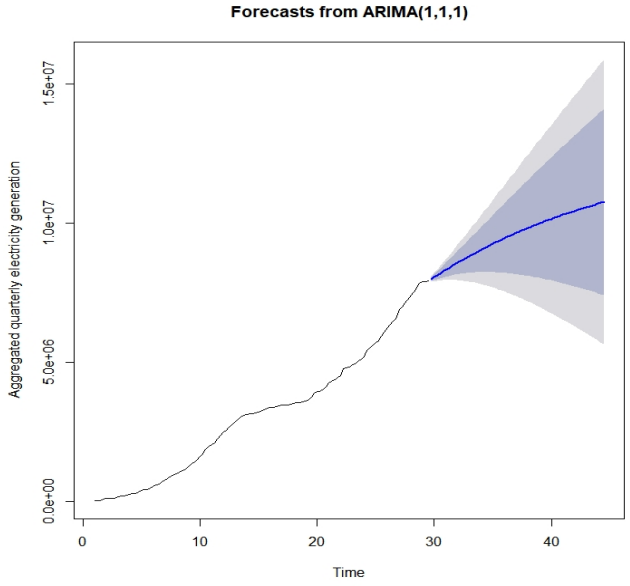

Figure 34 - Results: forecast from ARIMA (1,1,1).

3.4.5 Machine learning

The goal of this analysis is to develop a predictive model for future adoption of PV systems, and identify the most important features in the prediction model. Decision tree and random forest are among ensemble learning methods in which the multiple learning algorithms are developed and compared to gain the highest accuracy, which is addressed as better predictive performance.

Random forest technique is based on growing parallel weak decision tree learners, which reduces bias and variance [101]. Training process consists of randomly select sub-samples from the sample dataset, called bootstrap, and grow an unpruned classification tree based on them (Equation (7)). A small set of predictors are selected as the split sample. This process of bootstrap, grow tree, and select predictors is repeated and a prediction is then calculated based on the average prediction values of all trees. The random selection of sub-samples reduces the overall variance of the model. During the training process, one of the input variables is switched, the remaining constant is kept, and mean decrease in prediction accuracy is measured to assign relative importance score to the selected variable. This process continues until a binary tree of the predefined level is built.

$$\hat{f} = \frac{1}{N}\sum_{n=1}^{N} f_n(x) \quad \textbf{(7)}$$

where x represents input vector, $f_n$represents a constructed tree, N is the number of repeats. Out-of-bag error estimation is one of the advantages of the *random forest* technique, in which the samples that are not selected during the training of a tree are used to estimate the error without using an external data [101].

The *decision tree* is another efficient algorithm to develop a predictive model [102]. This method splits a problem into several simpler problems. This method constructs a decision tree with nodes: each tests the value of a certain attribute. Edges connect nodes, and leaves are each assigned to one class representing the most appropriate target value. The training process consists of recursive partitioning and multiple regressions. From the root of the tree and the node with no in-coming edge, the splitting process starts and continues until the stopping criterion is met. Some of the more common stopping rules are: all instances of the training sample belong to a single value, the process reaches a maximum tree depth, the number of cases in the terminal node are less than the minimum number of cases for the parent nodes, and if the node were split, the number of cases in one or more child nodes would be less than the minimum number of cases for child nodes[103].

Input dataset for the *decision tree* and *random forest* analysis methods contains 1969 rows, each represents `a census tract in Georgia. The dataset consists of 35 features (Table 14). The dataset is then cleaned and 15 rows that one or more features did not have data, are removed. The dataset is then split into two sets: a training set (60%) and a test set (40%). After training the model employing the random forest algorithm, the accuracy on the test set shows that the model can predict the existence of a PV system with *RMSE = 0.76.* This model is then tested for a range of depth to evaluate if increasing the depth of the tree will increase the accuracy of the model (Figure 35). The optimum depth of the tree is 20. A higher depth does not award a higher accuracy. With the same rate of split (60-40), the train and test sets are randomly selected. Employing the decision tree algorithm, the training set is also used to train the predictive model. The test set is then used to test

the trained model for its accuracy and the results shows *RSME = 0.65* for this model. Figure 36 is the graphical representation of the predictive model.

In the next step, the importance matrix of feature is extracted for both models. Figure 37 and Figure 38 show the results, in which the race, median income, and education are the common features with the highest impact in both models. Buildings with more than 2 units in both models have the lowest impact.

Table 14 - Input variables: decision-tree and random-forest models.

Category	Variable	Source
$(\text{Socio-economic})_k$	Population	U.S. census
	Number of households	U.S. census
	Median income (population over 15 years old)	U.S. census
	Number of people with minimum college degree	U.S. census
	People aged over 65	U.S. census
	Median age	U.S. census
	Unemployment	U.S. census
	Race - white	U.S. census
	Race - black	U.S. census
	Race - Asian	U.S. census
	Race - Hispanic	U.S. census
$(\text{Built Environment})_j$	Urban/Rural	U.S. census
	Number of housing units	U.S. census
	Number of vacant units	U.S. census
	Density	U.S. census
$(\text{Physical Structure})_j$	Unit type	U.S. census
	Number of bedrooms	U.S. census
Energy rate	Electricity rate per kWh (residential)	[94]
Solar radiation	Potential solar radiation (kWh/Sq. meter / day)	[92]
Predictive variable	Installed PV systems in the residential sector	[90]

Data source *U.S. Census* is extracted from the ACS (2003-2017) published by the U.S. Census bureau

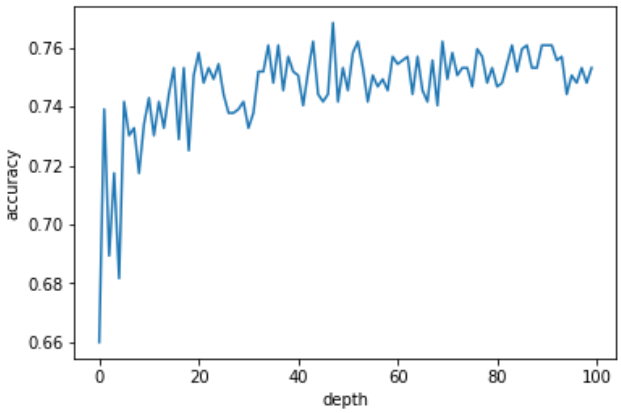

Figure 35 - Random forest: accuracy vs. depth of the tree.

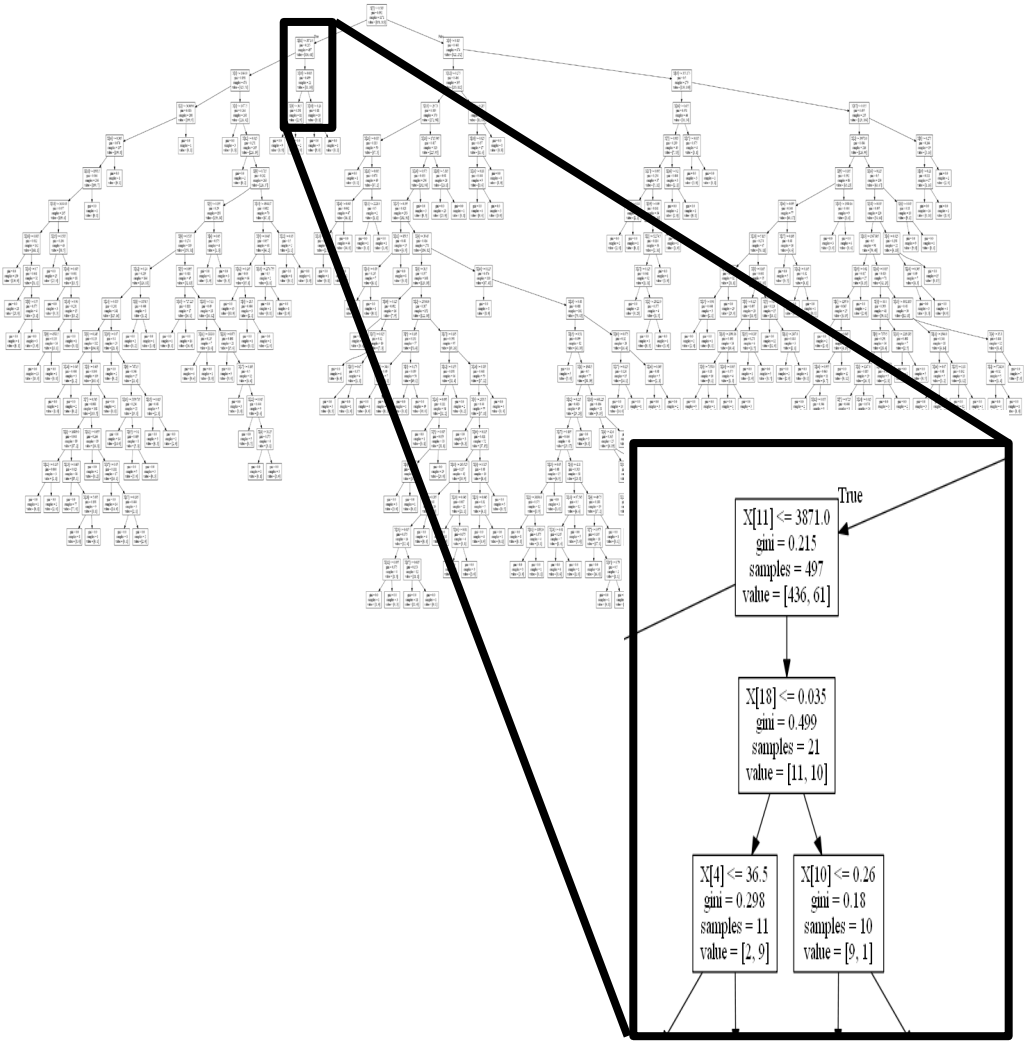

Figure 36 – Result: decision tree.

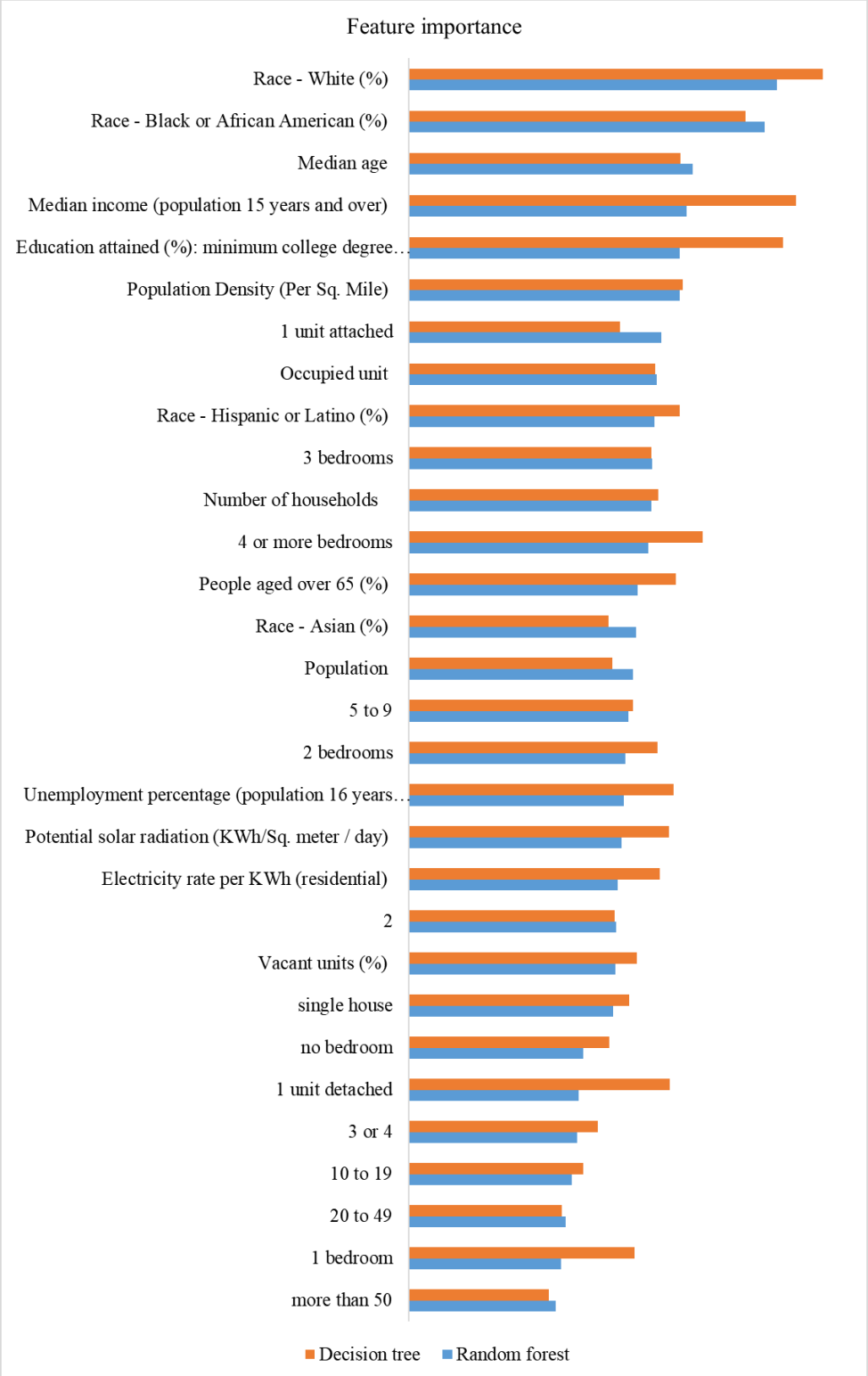

Figure 37 - Result: feature importance, sorted by importance (random forest).

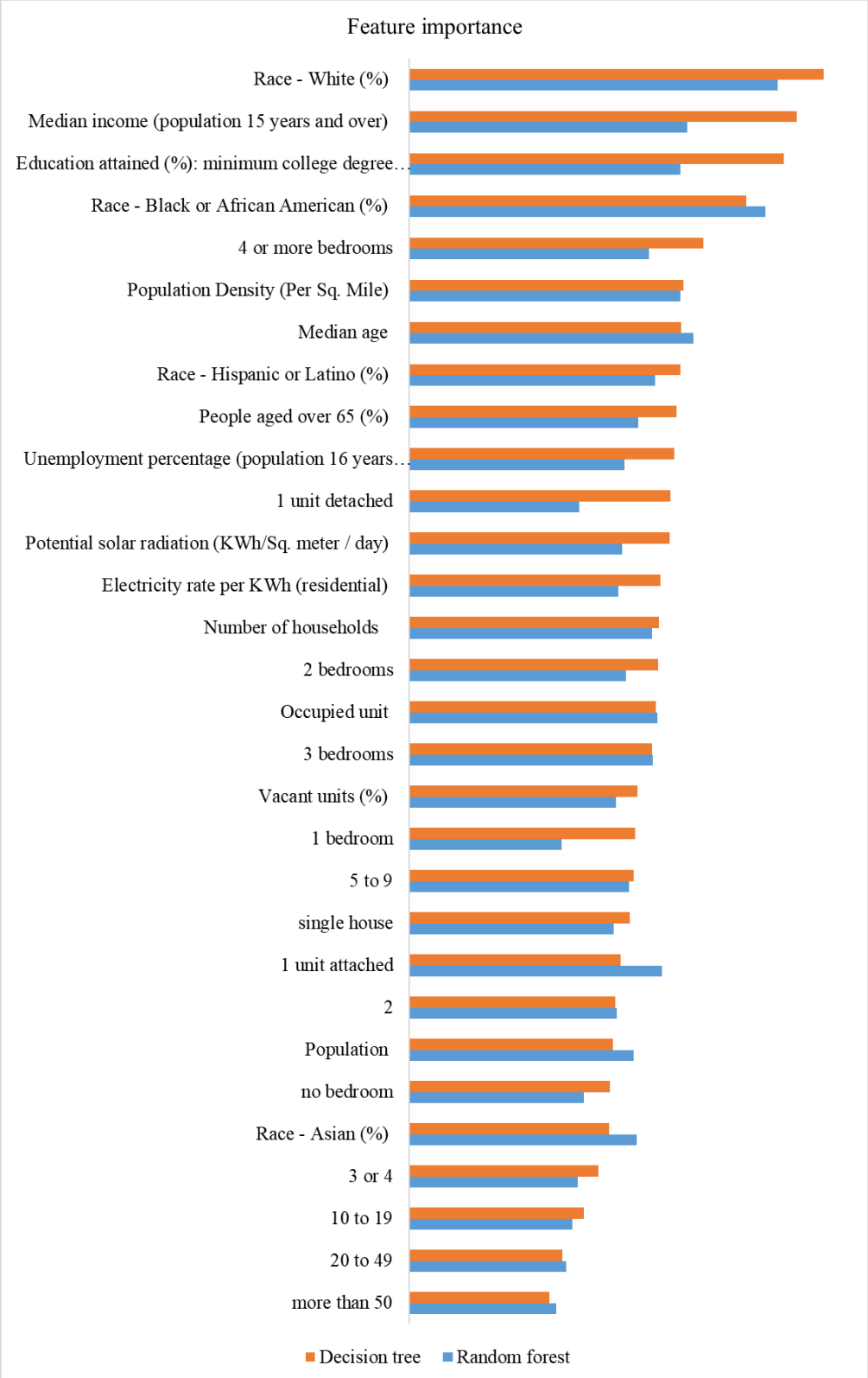

Figure 38 - Result: feature importance, sorted by importance (decision tree).

3.5 Discussion

Studies of diffusion introduced by Gabriel Tarde, a French socialist, and later adopted and published by Everett M. Rogers in 1962. Diffusion of innovation theory indicates the adoption of a new technology passes through five segments based on the propensity of customers to adopt it [49]: innovators, early adopters, early majorities, late majorities, and laggards. The diffusion of innovation theory helps to understand adapters of PV systems and their decision-making process [104]. This is a valuable outcome for shaping an effective policy to induce adoption of PV systems. The results of analyses expressed in this chapter are the base for investigating the adoption of PV systems in Georgia. Clearly, the adoption of PV systems has already the first segment. Results of pattern analysis show the adoption of PV systems in the utility sector has already passed *early adopters* phase and is currently at *early majority* phase. This explains the utility companies' efforts to build solar facilities across the state [105–107]. In the residential sector, the results of clustering analysis indicate the adoption is at the *early adopter* phase. Some of the early adopters' characteristics are being at the higher socio-economic level, being well-informed, being fashion conscious, and being open to change [104]. The results of first and fourth analyses indicate solar radiation, education, median income, are the important features to adopt PV systems, which represent the adopter profile.

The results of the forecast model indicate the share of solar energy in the residential sector will increase up to 300% by the next four years, from 3.3 GWh per year in 2018 to 10 GWh per year in 2022. To estimate the environmental impact of this change, the greenhouse gas emission (GHG) generated by power plants in Georgia is first calculated. In 2016, NREL published a report on GHG from the power plants in the U.S., in which it

provides the average GHG generated by power plants based on their fuel type (Table 15 - Power plants: average GHG generation by fuel source.) [108]. Assuming the generated electricity by PV systems will substitute the electricity generated by the power plants with coal as the fuel source, the adoption of the PV systems (additions) in the next four years will reduce GHG by 6,700 Ton CO_{2e} per year.

Table 15 - Power plants: average GHG generation by fuel source.

Fuel Source	GHG emission per MWh (Kg CO2e)
Natural Gas	430
Coal	1000
Nuclear	59

3.6 Summary

Theory of diffusion explains how the adoption of a new technology goes into five phases from the *innovators* phase to *laggards* phase. The adoption of PV systems gaining momentums during past years. In the U.S., the energy portfolio is on the pace to change, prone to adopt higher share of renewable energy sources. Georgia, with more than 1,800 installed PV systems, is among the top ten states with the highest solar capacity in the U.S. and GHG change during the past decade. While Georgia lack in state-wide policy for encouraging the adoption of PV systems, there are some local incentive programs. Furthermore, several utility companies have built solar facilities across the state. Shaping a new policy to induce the adoption of PV systems requires understanding the socio-economic characteristics of early adopters, to form a more effective policy. Furthermore, forecast the future adoption of PV systems based on the historical data on installed PV systems provides a benchmark to compare the outcome of a policy with business-as-usual scenario.

The results of this study indicate the adoption of PV system in the utility sector is in the third phase of diffusion, and while the initial observation of installed PV systems showed scattered systems across the state, the clustering analysis showed evidence of clustering. This indicates utility companies have already analysed the suitable sites for the adoption of PV systems. In the residential sector the diffusion pattern shows concentration in the north and the east areas, but the clustering analysis identified less evidence of clustering, indicating the adoption of PV systems in the residential sector is in the second phase of diffusion (early adopters). Two predictive models are developed employing two machine-learning techniques: decision tree, and random forest. The two predictive models could predict the adoption of PV system with high accuracy rated at $RSME_{decision\ tree} = 0.65$ and $RSME_{random\ forest} = 0.76$. The extracted values form future importance matrix shows white and African American races, education level, income, and median age are among the most important features in the two predictive models. Moreover, a forecasting model was developed by fitting the historical dataset of the installed PV system in the residential sector, employing ARIMA method. The results of the forecasting model indicate there will be a 300% increase in the generation of electricity via PV systems during the next four years. This change will reduce the GHG emission equivalent to 6,700 ton CO_{2e} per year, assuming additive generated electricity will substitute the electricity generated by the electricity plants with coal as their source of fuel.

This chapter makes two primary contributions to the existing body of knowledge: 1- identifies socio-economic and location-based factors influencing the adoption of PV systems in the residential sector and evaluate patterns of adoption in three sectors: utility, non-residential, and residential, and 2- creates a univariable forecasting model to predict future

adoption of PV systems in the residential sector. The results of this study can help both private industry to identify their target market, and government body to shape a more effective policy, aiming to adopt PV systems. Although this study was conducted in Georgia, assuming the availability of similar datasets, the proposed methodology can be used in other states and internationally.

CHAPTER 4. RENEWABLE REBOUND EFFECT

4.1 Introduction

Although in the U.S. the share of generated electricity by PV systems still is a small fraction of total annual electricity generation, the experience for renewable energy generation in countries like Germany and Denmark shows that the share of renewable electricity generation can change in a short time. A dramatic change in the supply of electricity creates an emerging task for utility companies and the stakeholders involved in the distribution of electricity to manage the merge of the decentralized PV systems into the existing electric infrastructure system, and still keep the balance between generation and consumption. To manage this balance between supply and demand, the electric infrastructure management system needs to compute the residual residential demand for power supplied from the grid. One challenging aspect of this task in the past was the intermittent electricity stream that derives from a group of non-dispatchable and decentralized PV systems. While the power grids were originally designed based on the concept of large controllable electric-generators, the renewable systems, due to the fluctuation in their generated electricity, create a challenge of constant disruptions. To mitigate the fluctuation in the electricity generated by the PV systems, past studies suggested to couple an energy storage system with a PV system [109,110]. However, on the demand side the power grid operators still need to estimate the impact of the adoption of the PV systems on the residual demand response.

One aspect of the demand response that is not yet fully explored is the potential impact of the renewable rebound effect. Rebound effect in general was first observed when

the improvement in energy efficiency did not match with reduction in energy [37]. This inconsistency is defined as the rebound effect, which is the gap between the pre-adoption assessment of the potential energy saving and the actual saving occurring after the implementation of new system or technology with a better energy efficiency [19,111]. The term e*nergy efficiency* is defined as either using less energy to provide the equal amount of service, or using the same amount of energy to provide a higher amount of service [112]. The same or higher service level is an important factor in defining energy-efficiency. The lower energy consumption resulting from a lower service level is considered as energy conservation and is beyond the scope of this study. In the content of the renewable energy systems, the renewable rebound effect explains how the lower average cost per unit of electricity generated by a PV system – with a zero-marginal cost – can cause an increase in household's total energy consumption. Previous empirical studies have revealed that the adoption of a solar PV system results in a statistically significant rebound in the residential sector [7,38]. However, there is a lack in knowledge for a method to predict the renewable rebound effect, for a future adoption of PV systems. This chapter addresses this gap in knowledge by introducing a data-driven econometric framework to estimate the renewable rebound resulting from the adoption of PV systems in the residential sector. The remaining sections of chapter one proceeds as follows: section two provides a brief literature review relevant to this study. Section three introduces the proposed econometric framework and methodology. Section four illustrates an application of the proposed framework and estimates the renewable rebound effect resulting from the adoption of the PV systems, under two scenarios, in Fulton County in Georgia. Conclusions are included in section four.

4.2 Literature review

The idea of rebound effect was first introduced by Jevons in 1865 [112]. Jevons argued the improvement in technology would reduce the price of such service, resulting in the increase of demand for that service [37]. Brookes and Khazzom followed the work of Jevons introduced the Khazzom-Brooks postulate (KBP) [113,114]. The KBP shows – considering the energy price does not change – "the cost effective energy efficiency investment will inevitably increase economy-wide energy consumption above what it would be without that improvement" [19]. While Khazzom emphasized on micro- rebound effect (the impact of energy efficiency standards for household appliances), Brookes addressed the macro effects of the rebound effect (the energy efficiency investment (production side) can lead to a net increase in energy demand). In a follow-up study, Saunders (2008) showed, under the Cobb-Douglas function, the increase in efficiency investment would result in an increase in fuel consumption [115]. Rebound effect, at its broad definition is expressed by the Equation (8). However, the scope and constrains of a study can change this formulation.

To overcome the mentioned issues, researchers decomposed the rebound effect into three main categories: direct, indirect, and economy-wide rebound effect [116,117]. Direct rebound effect includes the effect of two factors: income and substitution [19,111,112]. As the result, the consumers may make a greater use of that same product or service more often or more instantly. Indirect rebound effect considers three factors: income, change in embodied energy, and substitution. The economy-wide rebound effect contains factors in direct and indirect rebound effect, in addition to the effect of energy consumption due to a new equilibrium in the economy.

$$R = 1 - \frac{E_a}{E_P} \quad \textbf{(8)}$$

where

R: rebound effect,

E_a: actual energy saving, and

E_P : potential energy saving.

In a general term, if U represent consumer utility function on two axis chart, in which y-axis represents the consumption of all goods and services (Q) and x-axis represents the energy efficiency of energy service (S), the optimal bundle for a consumer with utility function U_0 is be the intersection of the utility function and budget constrain line (S_0, Q_0) (Figure 39). Since the budget constrain is a function of efficiency, the increase in efficiency will result in the move of the budget constrain toward up, while the intersection of budget-constrains line and y-axis remain constant (the price of other goods and services are constant).

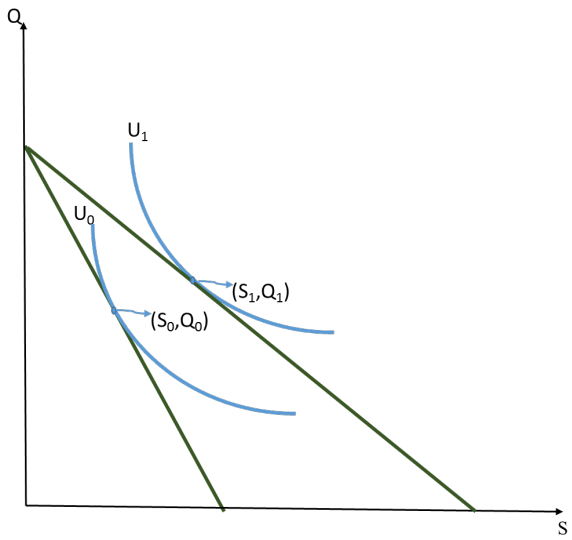

Figure 39 -Optimum bundle for energy service and efficiency, before and after the improve of efficiency (S: efficiency of an energy service, Q: consumption of service, and U: utility function).

The change in demand for the energy services and other goods and services can be decomposed into two categories: substitution effect, and income effect. The substitution effect results in a change in demand for energy services and other goods. The income effect leads to increase in demand for all services and goods to reach a higher utility level. The direct rebound effect is the net change in the demand for energy services (X axis), and indirect rebound effect is the net change in demand for other goods (Y axis) (Figure 40). A 0% rebound effect would maximize the cross-elasticity of rebound effect. The increase in rebound effect rate results in decrease in actual energy saving gained from utilizing the energy efficient service. In case of a 100% direct rebound effect, the cross-price elasticity will be zero and we gain no benefit from the efficiency improvement.

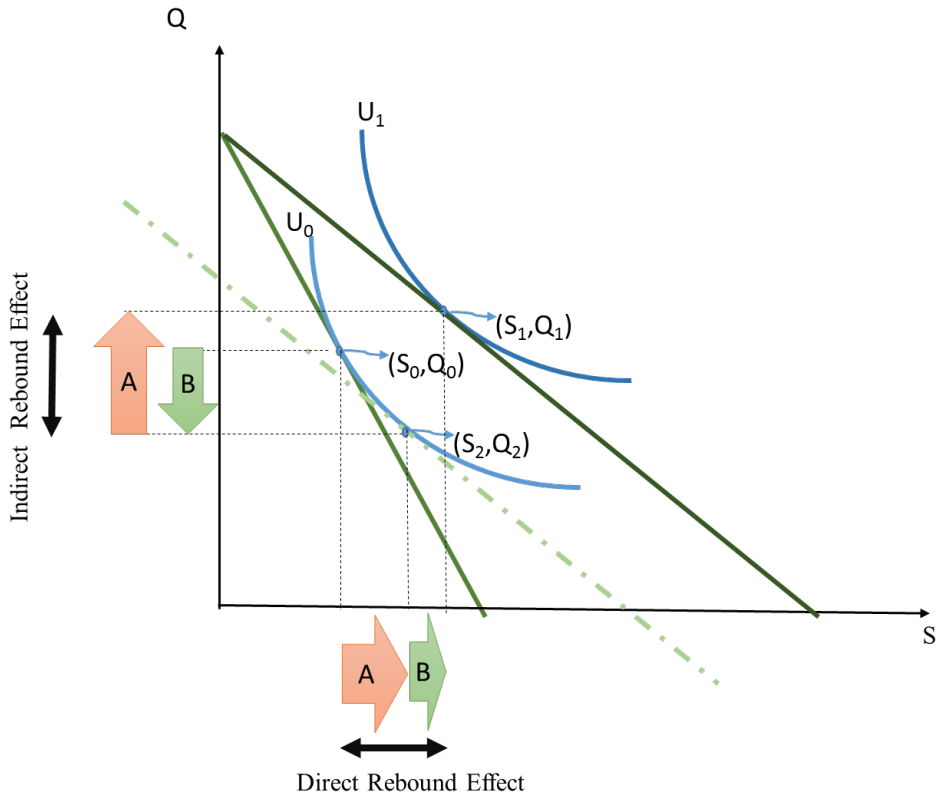

Figure 40 -Direct and indirect rebound effect.

A more common method to investigate different aspects of the electricity demand is empirical studies. For instance past studies provides estimates of the price elasticity of demand (a demand response resulting from an incremental change in a good's price) in the U.S. through empirical studies [19,118,119] range between -.0.02 to -0.12. The price elasticity of demand is the ratio of the percentage change in quantity demanded to the percentage change in price. The direct rebound effect also is typically measured by the elasticity of energy demand with respect to the change of the energy efficiency [19,120,121]. Nässén and Holmberg (2009) estimated the efficiency improvement in several vectors results in 5 to 15 percent direct rebound effect [122]. Direct rebound effect results from the improvement of efficiency for a range of vectors including: space heating [123,124], air conditioning and refrigeration [125]. Some recent studies found empirical evidences that the adoption of the PV systems results in rebound effect. Havas et. al. (2015) showed 15% rebound effect for the generated electricity of the early adaptors of the PV systems in Australia [38]. In another empirical study of 1.7 million homes over a course of four years since 2011, showed an average of 16% to 21% rebound effect per kWh electricity generated by the PV systems in Sydney and its adjacent areas [7].

4.3 Methodology

4.3.1 Renewable rebound effect

The proposed econometric formulation is developed on the basis of the existing economic model expressed by Chan and Gillingham [121]. Subject to a budget constrain, microeconomic theory of consumer behavior suggests a maximization of the household utility function. One of the most common used utility function to model a demand function

is the Cobb-Douglas utility function, in which household consumptions are separated into two main categories: electricity consumption and consumption of any other goods or services (Equation (9)).

$$U(X,Y) = X^{\alpha}Y^{1-\alpha} \quad s.t.\ budget\ constrain \tag{9}$$

where

X: $household\ electricity\ consumption$, and

Y: $consumption\ of\ all\ other\ goods$.

Assuming the electricity generated by a PV system is a perfect substitution for grid electricity, the total electricity consumption after installing the PV system is calculated by Equation (10). Equation (9) subjects to the budget constraint, in which price of Y is normalize to one (Equation (11)). To find the extrema of Equation (9), subject to the budget constraint, the Lagrangian multiplier is used (Equation (12)).

$$X = X_{pv} + X_{grid} \tag{10}$$

$$electricity\ rate * X_{grid} + Y' \leq Income \tag{11}$$

$$\mathcal{L} = U(X,Y) + \lambda\big(Income - electricity\ rate * X_{grid} - Y' =\big) \tag{12}$$

where

X_{pv}: $electricity\ generated\ by\ the\ PV\ system,$ and

X_{grid}: $electricity\ from\ the\ grid$.

The first order conditions are:

$$U_X - \lambda(electricity\ rate) = 0 \quad \textbf{(13)}$$

$$U_Y - \lambda = 0 \quad \textbf{(14)}$$

$$Income - electricity\ rate * X_{grid} - Y = 0 \quad \textbf{(15)}$$

The Marshallian demand function then mathematically shows the optimal choice of electricity consumption as a function of electricity rate and income (Equation (16)).

$$X^*_{grid} = \frac{\alpha * M - (1-\alpha) * X_{pv} * electricity\ rate}{electricity\ rate} \quad \textbf{(16)}$$

$$\alpha = \frac{X_{grid} * electricity\ rate}{income} \quad \textbf{(17)}$$

$$\mu = \frac{X_{pv}}{X} \cdot \frac{\partial X}{\partial X_{pv}} = \frac{\alpha * X_{pv}}{X_{pv} + X^*_{grid}} = \frac{\alpha * X_{pv}}{X_{pv} + \frac{\alpha * income - (1-\alpha) * electricity\ rate}{electricity\ rate}} \quad \textbf{(18)}$$

Equation (18) shows the direct rebound effect (μ), in terms of elasticity of total electricity consumption with respect to the electricity generated by the PV system (X_{pv}). The proposed formulation indicates a percentage increase in total electricity consumption resulting from a 1% incremental increase in the electricity generated by a PV system. The inputs for the proposed data-driven renewable rebound effect formulation are: household income, electricity rate, electricity consumption prior to the instating the PV system, and electricity generated by the PV system.

4.3.2 Estimating electricity consumption

While the electricity consumption data is available to a grid operator within its service area, it is not available for public access. To estimate the electricity consumption of household, a linear regression model is developed, given the available sample of household energy consumption provided by the U.S. Energy Information Administration (EIA) as the dependent variable and socio-economic, location, climate, built-environment, and physical and building structure as explanatory variables.

4.3.3 Estimate electricity generated by PV systems

While the annual electricity generated by the PV system can be obtained by an empirical method, an estimate of electricity generated by future adoption of PV systems requires a simulation technique. Previous studies have validated the use of geographic information system (GIS)-based method, in which a simulation model combines light detection and ranging (LiDAR) and rooftop datasets as inputs, estimate potential electricity generated by the rooftop PV system [69,126]. For an accurate estimation, not only the model needs rooftops' surfaces that would be available for PV installations, but it also must evaluate the geographical and spatial characteristics of the surfaces such as surface angle to the sun and possible shading effect caused by adjacent obstacles.

4.4 Numerical Example: Renewable Rebound Effect in Fulton County, GA

Through a case study the proposed method for estimating the DRE resulting from the adoption of PV systems in the residential sector is presented in this section. The scope of the study is Fulton County, Georgia, USA, in which the city of Atlanta and several major

suburbs are located. Table **16** presents basic summary data for Fulton County. The micro-boundary is census block-group. This is the smallest boundary for which the required explanatory variables are publicly available.

Table 16. Basic summary data, Fulton Co., GA, USA.

	Unit	Value	Source
Area	Square Mile	534	fultoncountyga.gov
Population	Persons	1,023,336	U.S. Census (v2016)
Housing	Unit	464,473	U.S. Census (v2016)
Families	Household	385,103	U.S. Census (v2016)

Neighborhoods in Fulton County vary in population densities and socio-economic attributes. The diversity provides a basis of comparison for how at a constant spatial adoption rate of PV systems, neighborhoods in a city may experience a range of DRE's. The DRE is calculated on annual level, which is governed by the time frame of explanatory variables. Figure 41 illustrates the spatial variation in population density and the average annual household income within Fulton County by census block-group.

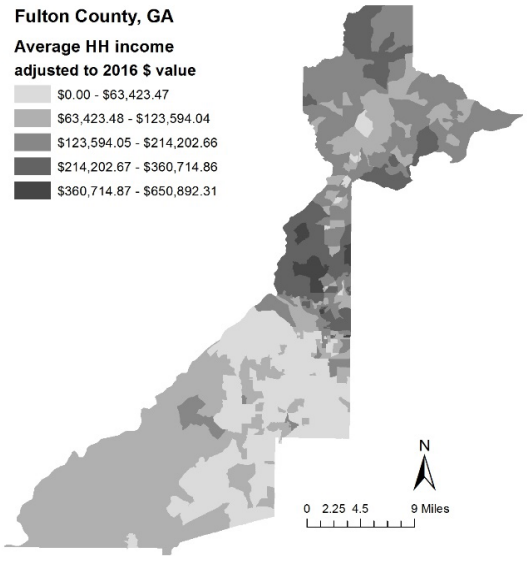

Figure 41 - Population density (left) and average household income (right), Fulton County.

4.4.1 Results – electricity consumption

To estimate of baseline energy consumption per household, a two-step computation method is employed: 1- a linear regression on available sample data of energy consumption, and 2- apply the obtained parameters to block-group specific data for the same variables for Fulton County. The electricity consumption sample is extracted from the residential energy consumption survey (RECS) (v2009), published in 2015 by EIA. Table 17 summarizes the explanatory variables and their sources.

Table 17. Summary of input variables – estimate baseline electricity consumption per household, Fulton County (Census block-group level).

Variables		Description	Sources
Dependent variable		Baseline electricity consumption (kWh)	RECS (2015)
explanatory variable	Location	Census region State Housing unit location: Metro- or Micro-politan areas Housing unit location: urban or rural	U.S. Census Bureau ACS (2003-2017)
	Climate	Building America climate region Heating degree day (HDD) (base temperature 65F) Cooling degree day (CDD) (base temperature 65F)	U.S. IECC; wunderground.com; U.S. Dept. of Energy
	Building	Average year housing units were built Average building type composition Average housing unit square footage	U.S. Census Bureau zillow.com
	Socio-economic	Average percent rent versus own Average race composition of block group Average employment status of householder Average education completed by householder Average number of household members Median household income	U.S. Census Bureau

Table 18. Common explanatory variables.

Census region	South
State	Georgia
Metro/micro	Metro
Urban/rural	Urban
Climate region	Mixed-humid
Heating Degree Days	2971
Cooling Degree Days	1965
Price per kWh ($)	0.125

Table 19 - Summary statistics and results.

Variables	**Mean**	**St. Dev.**	**Min.**	**Max.**
Avg. year built	1976	17.8	1939	2005
Building type (proportions)				
Single family detached	0.546	0.339	0	1
Single family attached	0.055	0.082	0	0.573
Apt. Bldg., 2-4 Units	0.061	0.082	0	0.537
Apt. Bldg., 5+ Units	0.338	0.315	0	1
Avg. square feet	2160.55	530.59	1120.26	5987.43
Rent (proportion rented)	0.369	0.231	0	0.976
Race (proportions)				
White	0.452	0.362	0	1
Black	0.463	0.389	0	1
Native American	0.002	0.011	0	0.215
Asian	0.045	0.084	0	0.67
Pacific Islander	0	0.003	0	0.039
Other	0.02	0.054	0	0.508
Two or more races	0.018	0.024	0	0.192
Employment (proportion employed)	0.585	0.149	0.139	0.952
Education (proportions)				
No HS diploma	0.116	0.124	0	1
HS diploma/GED	0.201	0.142	0	0.617
Some college/assoc. degree	0.231	0.101	0	0.682
Bachelor's degree	0.277	0.161	0	0.705
Master's degree	0.121	0.09	0	0.544
Professional degree	0.037	0.05	0	0.304
Doctorate degree	0.017	0.022	0	0.171
Avg. number household members	2.539	0.613	1.3	5.13
Median household income ($)	88,553.15	67,497.30	12,262.35	465,495.90
Estimated baseline electricity consumption per household (kWh)	13,516.00	2,718.86	7,568.87	21,497.13

Georgia Power Co. operates the electric grid in Fulton County and the average price of electricity for the city of Atlanta over the period 2013-2017, was roughly $0.125/kWh [127]. Table 18 presents common explanatory variables and Table 19 present results of summary statistics, and estimates of baseline electricity consumption per household. Figure 42 shows the results of the electricity consumption estimate. In Fulton County, compared to other Counties in Georgia, a significantly larger proportion of households occupying much smaller apartment homes. Neighborhoods located in the center and east of this county have the highest population density, in which the estimate of electricity consumption shows the households in these neighborhoods on average consume less than the mean predicted value for this County. Additionally, the variance of the electricity consumption in Georgia in the RECS dataset is greater than that of the predicted values for Fulton County.

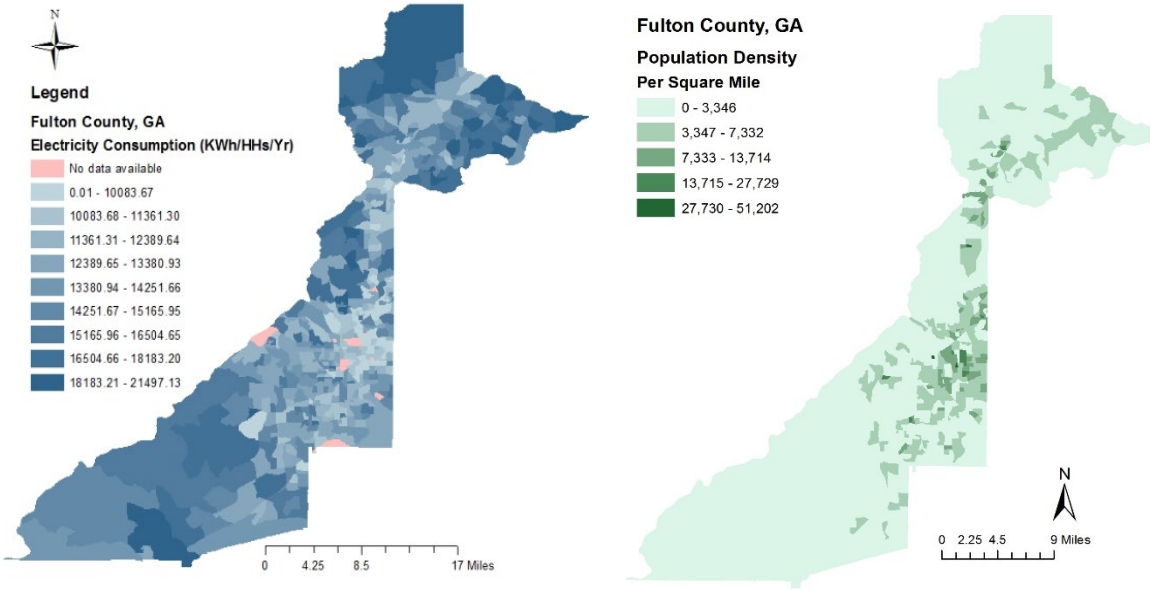

Figure 42 - Estimates of baseline electricity consumption per household (left) and population density (right) in Fulton County.

4.4.2 Results – potential electricity generation by PV systems

A GIS-based simulation model is developed and employed to estimate the generated electricity by a rooftop PV system under two hypothetical adoption scenarios: moderate and aggressive. The moderate scenario assumes 20% of the rooftop areas are covered with the PV panels whereas the aggressive scenario assumes PV systems cover 40% of the rooftop areas. A higher than 40% of rooftop area coverage may not be technically feasible since not all areas on the roof have an exposure to sunlight with the required angle. Moreover, the existing openings and utilities installed on roof areas reduce the available area to install PV systems. To develop the simulation model, first a digital surface model (DSM) is generated, from the LiDAR data, which identifies elevation, tilt, and azimuth of all surface areas.

A GIS model is developed to simulate the shading effects via the ArcGIS *solar radiation tool*, which analyzes the effect of the sun on a given geospatial location over predefined time intervals. This tool computes the seasonal and hourly shifted sun angle in addition to the effects of elevation, slope, orientation, and possible permanent shadows for the purpose of calculating the solar radiation at each time interval [128] (Figure 43). In the next step, a building footprint model is pruned to contain only the information from residential buildings and this dataset is then used to filter the potential solar radiation. The average efficiency rate of PV systems and rooftop coverage of PV panels are then applied to compute the potential electricity generation under two scenarios (Figure 44).

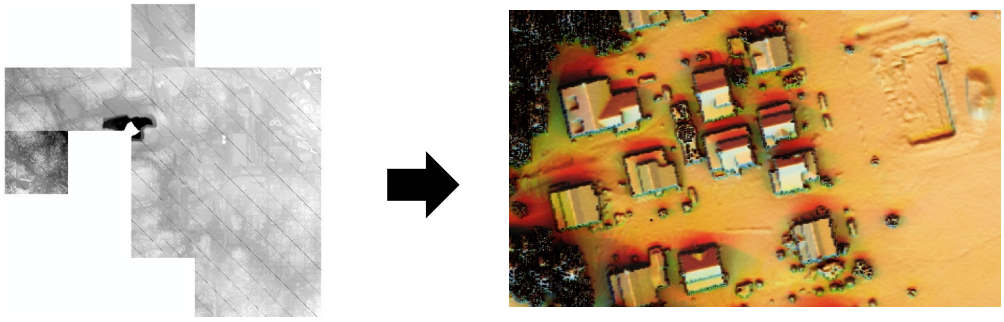

Figure 43 - Sample of results: estimate potential electricity generation via PV systems: DSM (left) and potential solar radiation (right).

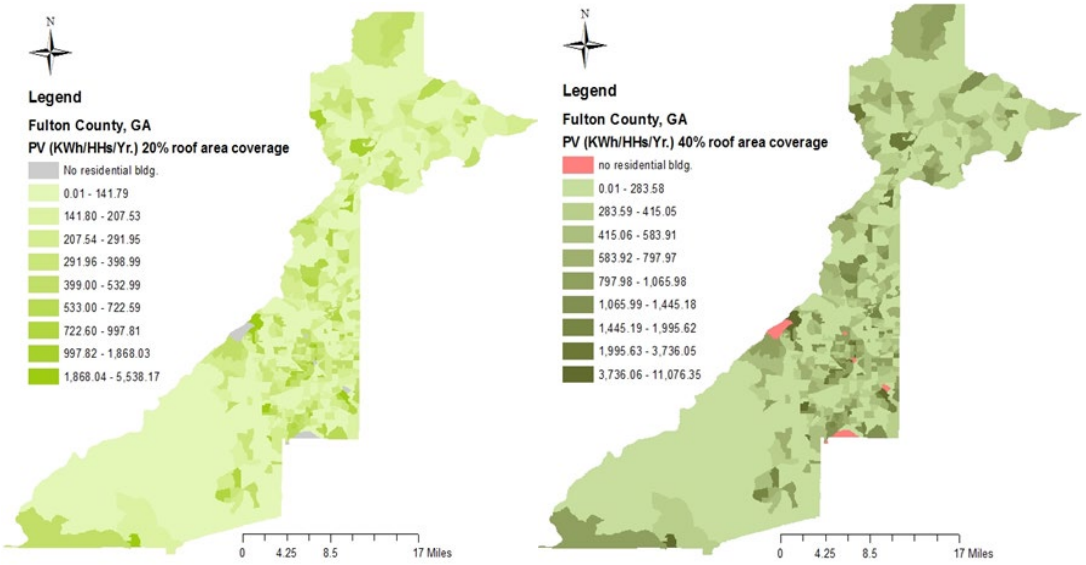

Figure 44 - Potential electricity generated via rooftop PV systems per household: moderate (left) and aggressive (right).

4.4.3 Results – renewable rebound effect

The calculated input variables are plugged into the Equation (18) and the annual renewable DRE per household are computed for the two adoption scenarios in each census block group. Table 5 presents summary statistics of the results. The computed DRE is measured as an elasticity at the margin, expressing the ratio of the marginal percentage change in total electricity consumption to a marginal percentage change in electricity

generated by a PV system. The results range between 0.000028 and 0.036 in the moderate diffusion scenario and between 0.000028 and 0.035 in the aggressive scenario, with a mean of 0.0016 (median of 0.0006) in either case (note that these numbers are not identical despite appearing so due to rounding). Translating these values of rebound effect as a percentage of marginal increase in the electricity generated by a PV system, the results for the moderate scenario range between 0.98 and 29.4 percent with a sample mean of 5.848 percent (median 4.426). The sample mean of 5.8% indicates that for each additional kWh of electricity generated by the PV system, we expect to have a 5.8% rebound. This mean if a PV system generates 100 kWh electricity in one year, the grid electricity consumption declines by 94.2 kWh, instead of 100 kWh. Figure 45 shows a graphical representation of the results.

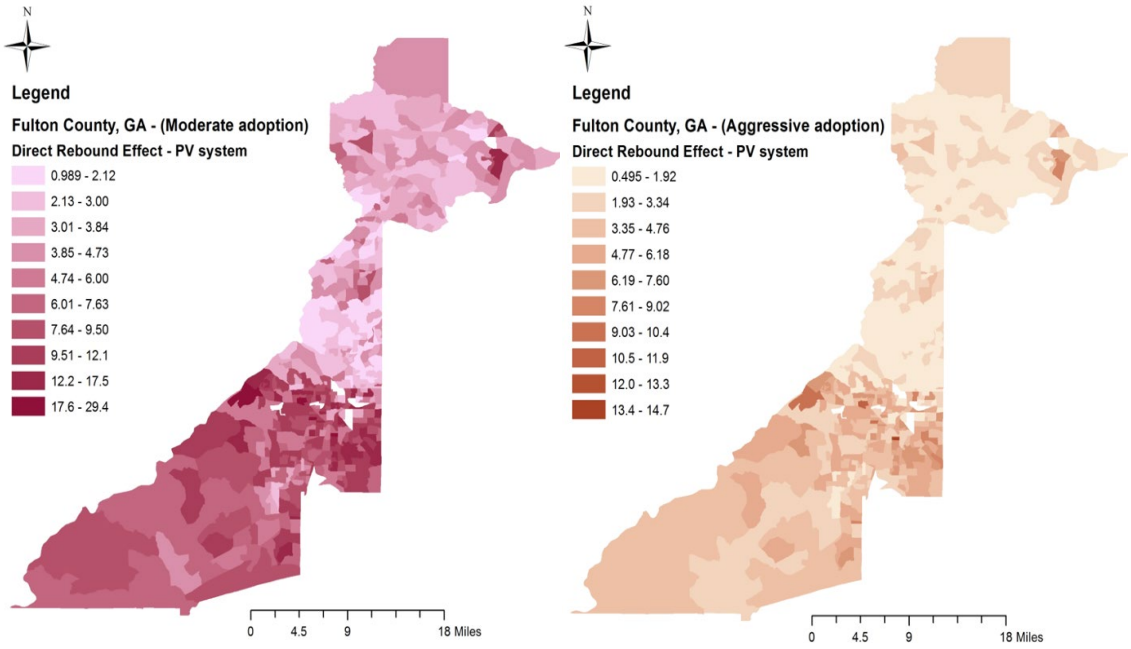

Figure 45 - Estimated renewable rebound effect, measured as percentage of marginal change in PV output: moderate (left) and aggressive (right) adoption.

Table 20. Direct rebound effect: summary statistics.

Renewable rebound effect	Mean	St. Dev.	Median	Min.	Max.
Calculated rebound effect as elasticity					
Moderate	0.00159	0.00368	0.0006	0.00003	0.03585
Aggressive	0.00158	0.00363	0.0006	0.00003	0.03522
Calculated as percentage of marginal increase in PV output					
Moderate	5.84767	3.94682	4.42628	0.98918	28.4043
Aggressive	2.92384	1.97341	2.21314	0.49459	14.70215

4.4.4 Discussion

The results show that under the two hypothetical scenarios, the highest potential rebound effect occurs in areas where the neighborhoods with a lower average income level are located. The primary reason for this is that households in these low-income neighborhoods typically spend a larger share of total income on electricity, as indicated by the spatial correlation between the demand parameter α and income. The availability of marginal free electricity supplied by a PV system results in an *income effect*, in which the reduced cost of electricity holding income constant acts in similar in effectively as it would in the case of an increase in income holding the cost of electricity constant; the household will spend a portion of that effective income increase on further consumption of electricity. This income effect is highest for those households who spend the greatest proportion of their income on electricity consumption. One implication of this result is that policies on inducing the adoption of PV systems may be more effective if they are enhanced with features to smooth the demand response in low-income neighborhoods. Such mechanisms range in a variety of forms, including coupling an incentive to install a PV system with another incentive for LED lights or time-switches.

A previous empirical study by Deng et. al. (2017) reported, after installing PV systems, rebound effect ranges between 4.5% to 8% [7]. However, there existed a FiT program

which boosts the rebound effect. Deng el. al. study concluded that the rebound effect for customers with FiT of 20 cents per Australian dollar ranges between 4.5% and 7.5% and for those with 60 cent per Australian dollar ranges between 5% and 8%. No FiT program is one of the relaxation assumptions in the proposed renewable rebound effect framework in this dissertation. Adding a FiT program can increase the renewable rebound effect more than the estimated values in this case study. While the estimated values for the rebound effect in Fulton County seam small, considering the aggregated rebound effect in the aggressive adoption scenario, we will have a 177,658 kWh increase in electricity consumption rather than a reduction in grid consumption by installing the PV systems. This calculation only covers one renewable technology. Other technologies with zero marginal resource cost, such as wind turbines or combined head and power systems can magnify the rebound effect. The cumulative renewable rebound effect, inclusive of all renewable energy technologies with zero or near zero monetary cost of resources can perturb the demand-supply balance in an electric infrastructure system even resulting in a blackout, which can cost $5 per kWh of lost electricity [129].

Consider a hypothetical case in which, during the summer, a cloudy day is followed by a sunny day. Under the moderate diffusion scenario, 268 MWh of electricity would be generated by PV in Fulton County on the sunny day, compared to 131 MWh on the cloudy day—a change of 137 MWh from one day to the next. At a 5.8% DRE, if the rebound were not incorporated into the grid manager's residual demand forecast, the forecast of the residual demand change would be off by 7.94 MWh, which may result in a significant voltage imbalance in some areas. A greater adoption rate of PV systems can result in a higher difference. Past studies showed that an imbalance rate higher than 2% can damage

transformers, voltage regulators, and electronic appliances such as computers and entertainment equipment [130].

4.5 Summary

Previous studies have found evidence of a rebound effect resulting from the adoption of a renewable energy generation technology: residential PV systems [7,38]. A high rate of adoption for residential PV systems is likely to have important consequences for electricity grid managers. This rebound effect not only has potential to perturb the demand-supply balance of an electric infrastructure system, but also diminishes a part of supposed substitution of grid electricity, and its positive environmental impact. There is a lack in knowledge for predicting the rebound effect resulting from the adoption of a renewable energy source such as a PV system. This study presents a data driven econometric framework for predicting this rebound by combining standard economic modeling with geographic information systems (GIS) based modeling and statistical methods. The required input data for the proposed framework, in the case of adoption of a PV system, include household income, an estimate of household electricity consumption prior to installation of the PV system, the retail electricity rate, and potential electricity generated by the PV system. An application of the proposed framework is demonstrated with a case study about the adoption of PV systems in Fulton County, Georgia. The results show that in Fulton County which has an aggressive adoption of PV systems, the estimated rebound effect is 5.8% which is within the reported rebound effect by previous empirical studies [7,38]. The results suggest that for a marginal increase in electricity generated by a PV system, the reduction of grid electricity will be 5.8% less than expected.

CHAPTER 5. RESILIENCE ASSESSMENT FRAMEWORK

5.1 Introduction

The electric infrastructure system acts as an enabling function for the other infrastructure systems, including transportation, water, food, financial institute, and healthcare systems. In the U.S., the electric infrastructure system consists of more than 6,413 power plants (generation) and approximately six million miles of high-voltage transmission lines (distribution), serving more than 300 million customers [2,3]. This widespread infrastructure system, however, is vulnerable to hazardous incidents, including natural disasters and cyberattacks [131]. Recent natural disasters have shown a disproportionate consequence of disruption in delivering the electricity or power failure on the entire country ranging from partial to complete power lost [28,132]. Between 2003 and 2012, 679 power outages occurred across the U.S. with annual costs between $18 and $33 billion [131]. Protecting the electric infrastructure system from unforeseen failures requires developing a complex system capable of providing a high level of safety and reliability. However, it is not viable to develop a system with 100% resistance to a mishap. As so, the concept of resilience with a core objective of withstanding to turbulence and returning rapidly to a near pre-incident service level was introduced to system engineering [39,52,133].

In general, the term “resilience” describes a capability of a system to remain in the state of equilibrium under an extreme condition, or a dynamic behavior of the system under stress [134]. The concept of resilience provides a new approach to address the system failure issue, with the focus on failure prevention and recovery efforts. To design a

resilience system as a capability augmentation that maintains a level of service function post-incident and manage to retrieve its service in a comparatively short time, is a relatively new concept. Resilience metrics enable system designers and strategy developers to compare system performance at different points in time, pre- and post-incident with a range of simulated incidents. Past studies introduced a range of resilience metrics. Bruneau et al. offered a broad definition of resilience covering actions that reduce losses from an incident, including the effects of mitigation and recovery [32]. The authors then introduced four dimensions of resilience: robustness, resourcefulness, redundancy, and rapidity. Later, they proposed a deterministic static metric that measures the loss of service performance in the case of a natural disaster (earthquake). Henry and Ramirez-Marquez presented a time-dependent resilience metric that defines resilience as the ratio of the performance recovery over the total loss due to a disruptive incident [35]. Cimellaro et al. proposed a resilience metric based on the quality of service with a weighting factor that represents the importance of pre- and post-incident service qualities and control time [135].

Though these previous studies introduced some metrics to assess the resilience capacity of a system, none of the proposed methods explicitly quantified the four dimensions of the resilience: robustness, redundancy, resourcefulness, and rapidity. While the design of most electric infrastructure systems in the U.S. is based on the core concept of centralized generation and distribution of generated electricity (distribution networks), during a power failure decentralized emergency generation systems – also known as distributed generation (DG) systems – can provide the needed electricity. Despite the conventional DG systems with a combustion engine, a PV system can also act as an emergency electricity generator [136]. However, previous studies did not count the contribution of decentralized

emergency DG systems in their evaluation of the resilience capacity of an electric infrastructure system. Furthermore, the consequences (both fatality and monetary) of a power failure are not equal among the end-users. For example, during the recovery process, addressing the needed electricity of critical end users such as hospitals has a higher priority than those of routine end users such as the residential sector. This leads to the third gap in knowledge; the previously proposed quantification resilience methods did not connect their resilience models with end-user types and focused only on the overall system performance.

This chapter addresses the expressed gaps in knowledge by developing a new quantitative resilience framework founded on the existing concept of resilience and the definitions of four resilience dimensions: robustness, resourcefulness, redundancy, and rapidity. Moreover, the proposed framework incorporates the contribution of both primary (centralized) and emergency (decentralized) service providers in a system. Unlike previous methods, the proposed framework differentiates among the end-users and presents a state of the art approach to evaluate the resilience capacity of a system. To achieve this objective, the remainder of this chapter is organized as follows: the second section reviews the existing concepts of resilience and presents a survey of previously proposed resilience metrics. Section three introduces the proposed resilience framework. Section four illustrates advantages of the proposed framework with two notional examples, and compares the results with a previously proposed metric. Section five includes conclusion and future works. The result of this study can help policy makers and system designers to measure four dimensions of resilience, compare the estimated resilience capacity of a system under a range of scenarios, and improve system resilience capacity.

5.2 Literature Review

Youn et al. (2011) defined engineering resilience as the sum of reliability (i.e., the passive survival rate) and restoration (i.e., the proactive survival rate) capacity [137]. The design of engineering resilience should capture the normal functioning of a technical system and incorporate the failures of the system in cases of hazardous incident [138]. The aggregated properties of a resilient system consist of one or more of the following abilities: to anticipate, to absorb changes, to resist, to adapt, to recover (quickly), to reduce the chance of failure, to provide minimum service while under stress, to provide minimum service during changes in the service level, and to sustain a shock [32,39,52,139,140]. Bruneau et al. (2003) expressed four dimensions of resilience of an infrastructure system [32]:

1- *Robustness*: the ability of a system to prevent the dissemination of damage during a hazardous incident,
2- *Redundancy*: the ability of a system to provide service using other resources in case of an incident,
3- *Resourcefulness*: the capability of a system to respond to a hazardous incident and mobilize needed resources/services, and
4- *Rapidity*: the speed of a system to return to its original state.

Later, they proposed a deterministic static metric for the resilience loss of community service in case of an earthquake, evaluating the resilience capacity by the system performance level over (Equitation (19)).

$$Resilience = \int_{t_0}^{t_1} [100 - Q(t)]dt \quad \textbf{(19)}$$

where

t_1: the time at which the system returns to its normal state,

t_0: the time at which the incident occurs,

$Q(t)$: the system performance level at time t (represents types of performance measurements).

Cimellaro et al. (2010) proposed a resilience metric based on the quality of service with a weighting factor that represents the importance of pre- and post-incident service qualities and control time (Equation (20) [141]. The authors used this measurement, in which they implied the waiting time for the patient as an important index for service quality, to quantify the resilience of the health care system. The weighting factor in their formulation enabled them to consider decision-making preferences. The four properties of resilience (rapidity, resourcefulness, redundancy, and robustness), however, are not explicitly included in their resilience metrics. In their paper, the authors presented a method that prioritizes demand for service and provided quality of service during the recovery process.

$$R = \propto \int_{T_{lc}} \frac{Q_1(t)}{T_{lc}}\, dt + (1-\propto) \int_{T_{lc}} \frac{Q_2(t)}{T_{lc}}\, dt \quad \textbf{(20)}$$

where

R : Resilience of a system

$\propto$: Weighting factor

T_{lc} : Control time of the system.

$Q_1(t)$: Pre-incident service quality

$Q_2(t)$: Post-incident service quality

Henry and Ramirez-Marquez (2012) developed a time dependent metric that quantifies resilience as the ratio of system performance to its performance loss [35]. To assess resilience, they proposed measuring the performance function at one point in time. The authors suggested dividing the performance-time chart into multiple stages to enhance the expression of the resilience of a system, and they concluded a system can go through three states:

1- Steady state represents the original state before an incident occurs,

2- Disrupted state presents the performance of the system after the disruptive incident occurs (t_e) and continues to a point at which the system reaches a new steady state (t_s), and

3- Stable recovered state is the new steady state after the recovery is initiated and completed at time t_s.

After concluding the above, from which they developed the plot of performance over time, the authors presented a time-dependent measurement (Equation (21), in which the numerator refers to the recovery until each point in time and the denominator reflects the total loss resulting from a disruptive incident. If a system, compare to the pre-incident performance level, reaches the same or almost the same performance level after the recovery process post-incident, the proposed metric returns a very large resilience capacity

in a system. Moreover, this proposed metric system does not differentiate the end-user and incident types.

$$Я_{\varphi}\left(t\middle|e^{j}\right) = \frac{\varphi\left(t\middle|e^{j}\right) - \varphi\left(t_{d}\middle|e^{j}\right)}{\varphi\left(t_{0}\right) - \varphi\left(t_{d}\middle|e^{j}\right)} \quad \textbf{(21)}$$

where

$Я_{\varphi}\left(t\middle|e^{j}\right)$: Resilience of a system at time t,

$\varphi\left(t_{0}\right)$: System performance (pre-incident),

$\varphi\left(t\middle|e^{j}\right)$: System performance at time t after the occurrence of incident e^{j}, and

$\varphi\left(t_{d}\middle|e^{j}\right)$: System performance once it stables after incidente^{j}.

Francis and Bekera (2014), based their dynamic measurement metric on three resilience capacities: 1- *absorptive*: capacity of a system to absorb the impact, 2-*adaptive*: the ability of a system to adjust to an undesirable situation by undergoing some changes, and 3-*recovery*: the speed of recovery for the system to return to a normal performance level [36]. Then they used performance and time- dependent variables to assess the resilience of the system (R_i) by a function of the three resilience capacity factors (Equation (22). The authors, however, did not clearly define the relationship between adaptive and absorption capacity. The authors used an exponential model to define the recovery capacity (Equation (23).

$$R = S_p \frac{F_r}{F_0} \frac{F_d}{F_0} \quad \textbf{(22)}$$

$$S_p = \begin{cases} \left(\frac{t_\partial}{t_r^*}\right)^{\exp(-a(t_r - t_r^*))} & t_r \geq t_r^* \\ \left(\frac{t_\partial}{t_r^*}\right) & t_r < t_r^* \end{cases} \quad \textbf{(23)}$$

where

F_r: performance level at a new stable level after recovery efforts,

F_d: performance level immediately following a disruption, and

F_0: performance level at its original state,

t_∂ : slack time, which is the maximum allowable time for the system to start the recovery process,

t_r : time to final recovery or time to reach a new equilibrium state, and

t_r^* : time to complete the initial recovery actions.

According the Francis and Bekera formula, if the system performance drops to zero after an incident, the resilience of the system is equal to zero, despite how fast it then recovers. The electric infrastructure system may experience a short blackout after a hazardous incident, at which the equation IV rates the system with zero resilience capacity. Moreover, any specific response by the electric infrastructure system, such as shut down service within the damaged areas or partial shutdown to protect the system from further consequences of the incident or due to safety protocol, would also be evaluated by equation IV as a system with no resilience capacity. Hosseini et al. (2016) suggested changing the absorptive capacity ratio from ($\frac{F_d}{F_0}$) to ($\frac{F_r}{F_0 - F_d}$), thereby providing a more effective formulation for the adaptive and absorptive capacities [52].

5.3 Proposed Resilience Framework

This section introduces a proposed resilience framework, which is an extension of the existing resilience concept and its four dimensions discussed earlier. The time dimension, emphasized in the previous methods and the department of homeland and security (DHS) protection plan is an important factor in the proposed framework [142]. In addition, this framework incorporates the prioritization of the end users, and the contribution of decentralized emergency electricity generators. The total electricity generated by emergency electricity generators is aggregated into a single variable named DG system (F_{DG}in Figure 46) [12]. The proposed framework divides the resilience capability of a system into two main phases: pre- and post-incident. In this framework incident is an event that causes damage to a system to the extent to which the system cannot absorb it and the service level, compared with its initial stable level, drops to a lower level ($F_d$in Figure 46). Because emergency (DG) systems still generate electricity post-incident, the overall system maintains some level of resilience, even when the primary system is down. The post incident recovery is divided into three phases: from the first stable stage after the incident (t_0), until the system reaches the level at which it satisfies the priority demands (t_1); and then the second phase starts at (t_1) and finishes once the system satisfies the urgent need (t_2). The last phase starts from the urgent satisfaction point (t_2) and finishes at t_3. At the end of the third phase (t_3), the system reaches its final stable stage and satisfies routine service needs. Four performance levels – $F_0, F_1, F_2, and\ F_3$ – represent the overall system performance level at which it satisfies the minimum required service level for each associated demand type:

F_0 - the performance level immediately after the incident, including the provided service by the DG systems,

F_1 - the system performance level at the point where it satisfies the need for the first tier of customers,

F_2 - the system performance level at the point where it satisfies the need for the second tier of customers, and

F_3 - the performance level at the new stable level. The recovery reaches its final stage and the system satisfies the required service for all tiers of end users.

Explicit recognition of customer types allows for a more meaningful characterization of resourcefulness and rapidity dimensions (i.e., the ability of the system to meet priorities in a timely manner).

5.3.1 Demand type

Electricity infrastructure supports a range of end-users, each of which has a unique demand pattern and impact associated with power disruption. The end-users are categorized into three categories: *Priority, urgent,* and *routine* (Table 21).

At the broadest level, end users are divided into two categories: supporting critical infrastructure, and standard consumption. *Routine* consumption category, which is defined as all electricity demand not recognized as critical infrastructure according to Presidential Policy Directive 21, consists mainly of residential demands [28]. Critical infrastructures, as defined by the U.S. Department of Homeland and Security, are conceptualized by two general categories: *priority* and *urgent* services [143]. The *priority* sector consists of a group of end-users that require continuous access to electricity to avoid a major loss of life or economic impacts, for instance to prevent a nuclear meltdown or to operate medical equipment. The *urgent* category consists of a group of end-users that require electric power

to operate and avoid major loss of life or economic impact, but they can tolerate interruptions or intermittent power. For instance, water infrastructure systems may operate for only a portion of a day without a significant loss of life, while the electricity infrastructure system is in a recovery mode.

Table 21 – Demand-type categorization.

	Demand Type		
	Priority	**Urgent**	**Routine**
Electricity Demand Sectors	Nuclear Reactors, Materials, and Waste	Water and Wastewater Systems	Residential
	Emergency Services	Transportation Systems	Others
	Healthcare and Public Health	Food and Agriculture	
	Energy	Chemical	
	Defence Industrial Base	Information Technology	
	Communications	Government Facilities	
		Commercial Facilities	
		Critical Manufacturing	
		Financial Services	
		Dams	

Depending on a specific infrastructure system in a given location, this proposed categorization may vary. For instance, in a financial hub, financial services may have a higher priority than a research facility. Furthermore, although the residential sector is categorized as *routine*, it does not diminish the importance of recovering a residential power outage in which a delay in the recovery process can cause a significant negative effect on economic and public welfare [131].

Although this distinction highlights the diverse need in terms of electricity infrastructure resilience, it may vary depending on the specific infrastructure of a given location. For instance, in a city that is a financial hub and conducts long-term medical research, financial services infrastructure may be a higher priority than research facilities. Furthermore, although residential power is categorized as routine, residential power outages have a significant economic and public welfare impact. Representing all demand types in a single performance-time chart does not properly reflect the consequence of an incident on each sector and leads to less accurate assessment of the resilience capacity of a system. To address this issue, the proposed framework has separate performance-time charts for the three end-user types, and the cumulative performance level of these three charts represents the overall system performance level (Equation (24)). By separating the system performance chart by the end-user categories our proposed metric system computes the resilience capacity for each end-user discretely.

$$F_i = F_i^{(P)} + F_i^{(u)} + F_i^{(r)} \qquad \textbf{(24)}$$
$$i = 0, 1, 2, 3, s, d$$

Figure 46 illustrates charts representing the system-performance over time, separated by the end-user type. Although these three charts represent three demand-type categories in a general format, an incident may only affect one or two demand-type categories. An example of such a case is a targeted attack against the urgent demand-type category. Alternatively, an incident may have a similar negative impact on each of the three demand type categories. An example of this scenario is a natural disaster such as a hurricane that causes damage at different levels to each demand type category depending on its path. The

initial system performance level (F_s) represents a stable performance-level prior to the incident in which the system is not under any stress.

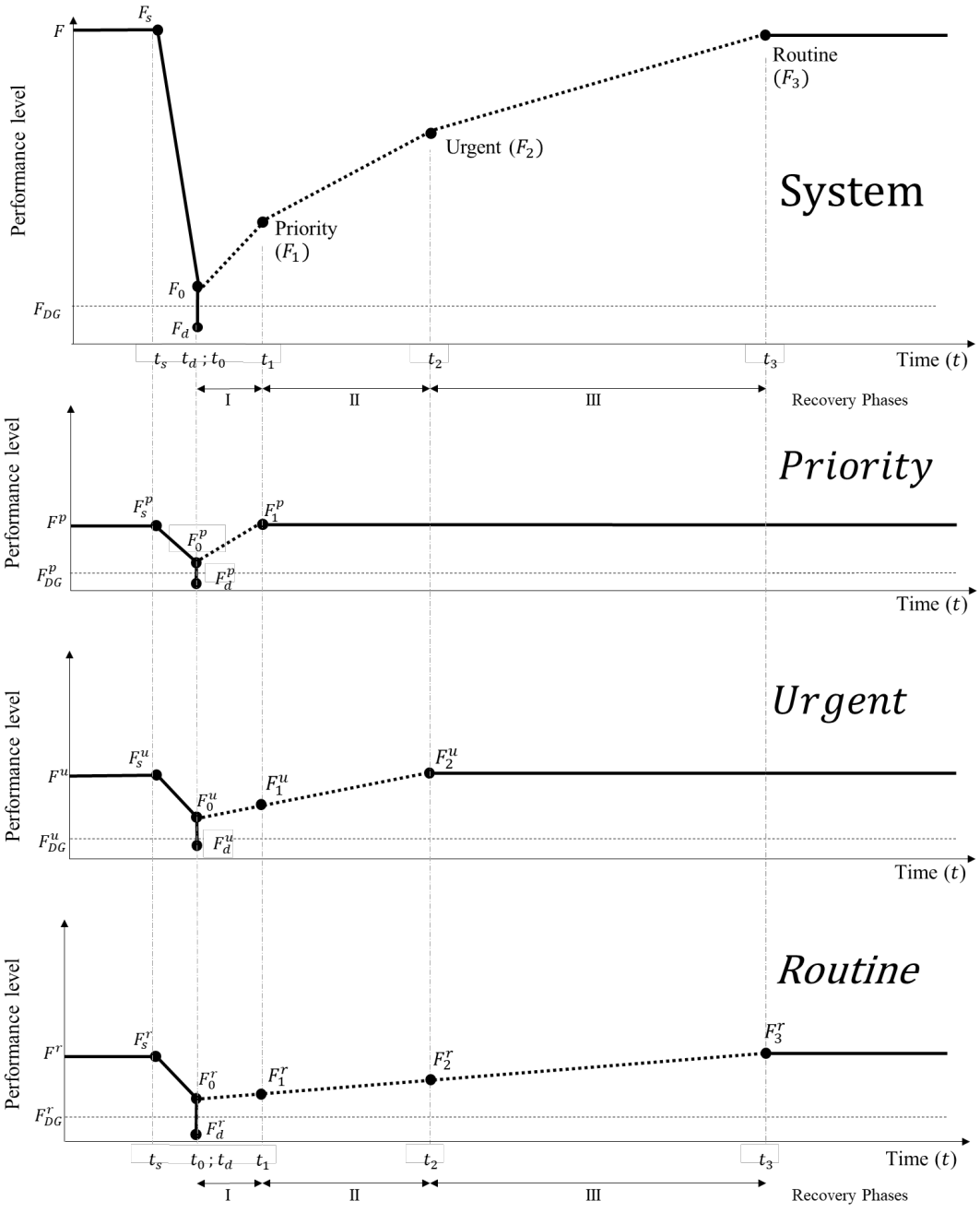

Figure 46 - Performance level over time: system, and demand types: priority, urgent, and routine.

The proposed performance-time chart (Figure 46) consists of four control points: $F_0, F_1, F_2, and\ F_3$. Each control point represents the system status at which the needed service of the all end-users in the associated demand type category are satisfied. During the recovery process, a system may allocate all of its available resources to one end-user category at each recovery phase (i.e., first urgent category and then priority category), or the resources may be distributed among all three end-user types. Hence, at the end of each recovery phase, the overall system performance level may represent the service provided to end-users of more than a category.

5.3.2 Resilience metric

The next step in examining the resiliency of a system is to develop a link between the system performance levels and time to the concept of the resilience. A set of formulation is developed on the basis of four unit-less resilience dimensions [32]: *robustness, redundancy, resourcefulness,* and *rapidity*. *Robustness* is a pre-incident capability of the system and evaluates the abortion of a short-term fluctuations in the system performance level. *Redundancy* expresses the availability of alternative resources to substitute its primary service. *Resourcefulness* defines the capability of system to mobilize the needed resources during the recovery process. *Rapidity* expresses how fast a system recovers to a stable state at which the primary system satisfies all the needed demands. The input variables of the proposed formulation are the performance levels and the associated time-stamps. In this formulation, the DG systems act as temporary electricity generators, which may not be evenly distributed across demand- type groups. To address this point, coefficient β_i in Equation (25) defines the share of generated electricity by the DG system for each end-user category. The system performance level at the beginning of

the first phase of recovery is the sum of the electricity generated by the temporary DG systems and grid electricity immediately after the incident (Equation (26)).

$$F_{DG}^{(i)} = \beta_i * F_{DG} \ , \qquad i = p, u, r \tag{25}$$

$$F_0^{(i)} = F_d^{(i)} + F_{DG}^{(i)}, \ \ i = p, u, r \tag{26}$$

Let R1 represents *robustness*, R2 *redundancy*, R3 *resourcefulness*, and R4 *rapidity*, all four of the variables are unit-less, and ranges from 0 to 1, the resilience capacity of the system is the weighted average of these four resiliency dimensions (Equation (27)).

$$Resilience = \ Weighted\ Avg.[\ \mathrm{R1}, \mathrm{R2}, \mathrm{R3}, \mathrm{R4}] \tag{27}$$

$$R1 = \ Weighted\ average \left(\frac{2}{1 + exp\left(\frac{F_s - F_d}{F_d}\right)} \right)_i \tag{28}$$

$$i = \ I, II, III$$

$$R2 = \frac{F_{DG}}{F_s} \tag{29}$$

$$R3 = \ Weighted\ Avg.\left(R3_p, R3_u\right) \tag{30}$$

$$R4 = \ Weighted\ avg \left(\frac{1}{1 + exp\left(\frac{\Delta t_i - t_{\delta_i}}{\gamma}\right)} \right)_i \tag{31}$$

$$i = \ I, II, III$$

Where

$$R3_p = \max[\ 1 - \left(\frac{\Delta F_I^u + \Delta F_I^r}{\Delta F_I^p}\right), 0\ ] \qquad\qquad R3_u = max[\ 1 - \left(\frac{\Delta F_{II}^u}{\Delta F_{II}^r}\right), 0\ ]$$

$\Delta F_I^u = F_1^u - F_0^u$ $\Delta F_I^r = F_1^r - F_0^r$

$\Delta F_I^p = F_1^p - F_0^p$ $\Delta F_{II}^u = F_2^u - F_1^u$

$\Delta F_{II}^u = F_2^r - F_1^r$ ɣ: $scalar\ factor\ (unit\ of\ time)$,

and

$$Constrains \begin{cases} F_{DG} = \sum_i F_{DG}^i \\ F_s = \sum_i F_s^i \end{cases} , i = p, u, and\ r\ .$$

The weight coefficients elaborate a system specific requirement for each resilience capacity dimension. For a system in which all resilience dimensions are equally important, the weighted average can be simplified to the average of the four resilience dimensions. The system *robustness* $(R1)$ defines how much a system can absorb turbulence and continue a steady service performance level in case of minor or major incidents (Equation (28)). Throughout a mishap, a perfectly robust system, $R1 = 1$, absorbs all the negative shocks on its components and maintain an optimum service level, at which $F_s = F_d$. The *redundancy* $(R2)$ is defined as the ratio of electricity generated by DG systems (temporary) to the grid electricity (primary) at the pre-incident level during a stable operation time (Equation (29)). This linear relation expresses the indifference between the electricity provided by the temporary and permanent systems. The upper boundary is limited to *1*, representing a system in which the DG systems generate electricity at a cumulative capacity equal to the capacity of the electric infrastructure system. The distribution of the ancillary systems is assumed similar to the electric infrastructure system.

The third resilience dimension, *resourcefulness (R3),* is computed based on how the system during the recovery process mobilizes its resources, assuming that the system always allocates all of its resources for the recovery process (Equation (30)). A resourceful

system mobilizes all of its resources to restore providing the needed electricity for the end-users at the highest priority category. The proposed formulation defines the resource mobilization capability as the ability of the system to manage the utilization of its resources for the purpose of the recovery according to the priority list of the end-user type. If end-users in the first category (priority) are not impacted by the mishap ($F_s^p = F_d^p$), $R3_p$ should be excluded from the *resourcefulness* calculation. The same rule governs for the exclusion of $R3_u$ in which end-users in the second category (urgent) are not experiencing a power outage ($F_s^u = F_d^u$). The upper boundary of the *resourcefulness* (*R3=1*) represents a system that allocates all of its resources to the recovery process addressing the needed service of end-users at the highest category The lower boundary of the resourcefulness, *R3=0*, represents a system with poor resource allocation and inefficient service mobilization. This lower boundary represents a system in which while the recovery process to address needed service for a higher tier is still in progress, same or higher resources are allocated to the recovery process of end users in the lower categories.

Rapidity (R4), evaluates how fast the system performs recovery process and is calculated by the weighted average of rapidity in the three recovery phases (Equation (31)). Some factors for determining the weight coefficients are fatality rate, financial loss, and negative environmental impacts in each end-user categories. Slack time (t_{δ_i}), a pre-defined variable, expresses the maximum allowance time for the system to recover, and is defined based on the sensitivity of end-users to the electricity outage. However, slack time does not give the system a free pass to delay its recovery process. If the recovery process is equal to the slack time, a *rapidity* value equal to *0.5* indicates that the system recovered within the maximum allowable time but the it did not occur immediately. The upper boundary

($R4 = 1$) represents a well-prepared system with an instant recovery. It was observed that an intense and widespread damage might delay the start of the recovery and create a shortage of the support of recovery services. An example of such an incident is the Nisqually earthquake in the Olympia-Seattle area [144]. In this case, the delay in starting the recovery is added to the recovery process time.

5.3.3 Sensitivity analysis

A sensitivity analysis is run to determine the impact of the input variables on the proposed metric. Figure 47 summarizes the sensitivity analysis on the four dimensions of resilience. At the two extreme boundaries, the *robustness* capacity changes less with the change in new stable performance level after mishap. This represent a situation in which when the system lost most of its performance level, it still provides service to a small fraction of end users. At the other extreme end, when a small fraction of end-users lose power, the system still has a high *robustness* capacity, indicating the system does not need to be 100% resistant to any mishap. This is aligned with the concept of resilience, which is to design a system with some level resistance to fluctuation but avoid over spending money and workforce to resist against any mishaps. For the *redundancy* dimension, a reasonable substitution of the electricity provided by the grid and DG systems implies a linear line stating a one-to-one relation of the sources of electricity. This study assumes that the DG systems generate a reliable and steady electricity during the recovery process. This can be achieved by coupling PV system with a storage, or in case of conventional electricity generators with combustion engine an adequate amount of fuel is provided by in the reserve fuel tanks.

Resourcefulness capacity is at its highest level ($R3 = 1$) when during the recovery all the required resources for conducting the recovery process are allocated to end-users at the highest category. An immediate recovery indicates the highest rapidity and recover time equal double of slack time indicates the lower boundary of the rapidity dimension. The scalar factor (γ) controls the slope of the sensitivity curve, and is defined based on the vulnerability of end-users to power outage. A lower scalar factor ($\gamma = 0.5$) represents a system with end-users who are extremely vulnerable to power-loss. In this scenario, if the recovery process time exceeds the slack time, end-users are not able to tolerate and the *rapidity* capacity drops to zero. This represents a situation in which the incident cuts the transportation network and end-users rely only on their limited stored resources.

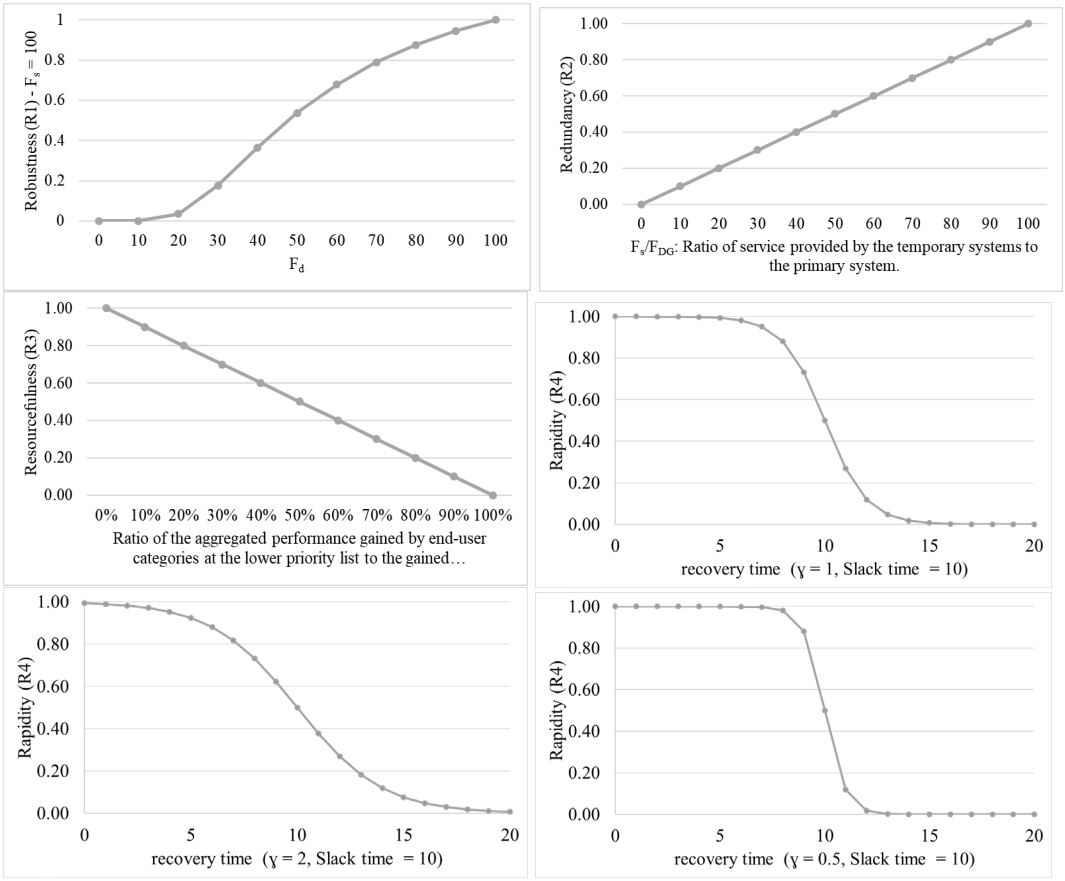

Figure 47 - Sensitivity analysis: proposed resilience metric.

5.4 Notional Examples

Though two notional examples, the application of the proposed framework is illustrated. The first notional example shows how the proposed framework incorporates the impact of emergency electricity generators on system resilience. Furthermore, it illustrates how this framework addresses the gaps in knowledge by comparing the results of resilience assessment with a previously proposed metric system. The second notional example aims to illustrate separating the end-users by type, resulting in a better assessment of resilience.

5.4.1 Notional example 1: contribution of DG systems to improve resilience capacity

5.4.1.1 System setup

The initial system performance level is assumed to be at 100%. The following two system setups represent three scenarios:

1- Conventional electric infrastructure system. The first system setup represents a typical conventional electric infrastructure system in which a group of centralized power plants and grid system generate and distribute the electricity to the end-users. This system is intended to represent a typical electric grid in the United States or elsewhere. Two scenarios define the post-incident performance-level: 1- A blackout in which the performance level drops to zero, and 2- partial power lost in which the performance level drops to 30% (distributed equally among end-user categories).

2- Conventional system coupled with DG systems. The second system setup presents the third scenario: an electric infrastructure system with both centralized and decentralized electricity generation systems. The centralized energy generation system is the primary

source, providing the electricity to the end-users through a grid system. The decentralized electricity generation systems are assumed to consist of coupled PV and electricity storage systems with the aggregated capacity equal to 30% capacity of the primary system. Immediately after the incident, the performance level of the primary systems drops to zero.

5.4.1.2 Input variables

All scenarios share the same proportion of performance level among the end-users' types. Figure 48 and Figure 49 illustrate the three scenarios. These graphical representations of system performance over time show how the incidents result in the drop in system performance, and the system effort to recover.

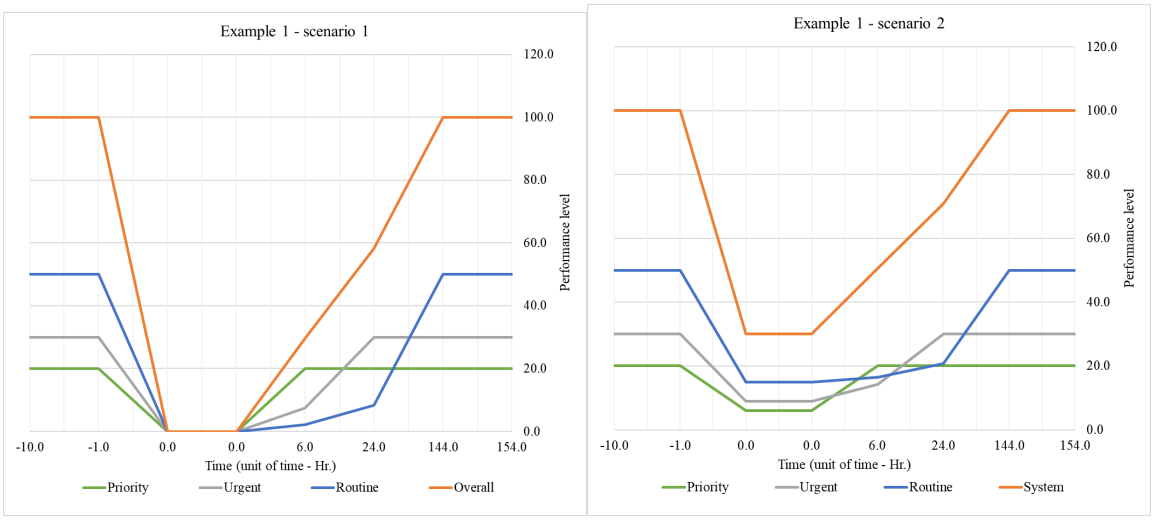

Figure 48 - Notional example 1 – scenario 1 and 2: performance-time charts.

Table 22 presents the input variables. Both system setups have similar slack time and recovery duration. In all three scenarios, the system fully recovers after 192 hrs. The recovery process in this example is linear. In the second system setup, as the system gains its performance during the recovery process, end-users switch back to the grid.

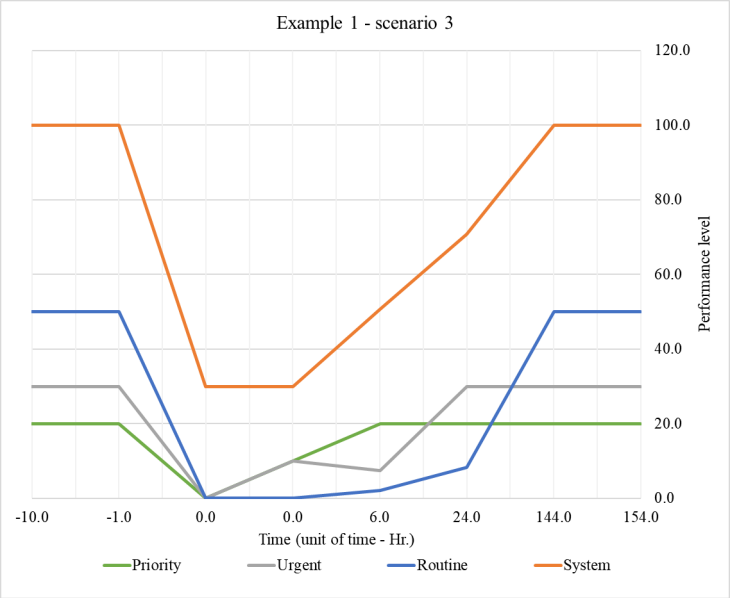

Figure 49 -Notional example 1 – scenario 3: performance-time charts.

Table 22 - Notional example 1: input variables.

Description	End-user type	Variables	scenario 1	2	3
Performance level pre-incident	priority	F_s^p	20	20	20
	urgent	F_s^u	30	30	30
	routine	F_s^r	50	50	50
	overall	F_s	100	100	100
Capacity: decentralized systems	overall	F_{DG}	0	0	30
Scalar factor		γ	1	1	1
Decentralized systems' capacity and distribution among end-user types	priority	F_{DG}^p	0	0	10
	urgent	F_{DG}^u	0	0	10
	routine	F_{DG}^r	0	0	10
Performance level post-incident	priority	F_d^p	0	6	0
	urgent	F_d^u	0	9	0
	routine	F_d^r	0	15	0
	overall	F_d	0	30	0
Slack time	priority	$t_{\delta I}$	8	8	8
	urgent	$t_{\delta II}$	24	24	24
	routine	$t_{\delta III}$	120	120	120
Recovery duration	priority	Δt_I	6	6	6
	urgent	Δt_{II}	18	18	18
	routine	Δt_{III}	168	168	168
	overall	Δt	192	192	192

5.4.1.3 Results and discussion

Figure 50 illustrates the calculated resilience capacity for each scenario. The second system has the highest resilience capacity, indicating a system that can resist against turbulence and maintain a level of performance has a higher resilience capacity. Comparing this second scenario with the third scenario shows the system that could maintain some level of performance has a higher resilience capacity than a system that could not resist, with DG systems with same capacity as the performance level immediately after incident in the second scenario.

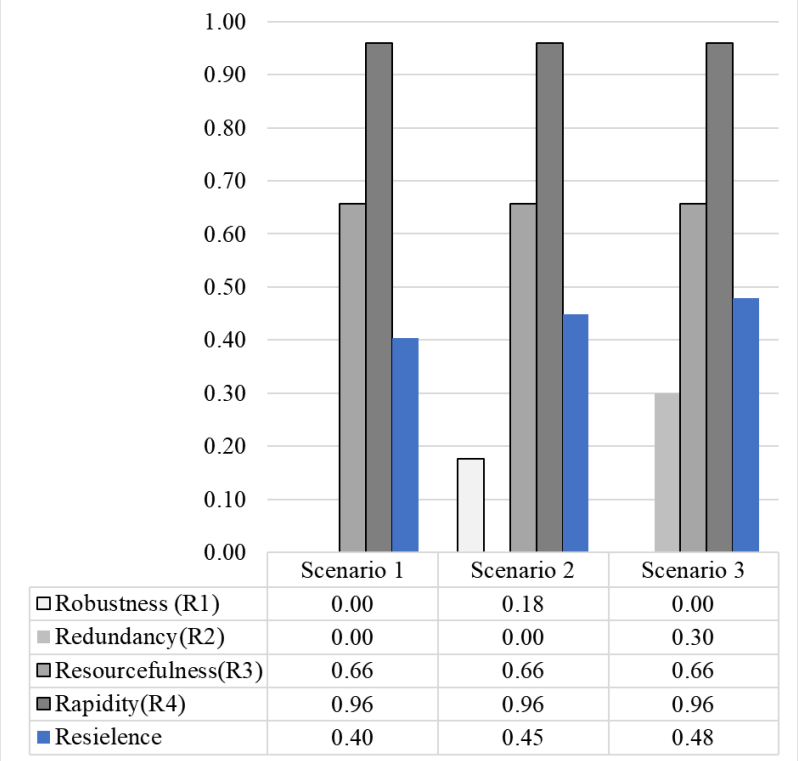

	Scenario 1	Scenario 2	Scenario 3
Robustness (R1)	0.00	0.18	0.00
Redundancy(R2)	0.00	0.00	0.30
Resourcefulness(R3)	0.66	0.66	0.66
Rapidity(R4)	0.96	0.96	0.96
Resielence	0.40	0.45	0.48

Figure 50 - Proposed resilience metric: results – example 1.

This example illustrates the proposed framework incorporates the contribution of the DG systems to improve the overall resilience capacity of the electric infrastructure system. A comparison between the results from the two methods:1- presented by Francis

and Bekera (2014), and 2- the proposed framework, reflects the proposed method 1-capable of including the contribution of the DG systems in improving the overall resilience capacity of the electric infrastructure system, and 2- in case of blackout, even for a short time, it can calculate the resilience capacity of a system based on the four resilience dimensions (Figure 51).

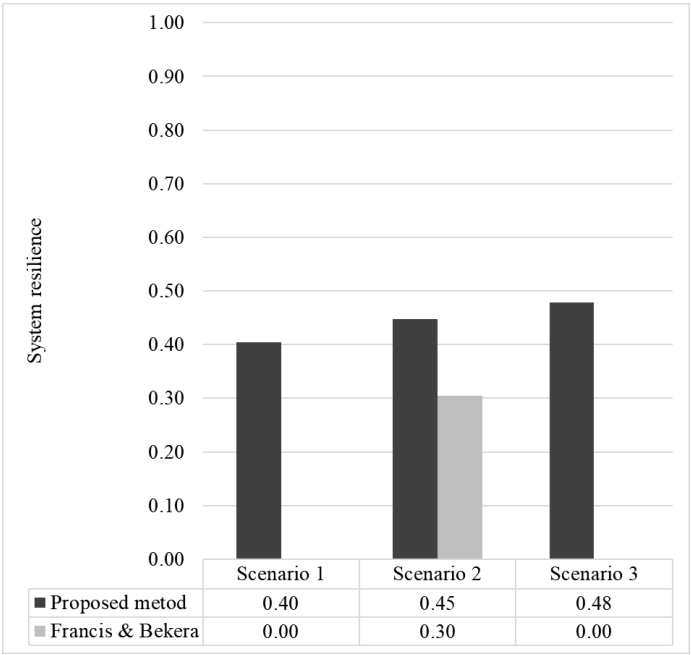

Figure 51 - Comparison two resilience metrics.

5.4.2 Notional example 2 – differentiate end-user types in evaluating resilience capacity

5.4.2.1 Input variables

The second notional example demonstrates separating the end-users by types in the proposed framework, a comparison with previously proposed resilience metric methods, results in a better assessment of the resilience. In this example, two scenarios are compared: 1- a targeted mishap, and 2- a random untargeted mishap. The system has a same

performance level proportion based on end-user types as the first example: 20% *priority*, 30% *urgent*, and 50% *routine*. Table 23 illustrates the input variables for the two scenarios. The targeted mishap causes 100% drops in system performance level of the und-users in priority category and 20% drops of performance level in each of the other two types. In the second scenarios end-users in the *priority* category are not affected by the mishap. However, the mishap results in drops of performance level from 30 to 14 in the *urgent* category and from 50 to 30 in the *routine* category. While in both scenarios the overall system performance levels drop to 64, immediately after the incident, each results in a completely diverse consequences.

Table 23 - Notional example 2: input variables.

Description	End-user type	Variables	scenario 1	scenario 2
Performance level pre-incident	priority	F_s^p	20	20
	urgent	F_s^u	30	30
	routine	F_s^r	50	50
	overall	F_s	100	100
Capacity: decentralized systems	overall	F_{DG}	30	30
Scalar factor		γ	1	1
Distribution of the decentralized systems' capacity among end-user types	priority	F_{DG}^p	10	10
	urgent	F_{DG}^u	10	10
	routine	F_{DG}^r	10	10
Performance level post-incident	priority	F_d^p	0	20
	urgent	F_d^u	24	14
	routine	F_d^r	40	30
	overall	F_d	64	64
Slack time	priority	$t_{\delta I}$	8	8
	urgent	$t_{\delta II}$	24	24
	routine	$t_{\delta III}$	120	120
Recovery duration	priority	Δt_I	50	0
	urgent	Δt_{II}	10	30
	routine	Δt_{III}	70	100
	overall	Δt	130	130

The recover duration values are selected based on the magnitude of the impact and aimed to illustrate that while the total duration of the recovery process is equal for both scenarios, the proposed metric framework, unlike previously proposed metric systems, can capture the differences among the two scenarios. Figure 52 illustrates the system performance-level over time of the two presented scenarios.

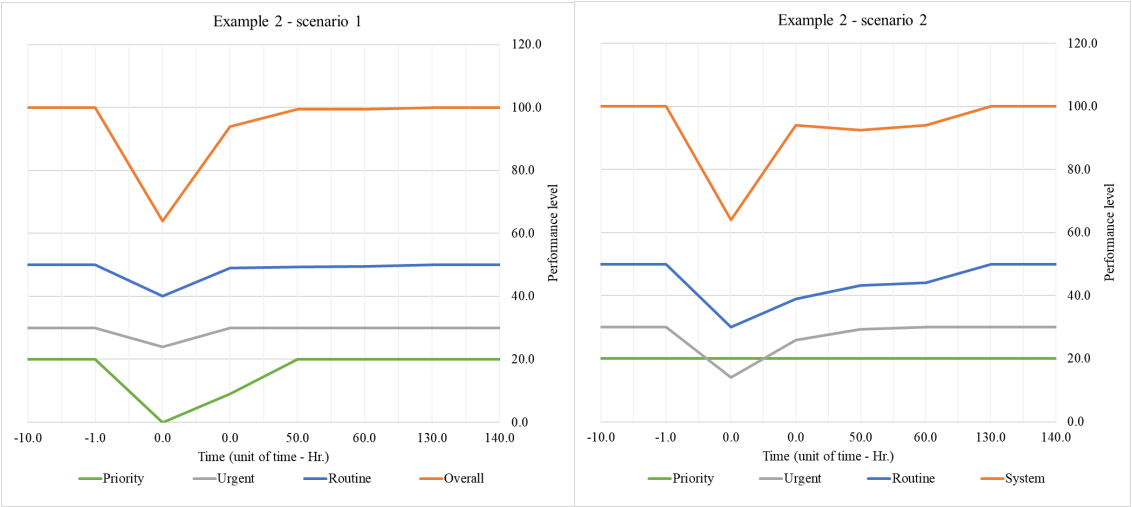

Figure 52 - Notional example 2: performance-time charts.

5.4.2.2 Results and discussion

The resilience capacity of the system is calculated based on two assumptions: 1- the four dimensions of resilience are equally important. 2-the recovery speed for all three end-user types are equally weighted. The results shows the system under targeted attack assuming simple weighting method for all the calculations, is less resilient than a system under random attack, in which end-users under *priority* category did not lose power. In the next step, the assumptions are changed and a higher weight factors are given to the end-users in higher priority group in calculation of robustness and rapidity as follow: 3 for *priority*, 2 for *urgent*, and 1 for *routine*. Figure 54 illustrates the results, under the un-equal

weight factor assumption. The results shows how the proposed method with differentiation of end-users by type more accurately assess the resilience capacity of a system. If the end-users were not separated, (orange line in Figure 52), the calculation of the resilience capacity would result in almost equal value for the two scenarios.

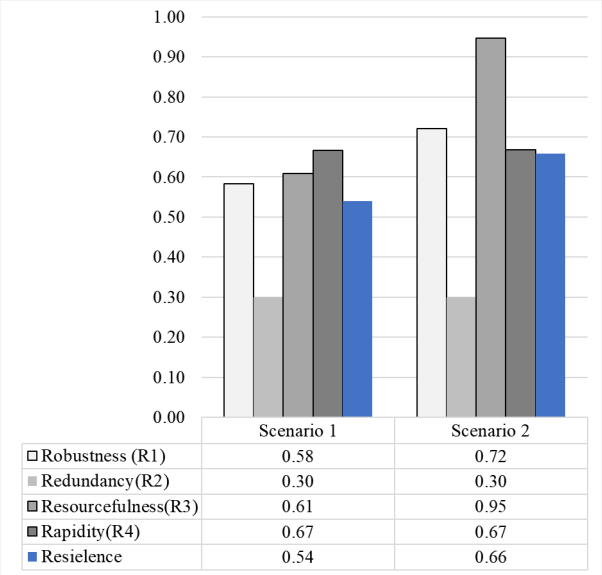

	Scenario 1	Scenario 2
Robustness (R1)	0.58	0.72
Redundancy(R2)	0.30	0.30
Resourcefulness(R3)	0.61	0.95
Rapidity(R4)	0.67	0.67
Resielence	0.54	0.66

Figure 53 - Proposed resilience metric: results – example 2 with equal weight factors.

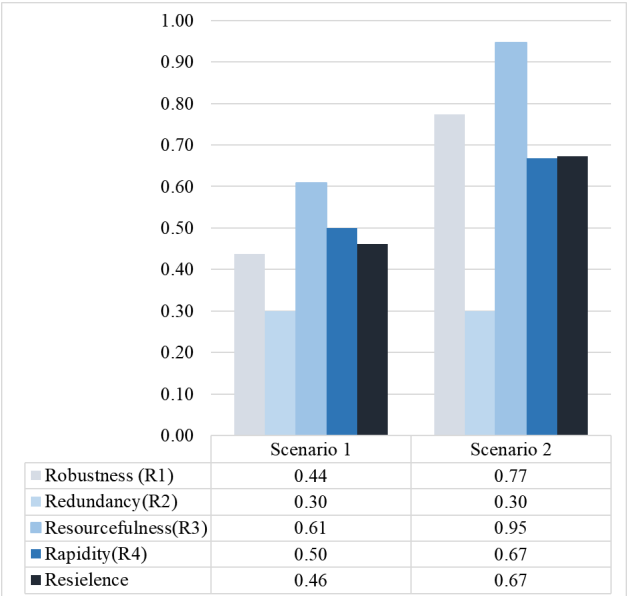

	Scenario 1	Scenario 2
Robustness (R1)	0.44	0.77
Redundancy(R2)	0.30	0.30
Resourcefulness(R3)	0.61	0.95
Rapidity(R4)	0.50	0.67
Resielence	0.46	0.67

Figure 54 - Proposed resilience metric: results – example 2 with varies weight factors based on the end-user types.

5.5 Conclusion

The electric infrastructure system faces many threats each year, both natural and man-made. Applying the resilience concept to the design and manage the electric infrastructure systems is a solution to reduce its vulnerability to hazardous incidents. This chapter proposed a new approach to assess the resilience capacity of an electric infrastructure system and addressed three shortcomings in the existing body of knowledge. There is no resilience metric method capable of evaluating the resilience capacity of a system according to the previously proposed four resilience dimensions: robustness, redundancy, resourcefulness, and rapidity. In case of a power outage, while it has a negative effect on all end-users, the fatality and monetary consequences of a blackout is not similar among end-user types. However, previously proposed resilience metric systems did not differentiate among end-user types, which leads to inaccurately assess the resilience capacity of a system. Furthermore, recent uptake of the decentralized electricity generation systems, including PV systems, creates an opportunity for them to substitute the grid electricity to some extends. However, the contribution of such systems in improving the resilience capacity of an electric infrastructure system is not yet accounted in the existing resilience metric system. Both of these shortcomings are addressed in the proposed resilience metric framework.

CHAPTER 6. CONCLUSION

6.1 Introduction

In 2016, the United Nations defined sustainable development in 17 areas, among which is affordable and clean energy [145]. Solar systems are among the key systems of clean energy [146]. During the past decade, the adoption of PV systems has gained a momentum. While the share of solar systems in the U.S., as a renewable energy source for generating electricity, was 2.4 % in 2017, five states – California, Hawaii, Nevada, Massachusetts, and Vermont – could reach the threshold of 10% solar capacity within their in-state electricity generation sources [147]. This dissertation presents three studies in which adoption of PV systems, as a sustainable energy solution, is the focal point.

The *first* study presents a comprehensive assessment of PV system diffusion in Georgia, which is among the top 10 states with the highest solar capacity. By 2018, in Georgia more than 1,800 PV systems are installed in three sectors: utility, non-residential, and residential. Understanding patterns of diffusion not only is important from a scholar's perspective, but also it has merits in policy and marketing. The *second* study addresses the issue of rebound effect as a subsequence of a major adoption of PV systems by introducing a novel computational framework for estimating the renewable rebound effect. In recent years, several scholars and intergovernmental organizations raised concerns about rebound effect – defined as the difference between achieved reduction in energy consumption to those forecasted – and suggested policy driven solutions to mitigate its impact [19,20,22–24], among which is the transition to renewable energy sources. Ironically, recent empirical studies showed adoption of PV systems resulted in rebound electricity consumption [7,38].

The first step to shape a policy to mitigate the rebound effect is estimating its magnitude and targeted areas [36]. The t*hird* study concentrates on a critical subject of the resilience electric infrastructure system by introducing a state of the art resilient assessment framework. To address the concern of hazardous-incident threats to the electric infrastructure system, DHS published a report in 2013, which a priority is developing tools to measure resilience and augment awareness of the disruption [27]. Improving diversity and resiliency and addressing environmental considerations are among efforts undertaken by DOE to improve energy security [30]. Studies in the aftermath of recent natural disasters (hurricanes Irma, Harvey, and Maria) showed several PV systems could survive, and if their design allows them to operate separate from the grid system, they are able to provide energy to customers during the blackout period [31]. Resilience metrics can provide knowledge about how a system is prepared for a future hazardous incident and enable design choice to improve resilience.

This dissertation addresses some critical questions in each study. The objectives of the first study are assessing PV system adoption and its future diffusion in Georgia, and this study aims to answer the following questions within two adoption time-frames – past and future: 1- what are the key socio-demographic and location-based variables and their comparative influence on the uptake of PV systems in the residential sector and the selection of its size (capacity)? 2- does the adoption of PV systems follow a pattern and how does this pattern differ in each sector (residential, non-residential, and utility)? 3- Based on the historical data on installed PV systems, what is the future projection of PV system adoption in Georgia? And 4- can socio-economic and location-based factors predict future adoption of PV systems in the residential sector? A range of methods is employed

to answer these questions. The scope of the study is Georgia and the micro-boundary of this study is U.S. census tract.

In the *first study* a statistical-based analysis answers the first question, in which two models are developed to test two hypotheses. The first model tests the relationship between the number of voters in the Republican and Green parties and the uptake of PV systems in the residential sector at the County level. The second model tests the relationship between a range of explanatory variables in four categories (socio-economic, building, solar radiation, electricity rate) and the adoption of PV systems in the residential sector at the Census block-group level. Explanatory variables are extracted from multiple sources and merged at the county level for the first model, and Census block-group level for the second model. The results of the first test show percentage of Republican voters has a negative relationship with the uptake of PV systems, while percentage of the Green-party voters has a positive impact. The results of the second study show wealth (median income) and electricity rate have a positive impact on the adoption of PV systems in the residential sector. The results also indicate solar radiation has minimal impact on the uptake of PV systems.

Two sets of spatial analyses are employed to assess the spatial pattern of installed PV systems in three sectors: standard deviational ellipse, and Moran's I cluster assessment. The results of the first analysis show installed PV systems in the utility sector are concentrated in the south of the state, while the residential and non-residential sectors are concentrated in the center and north of the state. Residential sector has a skewed concentration from the north to the center, while the center of the non-residential

concentration is shifted to the west. The results of the second analysis show a clear pattern of peer effect in the residential sector.

To answer the third question, an univariable time series model is developed. The result of Ljung-Box Q test shows the aggregated electricity generated by PV systems dataset from 2008 to 2018 is autocorrelated. The dataset is then tested for seasonality, trend, and cycle. The test is based on lag order of 4 and results show an increasing pattern. The Augmented Dicky-Fuller test revealed the dataset is stationary, and there is no need to apply a transfer function to the dataset to make it stationary. An auto-regressive integrated moving average (ARIMA) model is then fitted, by selecting autoregressive (AR) and moving average (MA) values. To select these two values first a visual test of autocorrelation (ACF) and partial-autocorrelation plots indicated $AR=MA=1$ is a good candidate. Quality of fit is then tested by applying two methods: Aakaike information criteria (AIC) and Bayesian information criteria (BIC). A forecasting model is developed and employing this model, the future adoption of PV systems in Georgia is projected.

The last step in the assessment of PV system adoption in Georgia is developing a predictive model for the adoption of PV systems in the residential sector at the census tract level. To achieve this objective two machine-learning models are employed: decision tree and random forest. The first step in developing the predictive model is forming the sample dataset. The goal of this model is to predict if in each census tract at least one PV system in the residential sector is installed. A group of 35 predictive features in five categories (socio-economic, built-environment, physical building, solar radiation, and electricity rate) are extracted from multiple sources. After pruning the dataset, it was divided into two sub-samples: training set (60%) and test set (40%). The training set was used to train the two

models. To check the accuracy of the two model, the root mean square error is computed for the test-set. The model trained by the random forest algorithm, compare with the decision tree, showed a higher accuracy rate with *RSME = 0.74*. The analyses of feature importance in two models revealed the percentage of White and African-American races, median age, median income, and education level are the most important features in the two predictive models, and buildings with 10 or more units are the least important features in both predictive models.

The objective of the *second study* is to answer an important question in the process of shaping a policy to mitigate the direct rebound effect: assuming a high rate of adoption for PV systems, how much is the magnitude of the rebound effect? While researchers have typically used empirical methods to investigate different aspects of electricity demand, the proposed methodology departs from the existing body of knowledge by introducing a novel methodology that combines standard economic modeling technique with data-driven method and GIS-based simulation model. Direct rebound effect typically measured as the elasticity of energy demand with respect to a change in energy efficiency or alternatively, it can be characterized as an increase in energy consumption relative to a counterfactual based on the improvement in energy efficiency. A standard Cobb-Douglas form is assumed to represent a household utility function. Assuming no FiT program or incentive available, electricity generated by PV systems is both exogenous and a perfect substitution for grid electricity. The direct rebound effect is then derived as a function of household electricity consumption, estimate generated electricity by PV systems, electricity rate, and household income. The proposed method is then applied to compute the direct rebound effect in Fulton County. The results show adoption of PV systems under a moderate diffusion rate

can generate an average 5.8% rebound effect. This translates to a 4.49 MWh increase in electricity consumption, which diminishes a portion of the environmental benefits resulting from the adoption of PV systems. Furthermore, a 5.8% rebound effect could change the forecast of the residual demand change by 7.94 MWh, which may result in a significant voltage imbalance in some areas.

The *third study* in this dissertation addresses an emerging concern of improving energy security. After a comprehensive review of the existing body of knowledge, a new framework is developed to quantify the resilience capacity of an electric infrastructure system. As a point of departure from the existing body of knowledge, the proposed framework is formed based on the four pre-defined resilience dimensions: 1- r*obustness*: the ability of a system to prevent the dissemination of damage during a hazardous incident, 2- *redundancy*: the ability of a system to provide service using other resources in case of an incident, 3-*resourcefulness*: the capability of a system to respond to a hazardous incident and mobilize needed resources/services, and 4-*rapidity*: the speed of a system to return to its original state. The second innovative characteristic of this approach is its capability to incorporate the contribution of emergency electricity generators, including PV systems, to improve the resilience capacity of the system. Finally, the proposed framework introduced a distinctive approach to estimate the resilience capacity of a system by separating the end-users by their type. Through two notional examples, the advantages of the proposed resilience framework are highlighted. The first example compares an electric system under three scenarios. The first scenario assumes the overall performance level of the system drops to zero. This is a typical example of a blackout. Since the computed resilience capacity is based on the average of the four dimensions of resilience, one could observe,

the blackout only expresses the *robustness* capacity of this system, while other demotions of resilience are calculated based on the other characteristics of the system, such as how fast the system can recover, is there a replacement system to generate electricity. In this scenario, the *redundancy* capacity is zero. The second scenario assumes the system will lose a portion of its performance. This is a representative of partial shutdown of an electric system. The third scenario also assumes a hazardous incident result in a blackout, while a portion of the consumers have emergency electricity generators. While the robustness capacity of the system is zero, the positive value of the computed *redundancy* capacity considers the contribution of the emergency electricity generators to improve overall resilience capacity. The second notional example illustrated how the proposed framework differentiates between concentrated incident and a widespread hazardous incident, even if both have similar impact on the overall system performance level.

6.2 Future Works and Directions

There remain some limitations regarding the study of PV system adoption that merits future effort.

- Examining the impact of the explanatory variable on the uptake of the PV system was limited to the residential sectors. To assess the uptake of PV systems in the other two sectors (utility and non-residential), a new set of explanatory variables is needed to form new models.

- Study of the spatial pattern can extend to examine the diffusion over time and space. This will reveal the impact of early adopters on the diffusion of technology. Third, development of the forecasting model in this study was

limited to the residential sector, which can be extended to forecast the adoption of PV systems in the other sectors.

The second study presented a new approach to compute the direct rebound effect, which can be further expanded.

- The proposed econometric framework is developed based on some relaxing assumptions. Future studies can improve the proposed method by advancing the proposed assessment framework by including the effect of a FiT policy on renewable rebound effect, or the cost of purchase and installation of a PV systems, in the calculation of renewable rebound effect.

- While the focus of this study was on developing a framework to estimate the direct rebound effect triggered by the adoption of PV systems, an expansion of this study will be shaping policy initiatives to mitigate the rebound effect.

The third study of this dissertation carried out a new approach to assess the resilience capacity of an electric system. For future development of knowledge in this area, the following recommendations are proposed for the future works.

- Linking the system components to the input variables of the proposed framework is an area with potential to explore. The scope of this study did not cover how a system setup and characteristics of each component in the generation and distribution sectors could impact the input variables in the proposed framework.

- Another extension of this study can expand the scope of this study to include the distribution network and examine its impact on the resilience capacity of an electric infrastructure system. For instance, the introduction of smart grid technology can improve the *rapidity* capacity of a system, by reducing the recovery process time.

One major contribution of the proposed framework is its capability to separately compute four resilience dimensions. While all four dimensions are important to maintain a reliable and sustainable flow of service, the monetary and fatality consequences of an incident are not equally distributed among these four dimensions. Future studies can investigate the consequences of a mishap separately by the four dimensions of a resilience system.

REFERENCES

[1] U.S. Energy Information Administration (EIA) - Total Energy 2018. https://www.eia.gov/totalenergy/ (accessed October 8, 2018).

[2] Spitzer A, Armstrong T, Lucas B. Transmission & Distribution Infrastructure. 2014.

[3] ASCE. A Comprehensive Assessment of America's Infrastructure. 2017.

[4] Maliszewski P, Larson E, Perrings C. Valuing the Reliability of the Electrical Power Infrastructure: A Two-stage Hedonic Approach. Urban Stud 2013;50:72–87. doi:10.1177/0042098012450482.

[5] Singal S, Singh R. Rural electrification of a remote island by renewable energy sources. Renew Energy 2007;32:2491–501. doi:10.1016/j.renene.2006.12.013.

[6] Zografakis N, Sifaki E, Pagalou M, Nikitaki G, Psarakis V, Tsagarakis KP. Assessment of public acceptance and willingness to pay for renewable energy sources in Crete n.d. doi:10.1016/j.rser.2009.11.009.

[7] Deng G, Newton P. Assessing the impact of solar PV on domestic electricity consumption: Exploring the prospect of rebound effects. Energy Policy 2017;110:313–24. doi:10.1016/j.enpol.2017.08.035.

[8] Electricity Information 2018: Overview. 2018.

[9] Wüstenhagen R, Wolsink M, Bürer MJ. Social acceptance of renewable energy innovation: An introduction to the concept. Energy Policy 2007;35:2683–91. doi:10.1016/J.ENPOL.2006.12.001.

[10] U.S. Energy Facts - Energy Explained, Your Guide To Understanding Energy - Energy Information Administration n.d. https://www.eia.gov/energyexplained/?page=us_energy_home (accessed October 26, 2018).

[11] EIA. Electricity in the United States - Energy Explained, Your Guide To Understanding Energy - Energy Information Administration. 2018.

[12] U.S. Energy Information Administration (EIA) - Electricity Data n.d. https://www.eia.gov/electricity/data.php (accessed October 23, 2018).

[13] SunShot 2030 | Department of Energy n.d. https://www.energy.gov/eere/solar/sunshot-2030 (accessed October 23, 2018).

[14] U.S. Solar Market Insight Q3 2018 | Wood Mackenzie n.d. https://www.woodmac.com/our-expertise/focus/Power--Renewables/us-solar-market-insight-q3-2018/ (accessed October 3, 2018).

[15] Fu R, Feldman D, Margolis R, Woodhouse M, Ardani K. U.S. Solar Photovoltaic System Cost Benchmark: Q1 2017. 2009.

[16] Top 10 Solar States | SEIA n.d. https://www.seia.org/research-resources/top-10-solar-states-0 (accessed October 19, 2018).

[17] State Energy Profile Data - Georgia n.d. https://www.eia.gov/state/data.php?sid=GA (accessed October 19, 2018).

[18] Jenkins J, Nordhaus T, Shellenberger M. Energy Emergence: rebound and backfire as emergent phenomena. 2011.

[19] Sorrell S, Dimitropoulos J. The rebound effect: Microeconomic definitions, limitations and extensions. Ecol Econ 2008;65:636–49. doi:10.1016/J.ECOLECON.2007.08.013.

[20] A. Greening L, Greene DL, Difiglio C. Energy efficiency and consumption — the rebound effect — a survey. Energy Policy 2000;28:389–401. doi:10.1016/S0301-4215(00)00021-5.

[21] Sorrell S, Dimitropoulos J, Sommerville M. Empirical estimates of the direct rebound effect: A review. Energy Policy 2009;37:1356–71. doi:10.1016/J.ENPOL.2008.11.026.

[22] Achieving energy efficiency through behaviour change: what does it take? (EEA Technical report No 5/2013). n.d. doi:10.2800/49941.

[23] Ryan L, Moarif S, Levina E, Baron R. Energy Efficiency Series 2011 ENERGY EFFICIENCY POLICY AND CARBON PRICING August. n.d.

[24] Girod B, van Vuuren DP, Hertwich EG. Climate policy through changing consumption choices: Options and obstacles for reducing greenhouse gas emissions. Glob Environ Chang 2014;25:5–15. doi:10.1016/J.GLOENVCHA.2014.01.004.

[25] Atkinson G, Dietz S, Neumayer E. Handbook of sustainable development. Edward Elgar; 2007.

[26] Font Vivanco D, Kemp R, van der Voet E. How to deal with the rebound effect? A policy-oriented approach. Energy Policy 2016;94:114–25. doi:10.1016/J.ENPOL.2016.03.054.

[27] ELECTRICITY: Federal Efforts to Enhance Grid Resilience. 2017.

[28] Security Committee I. Presidential Policy Directive 21 Implementation: An Interagency Security Committee White Paper. 2015.

[29] Department of Homeland Security U. 2015 Energy Sector-Specific Plan. 2015.

[30] Valuation of Energy Security for the United States. n.d.

[31] ELIZA HOTCHKISS. How Is Solar PV Performing in Hurricane-struck Locations? | State, Local, and Tribal Governments | NREL. NREL n.d. https://www.nrel.gov/state-local-tribal/blog/posts/how-is-solar-pv-performing-in-hurricane-struck-locations.html (accessed December 1, 2018).

[32] Bruneau M, Chang SE, Eguchi RT, Lee GC, O'Rourke TD, Reinhorn AM, et al. A Framework to Quantitatively Assess and Enhance the Seismic Resilience of Communities. Earthq Spectra 2003;19:733–52. doi:10.1193/1.1623497.

[33] Allan G, Eromenko I, Gilmartin M, Kockar I, McGregor P, Andújar JM, et al. Generic metrics and quantitative approaches for system resilience as a function of time. Reliab Eng Syst Saf 2014;42:1–8. doi:10.1016/j.ress.2011.09.002.

[34] Cimellaro GP, Reinhorn AM, Bruneau M. Framework for analytical quantification of disaster resilience. Eng Struct 2010;32:3639–49. doi:10.1016/j.engstruct.2010.08.008.

[35] Henry D, Emmanuel Ramirez-Marquez J. Generic metrics and quantitative approaches for system resilience as a function of time. Reliab Eng Syst Saf

2012;99:114–22. doi:10.1016/j.ress.2011.09.002.

[36] Francis R, Bekera B. A metric and frameworks for resilience analysis of engineered and infrastructure systems. Reliab Eng Syst Saf 2014;121:90–103. doi:10.1016/j.ress.2013.07.004.

[37] Jevons WS. The Coal Question; An Inquiry concerning the Progress of the Nation, and the Probable Exhaustion of our Coal-mines. Lib Fund, Inc 1865;1:1–323. doi:10.1038/031242a0.

[38] Havas L, Ballweg J, Penna C, Race D. Power to change: Analysis of household participation in a renewable energy and energy efficiency programme in Central Australia. Energy Policy 2015;87:325–33. doi:10.1016/j.enpol.2015.09.017.

[39] Faturechi R, Miller-Hooks E. Measuring the Performance of Transportation Infrastructure Systems in Disasters: A Comprehensive Review. J Infrastruct Syst 2015;21:04014025. doi:10.1061/(ASCE)IS.1943-555X.0000212.

[40] Preston Scott N Backhaus Mary Ewers Julia A Phillips Cesar A Silva-Monroy Jeffery E Dagle Alfonso G Tarditi John Looney Thomas J King BL. Resilience of the U.S. Electricity System: A Multi-Hazard Perspective. 2016.

[41] Menanteau P, Finon D, Lamy M-L. Prices versus quantities: choosing policies for promoting the development of renewable energy. Energy Policy 2003;31:799–812. doi:10.1016/S0301-4215(02)00133-7.

[42] Residential Renewable Energy Tax Credit | Department of Energy. US Intern Revenue Serv n.d. https://www.energy.gov/savings/residential-renewable-energy-tax-credit (accessed October 29, 2018).

[43] California Energy commision. Energy Commission Adopts Standards Requiring Solar Systems for New Homes 2018. http://www.energy.ca.gov/releases/2018_releases/2018-05-09_building_standards_adopted_nr.html (accessed October 3, 2018).

[44] Solar Power Free-Market Financing Act of 2015; enact. n.d.

[45] TVA - Green Power Providers n.d. https://www.tva.com/Energy/Valley-

Renewable-Energy/Green-Power-Providers (accessed October 29, 2018).

[46] Sun Power for Homes | Jackson EMC n.d. https://www.jacksonemc.com/solar-power-home (accessed October 29, 2018).

[47] Solar Power Rebates | Central Georgia Electric Membership Corporation n.d. https://www.cgemc.com/content/solar-power-rebates (accessed October 29, 2018).

[48] Solar Photovoltaic Program | GreyStone Power Corporation n.d. https://www.greystonepower.com/solarphotovoltaicprogram (accessed October 29, 2018).

[49] Rogers E. Diffusion of innovations. New York: Free Press of Glencoe; 1962.

[50] Hägerstrand T. The propagation of innovation waves. London: Royal University of Lund Dept. of Geography; 1952.

[51] Huijts NMA, Molin EJE, Steg L. Psychological factors influencing sustainable energy technology acceptance: A review-based comprehensive framework. Renew Sustain Energy Rev 2012;16:525–31. doi:10.1016/J.RSER.2011.08.018.

[52] Hosseini S, Barker K, Ramirez-Marquez JE. A review of definitions and measures of system resilience. Reliab Eng Syst Saf 2016;145:47–61. doi:10.1016/j.ress.2015.08.006.

[53] Rai V, Reeves DC, Margolis R. Overcoming barriers and uncertainties in the adoption of residential solar PV. Renew Energy 2016;89:498–505. doi:10.1016/J.RENENE.2015.11.080.

[54] Parkins JR, Rollins C, Anders S, Comeau L. Predicting intention to adopt solar technology in Canada: The role of knowledge, public engagement, and visibility. Energy Policy 2018;114:114–22. doi:10.1016/J.ENPOL.2017.11.050.

[55] Zhang H, Vorobeychik Y, Letchford J, Lakkaraju K. Data-driven agent-based modeling, with application to rooftop solar adoption. Auton Agent Multi Agent Syst 2016;30:1023–49. doi:10.1007/s10458-016-9326-8.

[56] Gooding J, Edwards H, Giesekam J, Crook R. Solar City Indicator: A methodology to predict city level PV installed capacity by combining physical capacity and socio-

economic factors. Sol Energy 2013;95:325–35. doi:10.1016/j.solener.2013.06.027.

[57] Assessment of potential for photovoltaic roof installations by extraction of roof tilt from LiDAR data and aggregation to census geography n.d. doi:10.1049/iet-rpg.2015.0388.

[58] Sommerfeld J, Buys L, Mengersen K, Vine D. Influence of demographic variables on uptake of domestic solar photovoltaic technology. Renew Sustain Energy Rev 67:315–23. doi:10.1016/j.rser.2016.09.009.

[59] Graziano M, Gillingham K. Spatial patterns of solar photovoltaic system adoption: The influence of neighbors and the built environment. J Econ Geogr 2015;15:815–39. doi:10.1093/jeg/lbu036.

[60] Caird S, Roy R, Herring H. Improving the energy performance of UK households: Results from surveys of consumer adoption and use of low- and zero-carbon technologies. Energy Effic 2008;1:149–66. doi:10.1007/s12053-008-9013-y.

[61] Grösche P, Schröder C. On the redistributive effects of Germany's feed-in tariff. Empir Econ 2014;46:1339–83. doi:10.1007/s00181-013-0728-z.

[62] Schaffer AJ, Brun S. Beyond the sun—Socioeconomic drivers of the adoption of small-scale photovoltaic installations in Germany. Energy Res Soc Sci 2015;10:220–7. doi:10.1016/J.ERSS.2015.06.010.

[63] Jayaweera N, Jayasinghe CL, Weerasinghe SN. Local factors affecting the spatial diffusion of residential photovoltaic adoption in Sri Lanka. Energy Policy 2018;119:59–67. doi:10.1016/J.ENPOL.2018.04.017.

[64] Snape J, Snape, Richard J. Spatial and Temporal Characteristics of PV Adoption in the UK and Their Implications for the Smart Grid. Energies 2016;9:210. doi:10.3390/en9030210.

[65] Kwan CL. Influence of local environmental, social, economic and political variables on the spatial distribution of residential solar PV arrays across the United States. Energy Policy 2012;47:332–44. doi:10.1016/J.ENPOL.2012.04.074.

[66] Wolske KS, Stern PC, Dietz T. Explaining interest in adopting residential solar

photovoltaic systems in the United States: Toward an integration of behavioral theories. Energy Res Soc Sci 2017;25:134–51. doi:10.1016/J.ERSS.2016.12.023.

[67] Brown LA. Innovation diffusion : a new perspective. Methuen; 1981.

[68] Chow A, Fung A, Li S. GIS Modeling of Solar Neighborhood Potential at a Fine Spatiotemporal Resolution. Buildings 2014;4:195–206. doi:10.3390/buildings4020195.

[69] Margolis R, Gagnon P, Melius J, Phillips C, Elmore R. Using GIS-based methods and lidar data to estimate rooftop solar technical potential in US cities. Environ Res Lett 2017;12:074013. doi:10.1088/1748-9326/aa7225.

[70] Zhao T, Zhou Z, Zhang Y, Ling P, Tian Y. Spatio-Temporal Analysis and Forecasting of Distributed PV Systems Diffusion: A Case Study of Shanghai Using a Data-Driven Approach. IEEE Access 2017;5:5135–48. doi:10.1109/ACCESS.2017.2694009.

[71] Lee M, Hong T, Jeong K, Kim J. A bottom-up approach for estimating the economic potential of the rooftop solar photovoltaic system considering the spatial and temporal diversity. Appl Energy 2018;232:640–56. doi:10.1016/J.APENERGY.2018.09.176.

[72] Leibowicz BD, Krey V, Grubler A. Representing spatial technology diffusion in an energy system optimization model. Technol Forecast Soc Change 2016;103:350–63. doi:10.1016/J.TECHFORE.2015.06.001.

[73] Vimpari J, Junnila S. Evaluating decentralized energy investments: Spatial value of on-site PV electricity. Renew Sustain Energy Rev 2017;70:1217–22. doi:10.1016/J.RSER.2016.12.023.

[74] Noll D, Dawes C, Rai V. Solar Community Organizations and active peer effects in the adoption of residential PV. Energy Policy 2014;67:330–43. doi:10.1016/J.ENPOL.2013.12.050.

[75] Small M. Applied nonlinear time series analysis : applications in physics, physiology and finance. World Scientific; 2005.

[76] Mikosch T, Kreiß J-P, Davis RA, Andersen TG, editors. Handbook of Financial Time Series. Berlin, Heidelberg: Springer Berlin Heidelberg; 2009. doi:10.1007/978-3-540-71297-8.

[77] Phinikarides A, Makrides G, Zinsser B, Schubert M, Georghiou GE. Analysis of photovoltaic system performance time series: Seasonality and performance loss n.d. doi:10.1016/j.renene.2014.11.091.

[78] Gürtler M, Paulsen T. Forecasting performance of time series models on electricity spot markets. Int J Energy Sect Manag 2018;12:617–40. doi:10.1108/IJESM-12-2017-0006.

[79] Paoli C, Voyant C, Muselli M, Nivet M-L. Forecasting of preprocessed daily solar radiation time series using neural networks 2010. doi:10.1016/j.solener.2010.08.011.

[80] Lee Woon W, Aung Stuart Madnick Z, Lee W, Aung WZ, Kramer O, Madnick S. Data Analytics for Renewable Energy Integration. n.d.

[81] Ulbricht R, Thoß A, Donker H, Gräfe G, Lehner W. Dealing with Uncertainty: An Empirical Study on the Relevance of Renewable Energy Forecasting Methods, Springer, Cham; 2017, p. 54–66. doi:10.1007/978-3-319-50947-1_6.

[82] Mellit A, Kalogirou SAA, Hontoria L, Shaari S. Artificial intelligence techniques for sizing photovoltaic systems: A review. Renew Sustain Energy Rev 2009;13:406–19.

[83] Hocaog FO, Gerek N, Kurban M. Hourly solar radiation forecasting using optimal coefficient 2-D linear filters and feed-forward neural networks 2008. doi:10.1016/j.solener.2008.02.003.

[84] Paoli C, Voyant C, Muselli M, Nivet M-L. Forecasting of preprocessed daily solar radiation time series using neural networks. Sol Energy 2010;84:2146–60. doi:10.1016/J.SOLENER.2010.08.011.

[85] Wu Y-K, Chen C-R, Abdul Rahman H. A Novel Hybrid Model for Short-Term Forecasting in PV Power Generation. Int J Photoenergy 2014;2014:1–9. doi:10.1155/2014/569249.

[86] Kardakos EG, Alexiadis MC, Vagropoulos SI, Simoglou CK, Biskas PN, Bakirtzis AG. Application of time series and artificial neural network models in short-term forecasting of PV power generation. 2013 48th Int. Univ. Power Eng. Conf., IEEE; 2013, p. 1–6. doi:10.1109/UPEC.2013.6714975.

[87] Abuella M, Chowdhury B. Random Forest Ensemble of Support Vector Regression Models for Solar Power Forecasting. 2017.

[88] Ahmad MW, Reynolds J, Rezgui Y. Predictive modelling for solar thermal energy systems: A comparison of support vector regression, random forest, extra trees and regression trees. J Clean Prod 2018;203:810–21. doi:10.1016/j.jclepro.2018.08.207.

[89] Wang Z, Wang Y, Zeng R, Srinivasan RS, Ahrentzen S. Random Forest based hourly building energy prediction. Energy Build 2018;171:11–25. doi:10.1016/J.ENBUILD.2018.04.008.

[90] Georgia Energy Data | Solar Map. Southface n.d. http://www.georgiaenergydata.org/solarmap (accessed January 14, 2019).

[91] Solar Data | Geospatial Data Science | NREL. NREL 2012. https://www.nrel.gov/gis/data-solar.html (accessed November 6, 2018).

[92] NSRDB Data Viewer. Natl Renew Energy Lab n.d. https://maps.nrel.gov/nsrdb-viewer/?aL=UdPEX9%255Bv%255D%3Dt%26f69KzE%255Bv%255D%3Dt%26f69KzE%255Bd%255D%3D1&bL=clight&cE=0&lR=0&mC=40.5137991550441 3%2C-42.978515625&zL=3 (accessed January 14, 2019).

[93] Utility Rate Database | Open Energy Information. OpeneiOrg n.d. https://openei.org/wiki/Utility_Rate_Database (accessed January 14, 2019).

[94] U.S. Electric Utility Companies and Rates: Look-up by Zipcode (2016) - Data.gov n.d. https://catalog.data.gov/dataset/u-s-electric-utility-companies-and-rates-look-up-by-zipcode-2016 (accessed November 8, 2018).

[95] ESRI. How Spatial Autocorrelation (Global Moran's I) works—ArcGIS Pro | ArcGIS Desktop n.d. http://pro.arcgis.com/en/pro-app/tool-reference/spatial-statistics/h-how-spatial-autocorrelation-moran-s-i-spatial-st.htm (accessed December 13, 2018).

[96] Anselin L. Local Indicators of Spatial Association-LISA. Geogr Anal 2010;27:93–115. doi:10.1111/j.1538-4632.1995.tb00338.x.

[97] Ljung GM, Box GEP. On a Measure of Lack of Fit in Time Series Models. Biometrika 1978;65:297. doi:10.2307/2335207.

[98] Fuller WA. Introduction to statistical time series. Wiley; 1996.

[99] Akaike H. Information Theory and an Extension of the Maximum Likelihood Principle, Springer, New York, NY; 1998, p. 199–213. doi:10.1007/978-1-4612-1694-0_15.

[100] Schwarz G. Estimating the Dimension of a Model. vol. 6. 1978.

[101] Breiman L. Random Forests. Mach Learn 2001;45:5–32. doi:10.1023/A:1010933404324.

[102] Mitchell TM (Tom M. Machine Learning. n.d.

[103] Rokach L, Maimon O. DECISION TREES. n.d.

[104] Rogers EM. Diffusion of innovations. Free Press; 2003.

[105] Community Solar Program | For Your Home n.d. https://www.georgiapower.com/company/energy-industry/energy-sources/solar-energy/solar/community-solar.html (accessed December 14, 2018).

[106] Georgia Power seeks 540 MW of new large-scale renewable generation n.d. https://www.prnewswire.com/news-releases/georgia-power-seeks-540-mw-of-new-large-scale-renewable-generation-300762895.html (accessed December 14, 2018).

[107] Georgia Solar | SEIA n.d. https://www.seia.org/state-solar-policy/georgia-solar (accessed December 14, 2018).

[108] NREL. Environment Baseline, Volume 1: Greenhouse Gas Emissions from the U.S. Power Sector. n.d.

[109] Yekini Suberu M, Wazir Mustafa M, Bashir N. Energy storage systems for renewable energy power sector integration and mitigation of intermittency. Renew

Sustain Energy Rev 2014;35:499–514. doi:10.1016/j.rser.2014.04.009.

[110] Aflaki S, Netessine S. Strategic Investment in Renewable Energy Sources: The Effect of Supply Intermittency. Manuf Serv Oper Manag 2017;19:489–507. doi:10.1287/msom.2017.0621.

[111] Berkhout PHG, Muskens JC, W. Velthuijsen J. Defining the rebound effect. Energy Policy 2000;28:425–32. doi:10.1016/S0301-4215(00)00022-7.

[112] Azevedo IMLL. Consumer End-Use Energy Efficiency and Rebound Effects. Annu Rev Environ Resour 2014;39:393–418. doi:10.1146/annurev-environ-021913-153558.

[113] Brookes LG. Energy policy, the energy price fallacy and the role of nuclear energy in the UK. Energy Policy 1978;6:94–106. doi:10.1016/0301-4215(78)90031-9.

[114] Khazzoom JD. Economic Implications of Mandated Efficiency in Standards for Household Appliances. Energy J 1980;1:21–40. doi:10.2307/41321476.

[115] Saunders HD. Historical Evidence for Energy Consumption Rebound in 30 US Sectors and a Toolkit for Rebound Analysts n.d.

[116] Hertwich EG. Consumption and the Rebound Effect: An Industrial Ecology Perspective. J Ind Ecol 2008;9:85–98. doi:10.1162/1088198054084635.

[117] Gillingham K, Rapson D, Wagner G. The rebound effect and energy efficiency policy. Rev Environ Econ Policy 2016;10:68–88. doi:10.1093/reep/rev017.

[118] Allcott H. Rethinking real-time electricity pricing. Resour Energy Econ 2011;33:820–42. doi:10.1016/J.RESENEECO.2011.06.003.

[119] Ito K. Do Consumers Respond to Marginal or Average Price? Evidence from Nonlinear Electricity Pricing. Am Econ Rev 2014;104:537–63. doi:10.1257/aer.104.2.537.

[120] Binswanger M. Technological progress and sustainable development: what about the rebound effect? Ecol Econ 2001;36:119–32. doi:10.1016/S0921-8009(00)00214-7.

[121] Chan NW, Gillingham K. The Microeconomic Theory of the Rebound Effect and

Its Welfare Implications. J Assoc Environ Resour Econ 2015;2:133–59. doi:10.1086/680256.

[122] Nässén J, Holmberg J. Quantifying the rebound effects of energy efficiency improvements and energy conserving behaviour in Sweden. Energy Effic 2009;2:221–31. doi:10.1007/s12053-009-9046-x.

[123] Haas R, Biermayr P. The rebound effect for space heating Empirical evidence from Austria. Energy Policy 2000;28:403–10. doi:10.1016/S0301-4215(00)00023-9.

[124] Guerra Santin O. Occupant behaviour in energy efficient dwellings: evidence of a rebound effect. J Hous Built Environ 2013;28:311–27. doi:10.1007/s10901-012-9297-2.

[125] Jin S-H. The effectiveness of energy efficiency improvement in a developing country: Rebound effect of residential electricity use in South Korea. Energy Policy 2007;35:5622–9. doi:10.1016/J.ENPOL.2007.05.028.

[126] Melius J, Margolis R, Ong S. Estimating Rooftop Suitability for PV: A Review of Methods, Patents, and Validation Techniques. Golden, CO (United States): 2013. doi:10.2172/1117057.

[127] Residential Rate Surveys. Georg Public Serv Comm n.d. http://www.psc.state.ga.us/electric/surveys/residentialrs.asp (accessed November 15, 2018).

[128] Understanding solar radiation analysis—Help | ArcGIS Desktop. ESRI, ArcGIS n.d. http://pro.arcgis.com/en/pro-app/tool-reference/spatial-analyst/understanding-solar-radiation-analysis.htm (accessed October 5, 2017).

[129] U.S. Department of Energy. Transforming the Nation'S Electricity System the Second. Install Quadrenn Energy Rev 2017.

[130] Shahnia F, Majumder R, Ghosh A, Ledwich G, Zare F. Sensitivity analysis of voltage imbalance in distribution networks with rooftop PVs. IEEE PES Gen. Meet., IEEE; 2010, p. 1–8. doi:10.1109/PES.2010.5590149.

[131] Office E, August P. Economic Benefits of Increasing Electric Grid Resilience To

Weather Outages. Exec Off Pres 2013:1–28.

[132] Roege PE, Collier ZA, Mancillas J, McDonagh JA, Linkov I. Metrics for energy resilience. Energy Policy 2014;72:249–56. doi:10.1016/j.enpol.2014.04.012.

[133] Yodo N, Wang P. Resilience Modeling and Quantification for Engineered Systems Using Bayesian Networks. J Mech Des 2016;138:031404. doi:10.1115/1.4032399.

[134] Holling CS. Resilience and Stability of Ecological System. AnnuRevEcolSyst 1973;4:1–23. doi:10.1146/annurev.es.04.110173.000245.

[135] Cimellaro G, Villa O, Bruneau M. Resilience-Based Design of Natural gas distribution networks. J Infrastruct Syst 2014;21:1–14. doi:10.1061/(ASCE)IS.1943-555X.0000204.

[136] Panda A, Pathak MK, Srivastava SP. Enhanced power quality based single phase photovoltaic distributed generation system. Int J Electron 2016;103:1262–78. doi:10.1080/00207217.2015.1092600.

[137] Youn BD, Hu C, Wang P. Resilience-Driven System Design of Complex Engineered Systems. J Mech Des 2011;133:101011. doi:10.1115/1.4004981.

[138] Pariès J, Hollnagel E, Pariès J, Woods D, Wreathall J. Resilience engineering in practice : a guidebook. n.d.

[139] Robbins J, Krishnan K, Allspaw J, Limoncelli TA. Resilience Engineering: Learning to Embrace Failure. Queue 2012;10:20. doi:10.1145/2367376.2371297.

[140] Klein RJT, Nicholls RJ, Thomalla F. Resilience to natural hazards: How useful is this concept? Environ Hazards 2003;5:35–45. doi:10.1016/j.hazards.2004.02.001.

[141] Cimellaro GP, Reinhorn AM, Bruneau M. Seismic resilience of a hospital system. Struct Infrastruct Eng 2010;6:127–44. doi:10.1080/15732470802663847.

[142] Chertoff M. National infrastructure protection plan. Dep Homel Secur (DHS), Washington, DC 2009:175.

[143] Critical Infrastructure Sectors | Homeland Security. Dep Homel Secur n.d. https://www.dhs.gov/cisa/critical-infrastructure-sectors (accessed January 14, 2019).

[144] Kafali C, Grigoriu M, California SEA of. Rehabilitation Decision Analysis Toolbox. Structural Engineers Association of California,; 2005.

[145] Sustainable Development Goals | UNDP. United Nation Dev Progr 2016. http://www.undp.org/content/undp/en/home/sustainable-development-goals/ (accessed December 7, 2018).

[146] Department of energy. Clean Energy | Department of Energy n.d. https://www.energy.gov/science-innovation/clean-energy (accessed December 11, 2018).

[147] ROSELUND C. Solar supplies more than 10% of electricity in five US states – pv magazine International. Pv-Magazine 2018. https://www.pv-magazine.com/2018/08/28/solar-supplies-more-than-10-of-electricity-in-five-us-states/ (accessed December 17, 2018).